Abstract

Renalase is a flavoprotein recently discovered in humans, which is ubiquitous in vertebrates and conserved in some other phyla. In 2005, it was identified within a project aimed to determine novel proteins secreted by the kidney, whose defect could explain the high incidence of cardiovascular complications in patients with chronic kidney disease (Xu *et al.*, 2005). The protein is preferentially expressed in the renal proximal tubules and heart, and it's secreted in blood and urine.

Genetic, epidemiological, clinical studies and animal experimental models have constantly accumulated evidence of the important role played by renalase in lowering blood pressure, decreasing the catecholaminergic tone and control heart function. A renalase knockout mouse model resulted in increased levels of catecholamines in plasma and heart, cardiac ischemia and myocardial necrosis more severe than WT littermates (Wu *et al.*, 2011). However, the possible molecular mechanism, the nature of the *in vivo* catalyzed reaction and the identity of renalase substrate(s) are still unclear.

Based on these premises, the main aim of the project was to provide a detailed biochemical and structural characterization of renalase in order to better elucidate its physiological function.

We solved the crystallographic structure of recombinant human renalase at 2.5 Å resolution. The general fold classified it as a member of the *p*-hydroxybenzoate hydroxylase family. Renalase contains non-covalently bound FAD with redox features suggestive of a oxidase or NAD(P)H-dependent monooxygenase activity (Milani *et al.*, 2011), in contrast with the proposed activity of catecholamine degradation via a superoxide (O_2^-)-dependent mechanism (Farzaneh-Far *et al.*, 2010). Furthermore, structural

evidence indicates that the proposed secretion signal of renalase could not be cleaved without disrupting the protein native conformation, suggesting that renalase trafficking occurs through an atypical secretory pathway.
The resolution of renalase crystallographic structure and the biochemical data available will hopefully provide the basis towards the understanding of the molecular mechanism of renalase physiological action, which is expected to favor the development of novel therapeutic tools for the treatment of kidney and cardiovascular diseases.

During the PhD program, I was also involved in a side project focused on the elucidation of the role of Y258 residue of *P. falciparum* Ferredoxin-$NADP^+$ reductase (PfFNR) in the control of NADPH specificity.
PfFNR is a FAD-containing enzyme able to promote the transfer of two electrons from NADPH to ferredoxin and represents a promising target of novel antimalarial drugs.
Rapid reactions kinetics, active site titrations with $NADP^+$ and anaerobic photoreduction experiments allowed us to conclude that the Y258 side chain favors the stabilization of the catalytically competent conformation of the MNM moiety of NADPH, enhancing the hydride transfer between the nicotinamide nucleotide and the FAD prosthetic group.
The almost complete abolishment of NADPH selectivity has never been accomplished before through a single mutation.

State of the Art

Discovery of renalase

In 2005, the research group of G.V. Desir at the Yale University reported the identification of a putative novel flavin adenine dinucleotide-dependent amine oxidase (renalase) that was proposed to be secreted into the blood by the kidney, to regulate blood pressure and to metabolize *in vitro* catecholamines (Xu *et al.*, 2005).

Kidney disease is one of the major pathologies that severely threaten people's health. The incidence of chronic kidney disease (CKD) is increasing all over the world (Levey *et al.*, 2003), and it's well documented that patients with end-stage renal disease (ESRD) are at significantly higher risk for developing cardiovascular complications (Park, 2012).

In addition to maintaining fluid and electrolyte homeostasis, the kidney also serves as endocrine organ and is, for example, the main source of erythropoietin and renin.

In order to identify novel proteins secreted by the kidney with important biological roles, Desir and coauthors analyzed all the cDNA clones published by the Mammalian Gene Collection Project (MGC) (Strausberg *et al.*, 1999) screening *in silico* for proteins predicted to possess the following three features:

1. protein with less than 20% sequence similarity to known proteins
2. presence of a signal peptide
3. lack of transmembrane domains

This *a priori* selection yielded a total of 114 candidate genes derived from 12,563 distinct open reading frames considered. For each gene, Northern blot analysis were then performed to assess its tissue expression pattern and one clone was found with robust and preferential expression in human kidney (MGC12474; GenBank accession number BC005364) (Figure 1) encoding a protein with a calculated molecular mass of 37.8 kDa.

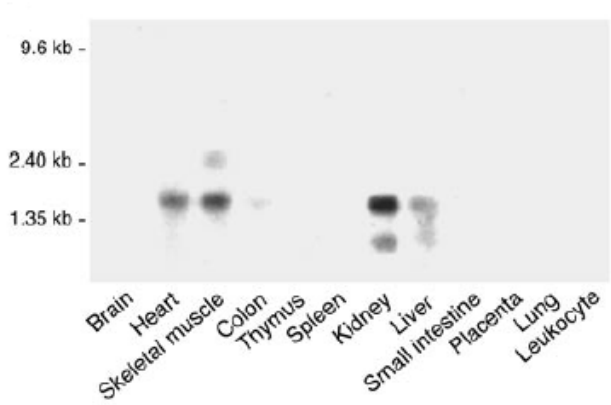

Figure 1. Tissue expression of renalase (Xu *et al.*, 2005). Northern blot analysis of human tissues using the MGC12474 clone as a probe. The major band of approximately 1.5 kb is visible in heart, skeletal muscle, kidney and liver. Two additional weaker bands detected in skeletal muscle (ca. 2.4 kb), kidney and liver (ca. 1.2 kb) may represent alternatively spliced variants.

Renalase gene

Human renalase gene (gene symbol: *RNLS*) resides on chromosome 10 at q23.33, encompassed 309,469 base pairs and has 10 exons. There is evidence for the existence of at least four alternatively spliced isoforms (Desir, 2009). The most highly expressed isoform (renalase1, NP_001026879) is 342 aa long, encoded by exons 1-4, 6-7 and 9. The second annotated protein isoform (renalase2, NP_060833) is 315 aa long,

encoded by exons 1-4, 6-7 and 10, thus differing from renalase1 at the extreme carboxy terminus. The other two characterized RNLS transcripts (AK296262 and BX648154) encode shorter deduced polypeptides (232 and 138 aa, respectively). The functional significance of the spliced isoforms is still not known.

The analysis of the renalase1 deduced amino acid sequence revealed the presence of a N-terminal signal peptide (SP) for the secretion (1-17 aa) and a dinucleotide binding motif (4-35 aa), which are partially overlapped. Renalase and flavoprotein-type monoamine oxidases share low degree of sequence identity (about 17%) concentrated in their N-terminal regions (Figure 2) (Desir, 2009). Renalase1 was detected in plasma, kidney, heart, skeletal muscle and liver, and efficiently secreted in the culture medium by transfected mammalian cells (Xu *et al.*, 2005).

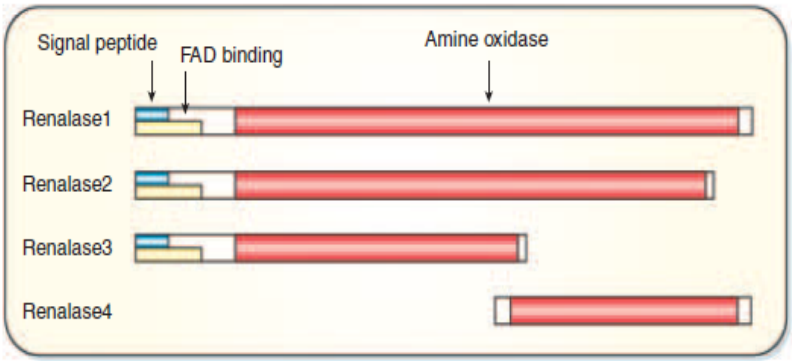

Figure 2. Functional domains of renalase isoforms 1-4 (Desir, 2009).

In 2008, the renalase homologous gene of mouse was cloned and characterized. Mouse renalase gene (DQ788834), isolated by RT-PCR from mouse kidney, shared 72% identity in amino acid sequence compared with the human counterpart (Wang *et al.*, 2008). Sequence analysis of the gene suggested that the coding region has an ORF encoding a protein of 342 aa with a predicted molecular mass of 37.6 kDa. The deduced protein sequence

presented a SP, a FAD binding motif and low identity with monoamine oxidases as the human renalase.

The renalase gene and its main protein product are highly conserved in vertebrates, with amino acid sequence identity above 60% (Xu *et al.*, 2007; Milani *et al.*, 2011) (Figure 3). Renalase-like proteins are present in some invertebrates, plants, fungi and prokaryotes.

Furthermore, renalase revealed less than 14% amino acid identity with well-known monoamine oxidase A (Xu *et al.*, 2005).

Figure 3. Amino acid sequence of human renalase (Milani *et al.*, 2011). Multiple alignment of human renalase with orthologs from different organisms: *Mus musculus* (110671808; 72% identity), *Danio rerio* (50540280; 60% identity), *Acyrthosiphon pisum* (193575653; 34% identity) and *Cyanothece* sp. (307154671; 28% identity. Partially conserved residues are boxed, with invariant residues highlighted in red.

Renalase expression pattern

In the most comprehensive study on the pattern of RNLS expression (Hennebry *et al.*, 2010), the authors investigated by immunoblotting the renalase distribution in autoptic human tissues that have earlier been shown to express MAO-A and B. In addition to kidney and myocardium (Xu *et al.*, 2005), renalase was found in forearm vein and artery, renal vein and artery, ureter, hypothalamus, pons, medulla oblongata, cerebellum, pituitary gland, cortex and spinal cord.

Immunolocalization studies, performed with anti-renalase monoclonal antibodies, confirmed that renalase is expressed in renal proximal tubules (Wang *et al.*, 2012) (Figure 4).

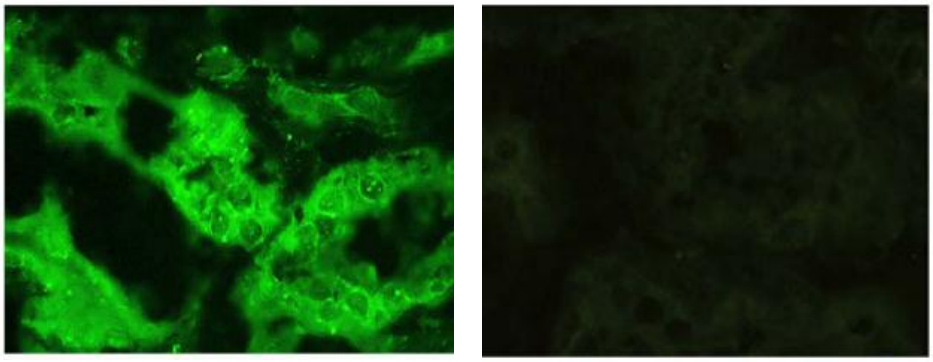

Figure 4. Immunofluorescence testing of renalase expression in renal tissue (Wang *et al.*, 2012). Left: renalase expressed in renal proximal tubules (Anti-renalase monoclonal antibody was used as primary antibody) (400X); right: renal proximal tubules negative control (PBS was used as control) (400X).

Renalase was detected in blood plasma and urine of healthy individuals (Xu *et al.*, 2005; Li *et al.*, 2008). However, data on the absolute concentration of renalase in human blood plasma have been explicity reported only recently as determined by ELISA, showing that it's about 4 μg/ml (Malyszko *et al.*, 2011).

The expression gene pattern of renalase homologue from mouse, defined by semiquantity RT-PCR, revealed the gene was predominantly expressed in kidney and testicle, followed by liver, heart, embryo (12.5 days) and very weakly detectable in brain and skeletal muscle (Wang *et al.*, 2008).

Cardiovascular complications in Chronic Kidney Disease

Chronic kidney disease is a progressive loss in renal function over a period of months or years; frequently clinically silent in the early stages, being detected shortly before when the impact of available therapies is markedly reduced (O'Seaghdha *et al.*, 2012). The clinical and public health importance of CKD is highlighted by several statistical analysis on the human population. In 2004, *National Kidney Foundation* defined the general criteria of CKD stages (Figure 5) considering an estimate glomerular filtration rate (GFR) below 60 ml/min/1.73 m^2, or evidence of structural kidney damage, such as proteinuria, or the requiring of renal replacement therapy (Cockcroft *et al.*, 1976; Levey *et al.*, 2003; Go *et al.*, 2006).

Clinical studies indicated that patients with either stage 3 through 5 CKD or end-stage renal disease (ESRD, sometimes considered as a subclass of CKD stage 5) receiving renal replacement therapy are at significantly higher risk for developing cardiovascular diseases (Go *et al.*, 2004; Li *et al.*, 2008; Rodriguez *et al.*, 2010). This increased propensity for cardiovascular events appeared to correlate with extensive arterial calcification, increased oxidative stress (Oberg *et al.*, 2004) and a heightened sympathetic tone (Koomans *et al.*, 2004; Joles *et al.*, 2004).

Stage	Criteria[a]
1	eGFR[b] $\geq$ 90 ml/min/1.73 m^2 with proteinuria[c]
2	eGFR 60–89 ml/min/1.73 m^2 with proteinuria
3	eGFR 30–59 ml/min/1.73 m^2
4	eGFR 15–29 ml/min/1.73 m^2
5	eGFR $<$ 15 ml/min/1.73 m^2 or requiring renal replacement therapy

Figure 5. CKD stages classification based on *National Kidney Foundation* criteria (Go *et al.*, 2006). eGFR (estimated glomerula filtration rate). [a]Criteria must be met for 3 months or longer, [b]eGFR based on abbreviated Modification of Diet in Renal Disease estimating equation or Cockcroft-Gault creatinine clearance equation, [c]Includes proteinuria or other evidences of structural kidney damage.

Interestingly, renalase was clearly detected in plasma of healthy individuals, but it was undetectable in ESRD patients (Xu *et al.*, 2005) (Figure 6). This evidence suggested that the kidney is the main source of renalase secreted in the blood. Since the molecular details underlying the regulation of renalase secretion are still unknown, low circulating renalase levels in ESRD might be due to increased catabolism or to a generalized decrease in secretion brought about by the metabolic abnormalities associated with severe renal failure.

Moreover, in rat model of unilateral renal artery stenosis, renalase expression and secretion were markedly reduced in the ischemic compared with the non-ischemic kidney (Gu *et al.*, 2011), confirming that the kidney is primarily responsible for renalase secretion in blood.

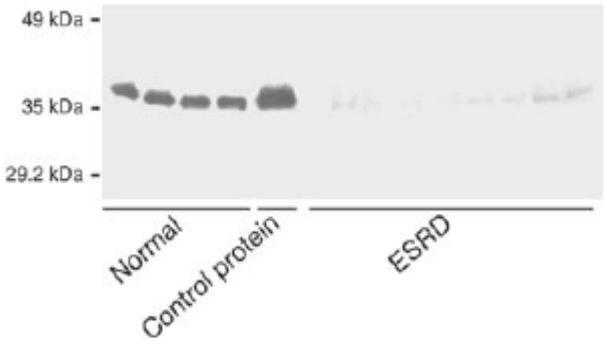

Figure 6. Western blot analysis of human plasma using an anti-renalase antibody (Xu *et al.*, 2005). Normal, plasma from individuals with normal renal function; Control protein, human recombinant renalase protein; ESRD, plasma from patients with ESRD receiving hemodialysis.

Physiological roles of renalase and their impact as possible pathogenic mechanisms of cardiovascular diseases

Despite the possible molecular mechanism of the renalase physiological activity, the nature of the catalyzed reaction and the identity of its substrate(s) are still very poor, there is quite solid and constantly accumulating evidence of the important roles played by renalase in the control of blood pressure and heart functions (Baroni *et al.*, 2012).

The *in vivo* effects of the protein was first analyzed on Sprague-Dawley rats (Xu *et al.*, 2005). The animals received a bolus injection of 0.5 mg of recombinant renalase and hemodynamic parameters were measured by a pressure/volume combination catheter inserted into the left ventricle. Renalase displayed the ability to lower blood pressure by decreasing cardiac contractility and mean arterial pressure. Renalase effect was dose-dependent (Figure 7).

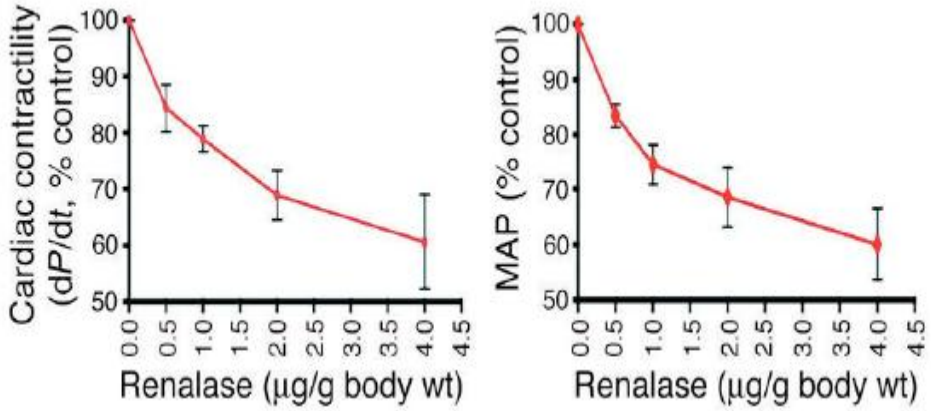

Figure 7. Renalase dose-response curve (Xu *et al.*, 2005). Left: cardiac contractility. Right: mean arterial pressure (MAP).

When injected on anesthetized rats at the dose of 4 mg/kg, recombinant human renalase significantly decreased systemic blood pressure (Pandini *et al.*, 2010) (Figure 8).

Parameters	Vehicle	Renalase	% Inhibition	*P*
MAP (mm Hg)	108.5 ± 7.4	87.4 ± 12.4	19.4	<0.033
SAP (mm Hg)	135.8 ± 11.3	102.1 ± 8.7	24.8	<0.040
DAP (mm Hg)	95.7 ± 6.9	74.9 ± 5.6	21.7	<0.041
LVSP (mm Hg)	128.4 ± 9.8	99.2 ± 6.3	22.7	<0.031
LVEDP (mm Hg)	6.2 ± 0.3	5.3 ± 0.4	14.5	ns
LVDevP (mm Hg)	122.1 ± 8.7	94.0 ± 7.7	23.0	<0.036
$LVdP/dt_{max}$ (mm Hg/s)	5095 ± 407	3724 ± 265	26.9	<0.018
$LVdP/dt_{min}$ (mm Hg/s)	4113 ± 258	3253 ± 204	20.9	<0.026
HR (beats/min)	371.6 ± 10.2	337.5 ± 12.9	9.2	ns
PRI (mm Hg/ min × 10^3)	40.2 ± 3.9	29.7 ± 3.7	26.1	ns

Figure 8. Effect of recombinant human renalase on hemodynamic parameters in anaesthetized rats (Pandini *et al.*, 2010). Data are expressed as mean ± standard error (n = 6); ns, not significant. Vehicle (PBS, containing 10% glycerol) and recombinant human renalase were given intravenously in a volume of 1 ml/kg body weight. MAP, mean arterial pressure; SAP, systolic arterial pressure; DAP, diastolic arterial pressure; LVSP, left ventricular systolic pressure; LVEDP, left ventricular end-diastolic pressure; LVDevP, left ventricular developed pressure; $LVdP/dt_{max}$, maximum positive rate of developed left ventricular pressure; $LVdP/dt_{min}$, maximum negative rate of developed left ventricular pressure; HR, heart rate; PRI, pressure rate index.

A single dose of recombinant renalase (0.5 mg/kg subcutaneous dose) significantly decreased systemic and diastolic blood pressure for up to 24 h in Dahl salt-sensitive rats (a genetic model of hypertension and renal disease that exhibits many phenotypic characteristics in common with human hypertension) (Desir, 2011) and in 5/6 nephrectomized rats (rats subjected to the removal of approximately 85% of kidney tissue) (Desir, Wang *et al.*, 2012). Moreover, in the latter animal model recent studies showed that four weeks treatment with 0.5 mg/kg body weight daily of recombinant renalase resulted in a significant decrease of blood pressure and cardiac hypertrophy (Baraka *et al.*, 2012).

Interestingly, using an isolated heart model of acute coronary syndrome, recombinant renalase perfusion was shown to exert a protective effect against ischemia, preserving ventricular function and reducing myocardial necrosis and infarct size (Desir *et al.*, 2007).

To gain insight into the link between renalase deficiency, hypertension and cardiovascular diseases, RNLS gene has been inactivated in mouse by homologous recombination, deleting the promoter region and a large part of the coding sequence (Wu *et al.*, 2011). Blood pressure and heart rate were higher in anesthetized knockout (KO) mice, while renal function was unaffected by renalase absence. KO mice also displayed higher plasma dopamine, epinephrine and norepinephrine levels than WT mice (Wu *et al.*, 2011).

A link between renalase and catecholamine metabolism emerged from several studies (Desir G.V., 2009; Ghosh *et al.*, 2009). In various rat models of chronic kidney and heart failures, lower concentrations of renalase in kidney, heart and blood were always accompanied by increased levels of epinephrine and norepinephrine in plasma and heart (Ding *et al.*, 2009; Quelhas-Santos *et al.*, 2010; Gu *et al.*, 2011).

Renalase KO mice also poorly tolerated cardiac ischemia and developed ischemic myocardial necrosis that was found to be 3-fold more severe than WT. Furthermore, reperfusion with recombinant renalase resulted in a dramatic reduction in ischemic myocardial damage in renalase KO heart (Wu *et al.*, 2011) (Figure 9).

Renalase deficiency was also associated with a significant decrease in the NAD/NADH ratio, indeed plasma NADH oxidase activity was found significantly lower in renalase KO mice, suggesting that plasma renalase contributes to the regulation of extracellular NAD level (Wu *et al.*, 2011) (Figure 20). However, the low turnover of renalase measured in NADH-dependent reaction *in vitro* (K_m^{NADH} = 15.2 ± 2.2 µM and V_{max} = 15.3 ± 0.8 nmol/min per mg protein) would exclude direct effects on NADH and/or NAD^+ concentrations *in vivo*.

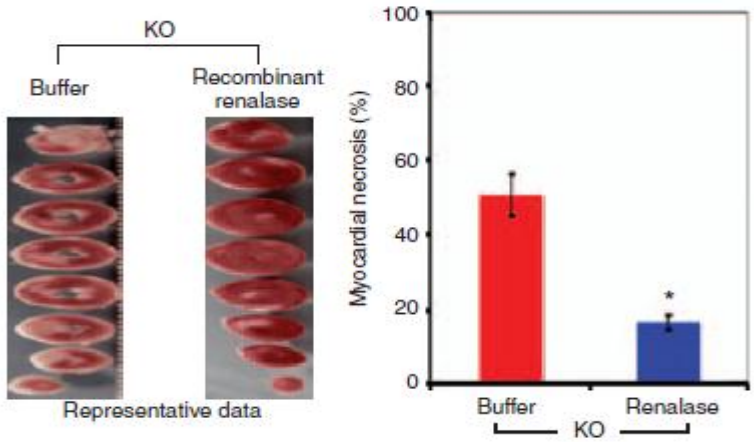

Figure 9. Cardioprotective effect of renalase (Wu *et al.*, 2011). Left: Cardioprotective effect of recombinant renalase. TTZ stains of KO heart exposed to 15 min of global ischemia followed by 90 min of reperfusion with or without recombinant renalase; red stain indicates viable myocardium. Right: Recombinant renalase cardioprotective effect quantified using ImaeJ. *P < 0.04, n = 4.

The involvement of renalase in kidney disease and hypertension

Recent evidence on the impact of kidney and heart transplantation on the level of circulating renalase unexpectedly revealed higher serum renalase content among recipients than in healthy volunteers and the degree of increase correlated with the severity of the kidney failure and the time after transplantation (Malyszko *et al.*, 2011; Przybylowski *et al.*, 2011). Indeed, in hemodialysis patients the mean serum renalase concentration was found ca. 17.5 μg/ml (significantly higher when compared with that reported for healthy volunteers, ca. 4 μg/ml) and ca. 8.5 μg/ml in the blood of heart transplant recipients.

These data were questioned by Desir and coauthors (Desir, Wang *et al.*, 2012) for two main considerations: first, the identity of the antibodies used in the ELISA kit, the epitopes they recognized and information on how they behaved in native Western blots were not available; second, the increase in renalase levels could be a reflection of accumulated renalase breakdown products or of cross-reaction with unrelated epitope.

Epidemiologic data implying renalase gene polymorphisms as disease risk factors

There are many entries of single nucleotide polymorphisms (SNP) for the renalase gene in the public NCBI *Single Nucleotide Polymorphism database* (dbSNP) (Zhao *et al.*, 2007).

Different independent genetic studies found a correlation between individual renalase SNPs and pathological conditions (Table 1).

Table 1. Single nucleotide polymorphisms of the renalase gene characterized for their association with pathological conditions (Baroni *et al.*, 2012). [b]MAF, minor allele frequency; [c]n.s., no significant correlation with the considered pathological conditions.

SNP accession no.	Location	Alleles	MAF[b]	Diseases and risk-associated allele
rs2576178	5' flanking region	G/A	0.46	Essential hypertension (G); hypertension in end stage renal disease (G); type 2 diabetes (G)
rs2296545	Exon 1	C/G Asp37/Glu37	0.44	Essential hypertension (C); hypertension in type 2 diabetes (C); cardiac hypertrophy, dysfunction and ischemia (C)
rs2765446	Intron 3-4	C/T	0.46	n. s.[c]
rs2437871	Intron 3-4	A/C	0.46	Type 2 diabetes (A)
rs11202776	Intron 4-5	C/T	0.12	n. s.[c]
rs1648512	Intron 5-6	A/G	0.32	n. s.[c]
rs10887800	Intron 5-6	A/G	0.50	Hypertension in end stage renal disease (G); stroke (G)
rs1035796	Intron 7 -7	C/T	0.47	n. s.[c]
rs2114406	3' flanking region	A/G	0.22	n. s.[c]

To investigate the possible association between renalase genetic variants and essential hypertension, in 2007 the first population genetic study was reported (Zhao *et al.*, 2007) on 1,317 hypertensive cases (from the *International Collaborative Study of Cardiovascular Disease* in Asia) and 1,269 normotensive controls in the northern Han Chinese population. Eight single nucleotide polymorphisms of the renalase gene were genotyped and analyzed. Two of them (rs2576178 located in the 5' flanking region and rs2296545 situated within the deduced FAD binding motif) showed significant association with essential hypertension.

The association between the rs2576178 renalase gene polymorphism and hypertension was confirmed by a case-control study on 369 Caucasian

subjects of Polish origin (200 hypertensive cases and 169 controls) undergone renal replacement therapy in a form of hemodialysis or peritoneal dialysis (Stec *et al.*, 2011). The authors also found a significant correlation between the rs10887800 polymorphism and the development of hypertension. Moreover, an independent study on 892 type 2 diabetic patients and 400 controls revealed a strong association of the rs10887800 polymorphism with stroke in patients with and without diabetes and a correlation between the rs2576178 and type 2 diabetes (Buraczynska *et al.*, 2011).

Among the renalase gene SNPs previously considered, rs2296545 is the only resulting in variants of the protein which differ for the presence of a Glu (G allele) or an Asp (C allele) residue at position 37. The functional missense polymorphism Glu37Asp was found to be associated with cardiac hypertrophy, ventricular dysfunction, poor exercise capacity and inducible ischemia in persons with stable coronary artery disease (Farzaneh-Far *et al.*, 2010).

Purification of endogenous and recombinant renalase forms

Any proposal about the mechanism of the physiopathological action of a newly discovered protein needs to be verified in the context of its functional and structural properties. In the case of renalase, the application of this general rule had to wait several years until sufficient amounts of stable recombinant holoprotein became available for its biochemical and structural characterization (Pandini *et al.*, 2010) (Baroni *et al.*, 2012).

The research group of Desir was the only who successfully isolated endogenous renalase from human urine of healthy volunteers (Xu *et al.*,

2005). After ammonium sulfate precipitation, renalase was purified by affinity chromatography using an anti-renalase antibody. Essentially, no biochemical characterization was performed on the purified material, except for electrophoretic analysis (Figure 10) and catalytic activity assay, not allowing definitive conclusions about the presence or absence of the signal peptide after post-translational processing. In addition to the band of the expected size (approximately 37 kDa), another doublet was also detected, possibly representing the product of either dimerization or aggregation of the protein.

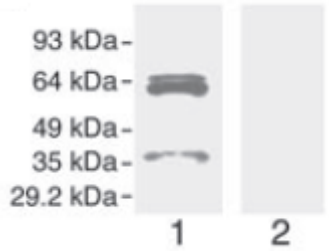

Figure 10. Affinity purification of human renalase. (Xu *et al.*, 2005). The anti-renalase polyclonal antibody was used to isolate protein from human urine. Lane 1: renalase from human urine. Lane 2: control with secondary antibody alone.

The production of recombinant mammalian renalase in different hosts using various expression strategies was described by many independent groups. Desir's team expressed and purified two recombinant forms of human renalase in *E. coli*: an N-terminal fusion protein with glutathione S-transferase (GST) was purified in soluble form using Glutathione Sepharose (Xu *et al.*, 2005), then an untagged variant was synthesized in soluble form, purified from inclusion bodies and *in vitro* refolded by dilution and gradual acidification in the presence of FAD (Wu *et al.*, 2011).

In order to obtain the monoclonal antibody against the recombinant renalase, Wang and coauthors produced a fusion protein containing the

pelB leader sequence (for cell periplasm localization) at the N-terminal and a C-terminal His-tag (Wang *et al.*, 2009).

Very recently, to improve the renalase protein production facilitating the expression in *E. coli*, Desir's group designed a synthetic renalase gene in which ≈ 30% of nucleotides were substituted to optimize codon usage and to remove putative translational pause signals while preserving the native amino acid sequence (Desir, Tang *et al.*, 2012). This resulted in a 200-fold protein expression increase and yielded about 20 mg/l *E. coli* culture *in vitro* refolded untagged protein, stable for several months at 4 °C.

Renalase homologue from mouse was obtained in *E. coli* by Zhang's group as an N-terminal fusion protein with GST, but no purification protocol has been reported (Wang *et al.*, 2008).

Although its isolation has never been reported, recombinant mouse renalase was also produced in eukaryotic cells (modified human embryonic kidney 293T cells) as a C-terminal EGFP-(enhanced green fluorescent protein) fusion protein (Wang *et al.*, 2008). Transfected cells displayed weaker cellular fluorescence than the EGFP control cells, but a brighter signal in the culture medium suggesting mouse renalase-EGFP was secreted out of the cells, although a proportion of the protein remained within the cells as well.

Even if many details of the cloning procedure were missing and no explanation was given of the very large apparent molecular mass of the purification product (85 kDa), the expression of human renalase in insect cells by a baculovirus-based system was described (Wang *et al.*, 2010). Moreover, the same authors also reported the production of human renalase in embryonic kidney cells (Wang *et al.*, 2011).

Recombinant renalase synthesis in the yeast *Pichia pastoris* was also reported in a patent by Desir (Desir *et al.*, 2008).

Despite the ability of renalase to incorporate a flavin nucleotide being a prerequisite for the enzymatic action, the presence of FAD or FMN in the recombinant renalase forms previously described was not reported.

Only in the first published paper, Desir and coauthors observed that the addition of 0.1 μM FAD in the bacterial culturing medium was required to isolate a recombinant protein functionally active (Xu *et al.,* 2005), even it's well known that FAD or FMN biosynthesis by *E. coli* is not a limiting factor in flavoprotein production (Kitamura *et al.,* 1998; Aliverti *et al.*, 2004). Based on these considerations, Medveded and coauthors clearly stated that a conclusive proof that renalase contained FAD was still lacking (Medveded *et al.,* 2010).

This proof was obtained in the same year. In our lab, two different protocols were set for the heterologous expression of human renalase and the purification of the resulting recombinant products in a holoprotein form (Pandini *et al.*,2010). Two plasmids were used to direct the synthesis of the protein in *E. coli*: one fused to a N-terminal polyHis extension and the other where a polyHis-tag, a small ubiquitin-like modifier (SUMO) unit and renalase were connected from N- to C-terminal.

Although yielding only 1.5 mg pure recombinant renalase spontaneously folded *in vivo* per liter culture, both purification protocols were very reproducible and easily scaled up, since they are based on small-volume affinity chromatographic columns. The identity of the final product as polyHis-renalase was confirmed by MALDI-TOF mass spectrometry which yielded a molecular mass of 39,496 Da in good agreement with the theoretical value of 39,626 Da.

A detailed spectroscopic characterization of polyHis-renalase and renalase was carried out in order to exclude their possible misfolding. Both proteins displayed identical absorption, fluorescence and circular dichroism spectra. The absorption spectra of renalase in the visible region is that

typical of a flavoprotein (Figure 11), with absorption maxima at 385 and 458 nm. This spectrum significantly differs from those of MAO-A and B (Hynson *et al.*, 2004). The flavin fluorescence of renalase was found almost completely quenched. Heating at 90 °C resulted in the formation of a colorless precipitate, while the liquid phase revealed to contain a flavin nucleotide on the basis of its absorption spectrum and to display a fluorescence spectrum matching that of a corresponding concentration of FAD. Moreover, an extinction coefficient of 11.3 mM^{-1} cm^{-1} at 458 nm was calculated for native renalase.

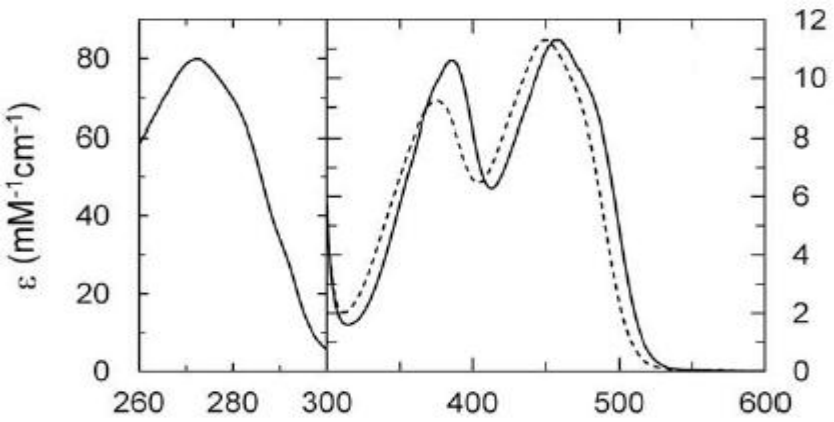

Figure 11. Absorption spectra of renalase (Pandini *et al.*, 2010). Spectrum of ca. 19 µM renalase in PBS, before (solid line) and after the addition of 0.2% SDS (dotted line), which resulted in FAD release from the apoprotein. The molar absorbance is reported.

Catalytic properties of renalase

To date, only two groups published data on the biochemical *in vitro* properties of renalase. In 2005, the research group of Desir found that both the recombinant GST-tagged renalase and the endogenous protein isolated from urine specifically metabolized catecholamines, with dopamine as preferred substrate, followed by epinephrine and norepinephrine (Xu *et al.*, 2005) whereas its activity towards other biogenic amines was negligible (Figure 12). The ability of renalase to oxidase biogenic amines was assessed using an Amplex Red Monoamine Oxidase Assay Kit, detecting H_2O_2 in a HRP-coupled reaction using 10-acetyl-3,7-dihydroxy-phenoxazine (Amplex Red reagent, Invitrogen Corp.) (Figure 13). Curiously, the authors observed that this activity was present only if the growth medium was supplemented with 0.1 µM FAD, suggesting the flavin cofactor is essential for the catalytic activity.

Furthermore, renalase enzymatic activity was not affected by known inhibitors of MAO-A and B, clorgyline and pargylilne.

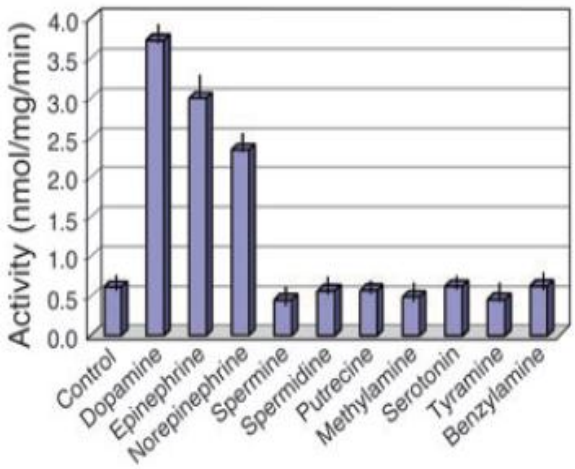

Figure 12. Renalase metabolizes catecholamines (Xu *et al.*, 2005). Ten micrograms of GST-renalase fusion protein was used for each assay; amine oxidase activity is expressed as H_2O_2 production (nmol/mg/min).

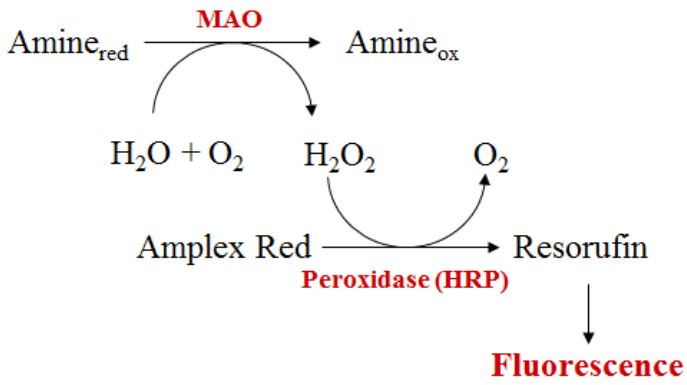

Figure 13. Amplex Red Monoamine Oxidase Assay. The Amplex Red reagent reacts with H_2O_2 in a 1:1 stoichiometry and the resulting fluorescence signal is directly proportional to H_2O_2 production and hence amine oxidase enzymatic activity.

After careful analysis of the data reported by Desir and coauthors, some authors (Boomsma *et al.*, 2007) concluded that the rate of H_2O_2 generation was too low to be ascribed to enzymatic conversion of catecholamines by renalase. They also noticed that plasma of many species contains the enzyme semicarbazide-sensitive amine oxidase which catalyzes the oxidative deamination of primary amines to form the corresponding aldehydes plus H_2O_2 and ammonia (Boomsma *et al.*, 2003). Moreover, the supposed activity of purified renalase, measured only as H_2O_2 production, might be due to catecholamine autoxidation, which is known to be relevant at pH values above neutrality, or to the oxidation of contaminant(s) that are common in commercial catecholamines. Finally, they argued that, even if renalase were able to degrade biogenic amines, its turnover number is so slow that it would hardly affect blood catecholamine concentration.

One year later, by comparison of the activities measured on both plasma and urine renalase, Desir and coauthors hypothesized that the circulating renalase would exist as inactive form (prorenalase) which needs catecholamine-triggered signals to be activated (Li *et al.*, 2008).

Amine oxidase activity was undetectable in rat plasma under basal conditions, but a 2 min infusion with exogenous epinephrine or dopamine significantly increased renalase activity (measured as H_2O_2 production inhibited by anti-renalase antibody) 10-fold within 30 s and remained high long after the catecholamines infusion (Figure 14), suggesting the possibility that the activating signal may be represented by an increase in plasma catecholamine levels. Since renalase plasma concentration didn't follow the same time course, the authors concluded that the rapid increase of amine oxidation activity was due to the conversion of an inactive prorenalase form to the functional enzyme.

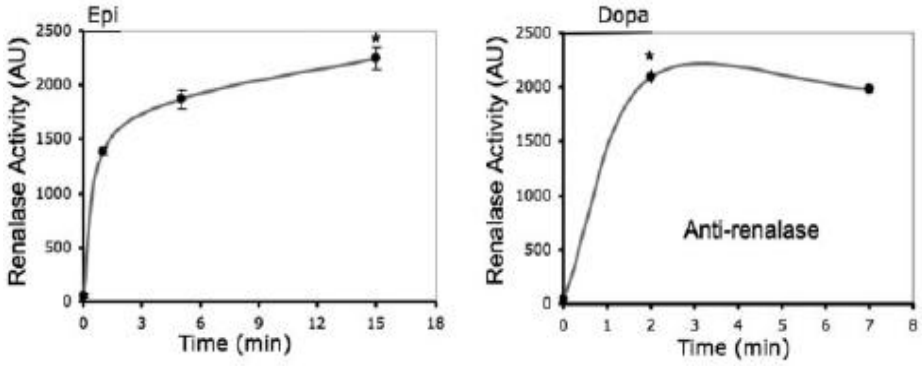

Figure 14. Catecholamines regulate renalase activity in rat plasma (Li *et al.*, 2008). Renalase activity in response to epinephrine (Epi; left) or dopamine (Dopa; right) infusion lasting 2 minutes. Renalase-specific amine oxidase activity is determined with an anti-renalase antibody that inhibits function.

As previously reported, in 2011 Desir and coauthors observed that renalase deficiency affected the cellular NAD/NADH ratio and found a markedly decreased NADH oxidase activity in renalase KO animals, supporting the hypothesis that renalase would possess a NADH oxidase activity (Wu *et al.*, 2011). They also reported that *in vitro* refolded recombinant human renalase displayed NADH oxidase activity, with a K_m^{NADH} of 15 µM and a k_{cat} of 0.4 min^{-1}. The enzyme was inactive towards NADPH.

Moreover, when epinephrine was included in the reaction mixture, it was degraded at a rate 18-fold faster than in the absence of NADH with a $K_m^{epinephrine}$ of 17 µM and a k_{cat} of 0.6 min^{-1} (Desir, Wang *et al.*, 2010). Based on these observations, renalase was proposed as a new NADH-dependent catecholamine degrading enzyme.

These conclusions were questioned by Eikelis and coauthors, who pointed out the observed renalase catecholamine-degrading rate was extremely low to be ascribed to a real enzyme activity (Eikelis *et al.*, 2011).

Recent data also reported the administration of human renalase in KO mice decreased plasma epinephrine, L-DOPA and dopamine by 82%, 63% and 31% respectively without significant increase in the urinary excretion of the deaminated, methylated and deaminated plus methylated metabolites, suggesting that renalase action on catecholamines differs significantly from that of catechol-O-methyl transferase (COMT) and MAOs (Desir, Tang, *et al.*, 2012; Desir, Wang, *et al.*, 2012; Quelhas-Santos *et al.*, 2012).

To further test if the NADH-dependent enzymatic activity of renalase was correlated with its hypotensive effect, 4 cysteine-to-alanine mutants were generated. The catalytic efficiency of C47A, C54A, C220A and C327A renalase variants was reduced by 20%, 95%, 95% and 94%, respectively, with a strong correlation to the capacity of decreasing blood pressure in renalase KO mice (Desir, Tang *et al.*, 2012).

Another aspect of renalase function is the role played by the residue 37 side-chain in catalysis. As previously mentioned, the renalase gene SNP rs2296545 was found to be associated to cardiovascular pathologies. The diaphorase activity of both Asp37 and Glu37 renalase isoforms revealed the Glu37Asp replacement determined an increase in K_m^{NADH} from 34 ± 4 to 820 ± 115 µM and a decrease in V_{max} from 58 ± 1 to 25 ± 2 nmol/min/mg (Farzaneh-Far *et al.*, 2010) (Figure 15).

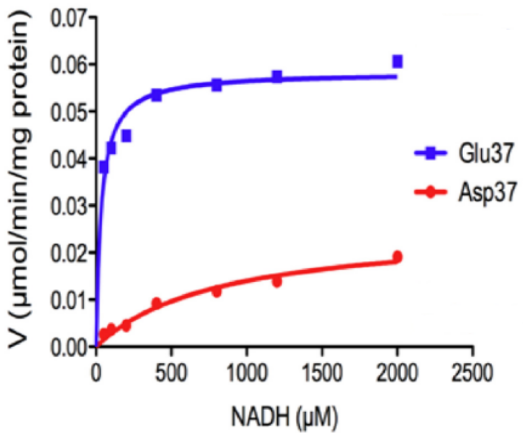

Figure 15. Calculated kinetics parameters (Farzaneh-Far *et al.*, 2010). The NADH/FAD dependent enzymatic activity was assessed by measuring the rate of reduction of 2-(4-iodophenyl)-3-(4-nitrophenyl)-5-(2,4-disulfophenyl)-2H tetrazolium monosodium salt (WST-1). Reduction of WST-1 resulted in the formation of a yellow, water-soluble product, quantified by measuring absorbance at 450 nm.

Recently, we confirmed that recombinant human renalase slowly reacts with nicotinamide dinucleotides and weakly binds the corresponding oxidize forms (Milani *et al.*, 2011). We clearly showed that the FAD cofactor is involved in these reactions, since its reduction rates are compatible with the catalysis. Differently from the data published by Desir and coauthors, we demonstrated that the recombinant *in vivo* folded FAD-containing human renalase is not strictly specific for NADH and found completely lacking of any amine oxidase activity.

Flavoenzymes

Flavoenzymes have the unique ability to catalyze a wide range of biochemical reactions (Fraaije *et al.*, 2000). They are involved in the dehydrogenation of a variety of metabolites, in one- and two-electron transfer from and to redox centers, in light emission, in the activation of oxygen for oxidation and hydroxylation reactions (Massey, 1995). Moreover, they catalyze other types of reactions involved in a wide array of biological processes including protein folding, DNA repair and apoptosis. At present, the Protein Data Bank (PDB) contains hundreds entries for FAD- and FMN-dependent proteins. Flavoenzymes (Massey, 2000; Joosten *et al.*, 2007) are colorful oxidoreductases that contain a flavin (flavin mononucleotide, FMN or flavin adenine dinucleotide, FAD) as cofactor, non-covalently or covalently bound to the apoprotein. Topologically similar flavoenzymes can catalyze different reactions, whereas proteins performing similar functions can have dissimilar folding architectures (Fraaije *et al.*, 2000).

The spectroscopic properties of the flavin cofactor make it a natural reporter for changes occurring within the active site, a feature which makes flavoproteins one of the most studied enzyme family.

Well-studied classes of flavoenzymes are flavoprotein oxidases and monooxygenases.

Flavoproteins oxidases, such as D-amino acid oxidase, glucose oxidase, glycolate oxidase, catalyze the oxidation of a specific substrate involving molecular oxygen (O_2) as electron acceptor, which is reduced to H_2O_2. The stabilization of the anionic flavin semiquinone and the formation of a flavin-sulfite adduct at the N-5 position are typical of flavin-dependent oxidases. However, there are many exceptions, as in the case of

monoamine oxidases, which are not able to react with sulfite ion (Li *et al.*, 2002).

Flavoprotein monooxygenases introduce a single atom of molecular oxygen into the substrate, while the other oxygen atom is reduced to water. The reaction needs NADH or NADPH cosubstrates as electron donor. Activation of molecular oxygen in these enzymes is achieved by the generation of a (hydro)peroxyflavin, which in the presence of the substrate transfers an oxygen atom to the substrate and subsequently returns to its resting state by losing a molecule of water.

P-hydroxybenzoate hydroxylase protein superfamily

Enzymes belonging to the *p*-hydroxybenzoate hydroxylase (PHBH) structural family catalyze highly diverse reactions and include both oxidases and non-oxidases. In particular, the enzymes catalyzing the oxidation of amines belong to one of the two possible structural groups: the MAO family and the D-amino acid oxidase family (Fitzpatrick *et al.*, 2010).

Monoamine oxidases

Monoamine oxidases (Edmonson *et al.*, 2007; Edmonson *et al.*, 2009) are mitochondrial outer membrane-bound flavoproteins that catalyze the oxidative deamination of neurotransmitters and biogenic amines using O_2 as electron acceptor. Two distinct forms of MAOs, named MAO-A and MAO-B sharing about 70% identity in amino acid composition, are known. It's currently thought that the gene encoding MAO-A and B

evolved from a single ancestral gene by a duplication event, since lower animals were found to contain only a single MAO gene (Setini *et al.*, 2005).

The flavin cofactor is covalently bound to the enzyme via a Cys residue, forming an 8α-S-cysteinyl-FAD in both MAO-A (Cys406) and B (Cys397) (Edmonson *et al.*, 2004).

The catalytic pathway of MAOs implies the formation of the enzyme-substrate complex resulting in the reduction of FAD and the formation of an imine intermediate. During this phase, oxygen reacts with reduced FAD to regenerate the oxidized flavin and H_2O_2. Released imine undergoes non catalyzed hydrolysis to form NH_4^+ and the corresponding aldehyde (Edmonson *et al.*, 2009).

The crystal structure of human and rat MAO-A (De Colibus *et al.*, 2005; Son *et al.*, 2008) and human MAO-B (Binda *et al.*, 2002) have been determined (Figure 16). Both MAO-A and B showed a C-terminal protruding transmembrane region, folded as an α-helix. The position of the FAD cofactor is highly conserved between the two forms.

Human MAO-B crystallized as a dimer. The structure revealed an "entrance" and a "substrate cavity" at the end of which the FAD cofactor is located. Ile199 side chain serves as a "gate" between the two hydrophobic cavities and can exist in "open" or "close" conformation. Human MAO-A crystallized as a monomer, while the rat homologue as a dimer. It displayed a single substrate hydrophobic cavity with protein loops at the entrance.

The presence of different residues in the active site in the two enzymes is at the base of their distinctive substrate and inhibitor specificities. Indeed MAO-A specifically deaminates serotonin and epinephrine and is inhibited by clorgyline, whereas MAO-B is specific for phenylethylamine and benzylamine and inhibited by pargylilne and selegine.

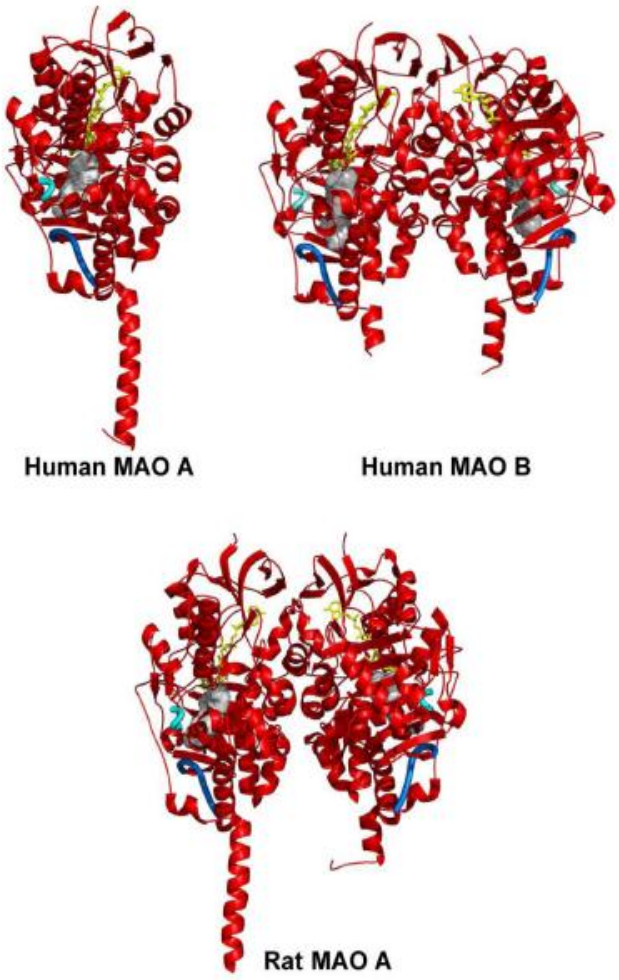

Figure 16. Ribbon diagram showing the three-dimensional structures of human MAO-A, human MAO-B and rat MAO-A (Edmonson *et al.*, 2009). All structures are oriented with the C-terminal transmembrane helices pointing downwards. The FAD cofactor is in yellow ball-and-stick representation. Active site cavity in each enzyme molecule is drawn as a gray surface. The cavity-shaping loop is highlighted in cyan. The loop lining the entrance cavity in human MAO-B is featured in blue. The corresponding residues in rat and human MAO-A adopt the same conformation.

p-hydroxybenzoate hydroxylase

Another important class of flavoproteins is the monooxygenase family, which uses NAD(P)H and O_2 as co-substrates and inserts one atom of oxygen into the substrate. They are involved in a wide variety of biological processes including drug detoxification, biodegradation of aromatic compounds, biosynthesis of antibiotics and many others (Ballou *et al.*, 2005).

P-hydroxybenzoate hydroxylase is one of the most thoroughly studied enzymes. It displays significant protein and flavin dynamics during catalysis (Ballou *et al.*, 2005). There is an *open* conformation that gives access of substrate and product to solvent, and a *in* conformation for the reaction with oxygen and the hydroxylation to occur. This *in* form prevents solvent from destabilizing the intermediate. Finally, there is an *out* conformation achieved by movement of the isoalloxazine towards the solvent allowing the access of NADPH which transfers an hydride to the N-5 of the flavin (Figure 17).

The catalytic process starts while the enzyme is in a dynamic equilibrium between the *open* and *in* conformations. In the *open* conformation the enzyme can bind *p*-hydroxybenzoate and the formation of the ES complex shifts the equilibrium to the *in* position. The presence of the substrate increases the rate of reduction of the flavin by NADPH by > 10^5-fold. On the contrary in the absence of the substrate, flavin reduction is quite ineffective, preventing the wasteful use of NAD(P)H which would produce unwanted reactive oxygen species (such as H_2O_2). When the substrate is in the place, the transition to the *out* conformation is triggered by NADPH binding with the subsequent reduction of the flavin. After $NADP^+$ release the anionic isoalloxazine moves back to the *in* position, where it can react efficiently with O_2 to form C4a-hydroperoxy-FAD, with the consequent

electrophilic attack of the hydroperoxide on the phenolate, resulting in the hydroxylation of phenolate to yield the dienone form of the product and the C4a-flavin alkoxide. The final product is achieved by rearomatization of the dienone.

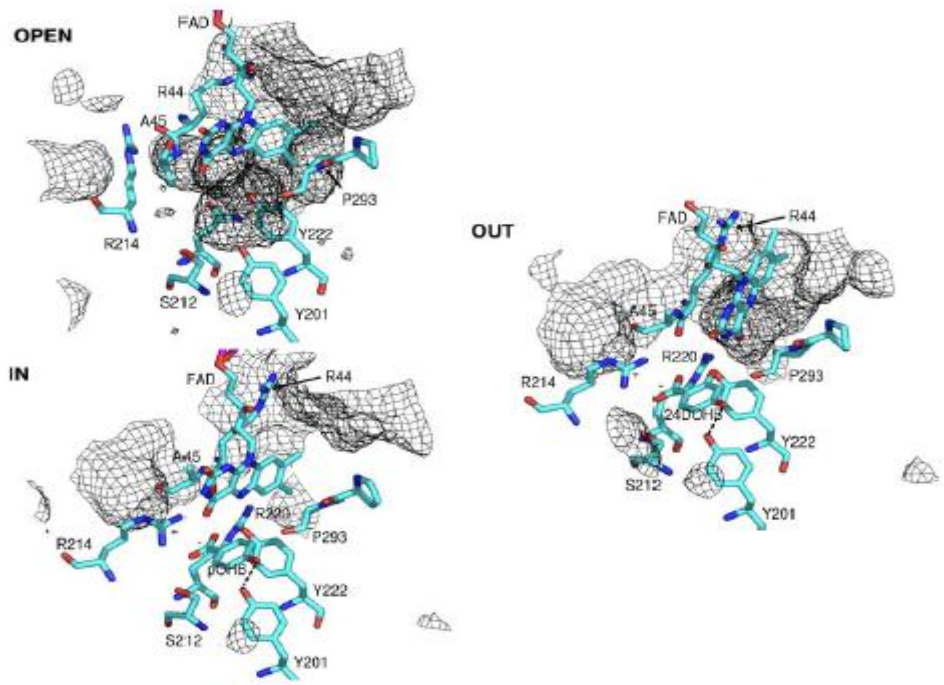

Figure 17. Conformations of PHBH important for catalysis (Ballou 2005). Left top, *open*; left bottom, *in* ; right, *out* conformation.

Uunconventional protein secretion

The vast majority of extracellular proteins are secreted by the classical endoplasmic reticulum (ER)/Golgi-dependent pathway, however numerous exceptions have been identified (Nickel, 2010). "Unconventional protein secretion" has become a generally used term to collectively describe several kinds of unusual trafficking pathways that lead to the exposure of proteins on cell surface or to their release into the extracellular space (Nickel *et al.*, 2009). Unconventional secretion is not characterized by a common mechanism, but rather represents a collection of at least four distinct transport pathways. They can be classified into non-vesicular and vesicular mechanisms.

Non-vesicular mechanisms are based on direct translocation of cytoplasmic proteins across the plasma membrane, followed by deposition on cell surfaces or by release into the extracellular space. Fibroblast growth factor 2 is a key example (Schäfer *et al.*, 2004; Nickel *et al.*, 2009).Vesicular mechanisms depend on intracellular membrane bound intermediates that need to fuse with plasma membrane to release cargo into the extracellular space. Such mechanisms have been described to involve either secretory lysosomes, exosomes derived from multi-vesicular bodies or microvesicles shedding from cell surface. The export involving intracellular transport intermediates has been shown for acyl-CoA binding protein (Pfeffer, 2010).

The amino terminus of renalase contains a putative signal peptide for the secretion through the classical pathway. However, structural evidences suggest that the SP could not be cleaved without the loss of the protein native conformation (Milani *et al.*, 2011).

Aim of the Project

Renalase is an intriguing protein, which has been proposed to represent a novel player in the regulation of blood pressure and cardiac function (Xu *et al.*, 2005). Despite its potential medical relevance, a deep biochemical characterization of this protein is still lacking.

The general aim of this work has been to assess the molecular mechanism of renalase action thorough the structural and functional characterization of the recombinant protein isolated in purified form.

Since only very small amounts of renalase were produced using previously developed expression systems, strongly limiting its biochemical study (Desir, Wang *et al.*, 2012), this project was initially focused on developing new strategies to increase the yield of recombinant renalase. Attempts to produce human renalase and its mouse homolog using various fusion strategies, as well as to express the human protein in the eukaryotic host *Saccharomyces cerevisiae,* have been carried out.

The solution of the three-dimensional structure of the protein by X-ray crystallography has been another important aim of the project, since such achievement was expected to open the way to the understanding of the catalytic mechanism of the enzyme. After many efforts, in collaboration with Dr. Bolognesi, I finally obtained the crystal structure of human renalase (Milani *et al.*, 2011).

Its general fold classified it as a member of the *p*-hydroxybenzoate hydroxylase protein superfamily, which includes both NAD(P)H-dependent enzymes, as the aromatic monooxygenases, and O_2-dependent ones, catalyzing either monooxygenase or oxidase reactions. For this reason, specific aims of the project were the detailed analysis of the interaction of

renalase with nicotinamide dinucleotides and the study of its reactivity towards O_2, by means of equilibrium, steady-state and rapid reaction kinetic approaches, in order to define the general features of the possible catalytic activity of the protein.

The allelic form of human renalase whose crystal structure was obtained within this project, represents its Asp37 variant. Since a recent study reported that an alternate form, carrying Glu at the same position, had a higher catalytic activity (Farzaneh-Far *et al.*, 2010), I decided to produce the latter isoform by site-directed mutagenesis in order to assess its *in vitro* properties. Indeed, should the supposed functional difference between the allelic variants be confirmed, this would represent an important step towards the localization of renalase NADH binding site, which was not obvious from structural data.

Furthermore, an additional specific aim of the project was to compare the catalytic properties of the spontaneously *in vivo* folded renalase produced in my laboratory with those of the *in vitro* refolded, FAD-reconstituted protein produced by Desir's group, in order to ascertain the source of the reported differences between them, the latter being much more active as a NADH-oxidase.

Finally, during the third year of the PhD program, I started a formal collaboration with Dr. Desir at the Yale School of Medicine, in order to elucidate the subcellular localization of endogenous renalase by immunofluorescence microscopy and cell fractionation approaches. Renalase presents a signal peptide which could mediate the secretion through the classical pathway, but I provided structural evidence suggesting that could not be removed without disrupting protein's native conformation, implying that renalase secretion would occur *via* atypical secretory pathway.

Main Results

The major aim of the project was to provide a detailed functional and structural characterization of renalase, in order to collect new precious details on the biochemical properties of this protein and to obtain a general firm framework for assessing its possible molecular mechanism of action.

The lab where I carried out this work, had previously succeeded in producing recombinant human renalase in *E. coli* as a soluble, correctly folded protein containing an equimolar amount of FAD, thus showing for the first time that renalase is actually a flavoprotein (Pandini *et al.*, 2010). Two recombinant renalase forms were purified to homogeneity exploiting their N-terminal tags (polyHis and polyHis-SUMO tags), obtaining about 1.5 mg of pure protein per liter culture.

With the aim to increase the yield of the recombinant flavoprotein, I first expressed human renalase in *Saccharomices cerevisiae*, since the eukaryotic host could provide a more appropriate environment for the correct folding of the protein. Unfortunately, the amount of soluble renalase produced in yeast was very low and only recovered in apoprotein form. Then, to test the possibility that previously used N-terminal extensions could hamper the correct folding of the recombinant renalase, I produced the protein in *E. coli* as a fusion with a C-terminal polyHis-tag. The new expression/purification system yielded about the same amount of soluble renalase as the previous ones, suggesting the low expression level of the soluble fraction in the heterologous hosts could be an intrinsic property of the protein. Thus, despite representing no improvement in terms of amount of protein obtained (Table 2), the new expression strategies allowed us to demonstrate that the biochemical properties of recombinant human renalase are not affected by

the position of the tag added to facilitate its purification. Moreover, in order to extend our studies to homologs of the human protein, N-terminally GST-fused murine renalase (whose plasmid was kindly provided by Dr. Zhang, Tsinghua University of Beijing) was produced in *E. coli*. Unfortunately, the *in vivo* folding behavior of this protein was similar to that of the human one: the amount of soluble product was very low and the purified protein was found to lack bound FAD.

Interestingly, in contrast with the data reported in literature (Xu *et al.*, 2005), we didn't observe any monoamine oxidase activity associated to any of the purified recombinant renalase.

Table 2. Purification yields of different renalase variants expressed in *E. coli*.

	culture volume (l)	cell yield (g/l)	purified renalase (mg/l)
renalase	12	6	1.5
renalase-His	2	6	1.25
His-renalase	12	6.5	1.5
GSTm-renalase	2	6	1

Though very low, the amount of purified renalase was enough for its structural characterization. In collaboration with Dr. Bolognesi, the three-dimensional structure of recombinant human renalase has been determined by X-ray crystallography (Milani *et al.*, 2011) (Figure 18). Diffraction data were interpreted by the molecular replacement method using the structure of an oxidoreductase from *Pseudomonas siringae* as the starting model. The renalase molecule is monomeric and adopts a compact conformation. It presents two main domains: the FAD binding domain and the putative substrate binding domain. The two domains are bent, forming a wide and

deep cleft at the center of the protein. The FAD cofactor is buried within the protein, except for part of the isoalloxazine ring and it's firmly, but not covalently, bound to the protein through several H-bonds and other contacts. The active site cavity can be roughly divided into two hemispheres: one composed of aromatic amino acids and the other of polar residues, centered on the isoalloxazine ring (Figure 18). The general fold of renalase classifies it as a member of the *p*-hydroxybenzoate hydroxylase superfamily, more similar to MAO- than to D-amino acid oxidase-like enzymes.

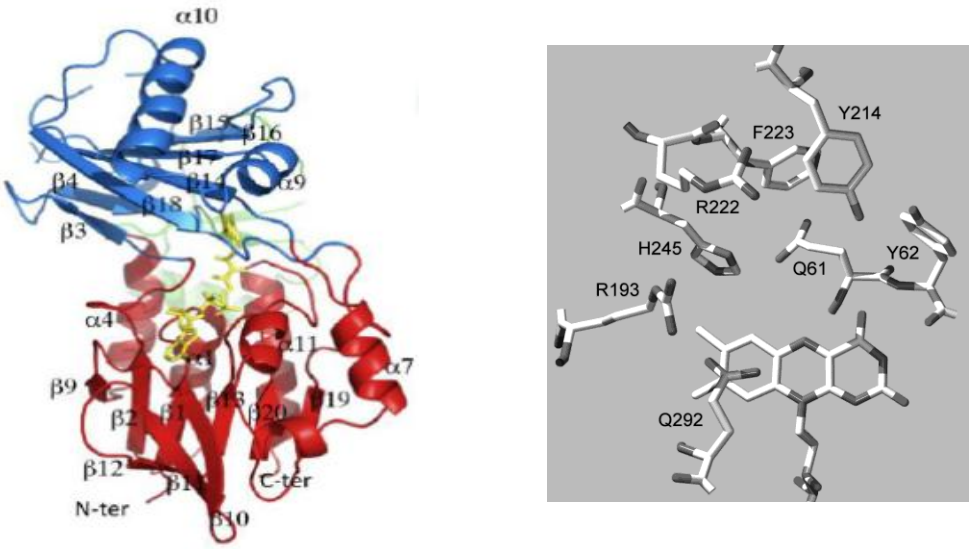

Figure 18. Renalase three-dimensional structure and active site cavity (Milani *et al.*, 2011). Left: The FAD binding domain is shown in red, the substrate binding domain in blue and the 62-108 subdomain in green. Right: the FAD prosthetic group and the amino acid residues lining the active-site cavity are shown.

Since renalase was reported to catalyze O_2 reduction in the presence of NADH, suggesting the possibility that it could be either a dehydrogenase or a monooxygenase, we studied in detail its reactivity towards the nicotinamide dinucleotides. Both the NADH- and NADPH-dependent diaphorase activities of renalase using a tetrazolium salt

(iodonitrotetrazolium, INT) as artificial electron acceptor were tested to verify the hypothesis that renalase could be a NADH-dependent enzyme. Renalase displayed a low but measurable catalytic activity *versus* INT and the steady-state kinetic parameters showed a slight preference for NADH over NADPH (Table 3).

Table 3. Kinetic parameters of renalase for the NADH- and NADPH-dependent INT reductase reactions (Milani *et al.*, 2011).

Cosubstrate	k_{cat} (min^{-1})	K_m (μM)	k_{cat}/K_m (min^{-1} μM^{-1})
NADH	0.14	18	$(7.8\times10^{-3})\pm(1.2\times10^{-3})$
NADPH	0.26	175	$(1.5\times10^{-3})\pm(1.4\times10^{-4})$

The poor reactivity of renalase towards nicotinamide dinucleotides was confirmed by studying under anaerobic conditions the pre-steady state reactions with either NADH or NADPH. Both nucleotides were able to transfer reducing equivalents to the renalase flavin cofactor, with very low apparent first-order constant (Figure 19).

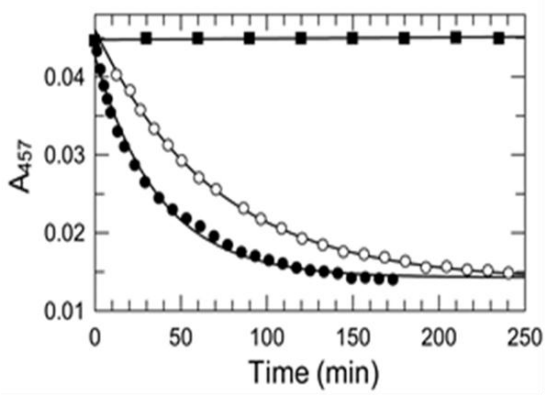

k_{red}^{NADH} (min^{-1})	k_{red}^{NADPH} (min^{-1})
$1.5\times10^{-2}\pm2\times10^{-3}$	$2.7\times10^{-2}\pm1\times10^{-3}$

Figure 19. Time course of anaerobic reduction of renalase FAD cofactor by NADH (open circles) and NADPH (filled circles), control data obtained in the absence of reductant are shown as filled squares (Baroni, Milani *et al.*, 2012).

In order to further investigate the interaction of the protein with nicotinamide dinucleotides, spectrophotometric titrations of the renalase active site with both NAD^+ and $NADP^+$ were performed. Renalase clearly interacted with both the oxidized forms of the dinucleotides, forming complexes whose difference absorption spectra were very similar. Both titrations followed the theoretical curve expected for a 1:1 stoichiometry yielded K_d values for the enzyme-ligand complexes in the millimolar range.

The absence of a recognizable NADP binding site in the protein structure and its poor affinity for, and poor reactivity towards, NADH and NADPH suggest that these are not physiological ligands of renalase.

With the aim of identifying possible renalase substrates, I screened a small library of compounds (Prestwick Chemical Library). More than one thousand small molecules were tested as possible electron donors to the enzyme, using INT as chromogenic electron acceptor. Unfortunately, this preliminary screening identified no renalase substrate.

Since the general fold of renalase classifies it as a member of the flavoprotein superfamily sharing the *p*-hydroxybenzoate hydroxylase fold topology, which includes both oxidases and monooxigenases, the study of the reactivity of the reduced flavin cofactor ($FADH_2$) of renalase with O_2 was performed in order to provide precious information about the nature of the reaction catalyzed by the flavoenzyme (more details in 'Supplemental Results'). After anaerobic stepwise photoreduction in order to completely reduce the bound flavin, renalase was reacted with O_2 by mixing it with different air-equilibrated buffers prepared at diverse pH. The reactions proceeded monotonically in all the conditions tested and no evidence of transient semiquinone and/or peroxide intermediate of flavin was observed. The second-order constant value range from $4.56 \cdot 10^3$ $M^{-1}s^{-1}$ to $10.2 \cdot 10^3$ $M^{-1}s^{-1}$, 20/40-fold higher compared to the free FAD (250 $M^{-1}s^{-1}$), but lower than typical flavin oxidases (10^5-10^6 $M^{-1}s^{-1}$). These results suggested that

renalase might be an oxidase, assuming the presence of not yet known substrate(s) could increase the rate of the reaction to typical oxidases values. The recombinant form of human renalase crystallized and biochemical characterized corresponds to its Asp37 allelic variant. Recently, Farzaneh-Far and coauthors reported that the allelic variant of the protein carrying a Glu residue at position 37 possessed a much higher NADH-dependent activity than the Asp variant. Since this observation, when confirmed, would contribute to assign a catalytic activity to the protein and help in localizing its NAD binding site, I introduced the Asp37Glu replacement in the recombinant protein by site-directed mutagenesis. The steady-state kinetic parameters for both NADH- and NADPH-dependent diaphorase activity *versus* INT were found not significantly different from those of the Asp variant (Table 4).

Table 4. Kinetic parameters of Asp and Glu renalase for the NADH- and NADPH-dependent INT reductase reactions.

	k_{cat}^{NADH} (min^{-1})	K_m^{NADH} (μM)	k_{cat}/K_m^{NADH} (min^{-1} μM^{-1})
Asp37	$0.14 \pm 4 \times 10^{-3}$	18 ± 3	$7.8 \times 10^{-3} \pm 1.2 \times 10^{-3}$
Glu37	$0.19 \pm 8 \times 10^{-2}$	46 ± 10	$4.1 \times 10^{-3} \pm 0.8 \times 10^{-3}$

	k_{cat}^{NADPH} (min^{-1})	K_m^{NADPH} (μM)	k_{cat}/K_m^{NADPH} (min^{-1} μM^{-1})
Asp37	$0.26 \pm 6 \times 10^{-3}$	175 ± 20	$1.5 \times 10^{-3} \pm 1.4 \times 10^{-4}$
Glu37	$0.34 \pm 2.6 \times 10^{-2}$	172 ± 44	$1.9 \times 10^{-3} \pm 6 \times 10^{-4}$

Furthermore, the study of the reductive half-reactions and the $NAD(P)^+$ binding properties of the Glu37 enzyme form confirmed that the two

variants of renalase have indistinguishable features *in vitro*. These data are consistent with the localization of the residue 37 within a surface loop at the interface between the two domains, far from the active site.

In order to ascertain the differences in the catalytic features, I compared the properties of the spontaneously *in vivo* folded recombinant holo-renalase produced in our lab with those of the *in vitro* refolded, FAD-reconstituted protein prepared by Dr. Desir (more details in 'Supplemental Results'). The protein preparation provided by Dr. Desir was found to bound FAD very loosely and lack of the NADH-oxidase activity in the absence of the flavin cofactor added to the assay mixture. A preliminary evaluation of the enzyme specificity, assayed with all possible combinations of NADH or NADPH as the reducing substrate, and FAD, flavin mononucleotide or riboflavin as the electron acceptor, suggested that the flavin compounds behave as substrates of the enzyme rather than prosthetic groups. Interestingly, such catalytic features resulted very similar to those of the *E. coli* flavin reductase (FRE). In collaboration with Dr. Tedeschi, tandem mass spectrometry analysis of the renalase preparation was performed, which confirmed the actual presence of FRE as a major contaminant of the protein solution, strongly suggesting this protein as the responsible of the observed NADH-dependent flavin reductase activity of the *in vitro* refolded renalase sample.

The last part of the project was focused on the subcellular localization of mammalian endogenous renalase through a collaboration with Dr. Desir, at the Yale School of Medicine (more details in 'Supplemental Results'). Indeed, structural evidence has indicated that the proposed secretion signal peptide could not be cleaved without the loss of the protein native conformation, suggesting that renalase trafficking would occur through an atypical secretory pathway. The presence of endogenous renalase was studied by immunofluorescence microscopy in human immortalized HK-2 cells, pig and mouse kidney tissues. Renalase was clearly detected in all the

samples, preferentially localized in the cytoplasm of the cells, where it showed a punctate distribution suggestive of an organelle association. Co-localization approaches with E-cadherin (distal tubule marker) and megalin (proximal tubule marker), performed in pig kidney, demonstrated that renalase is exclusively expressed in proximal tubule (Figure 20).

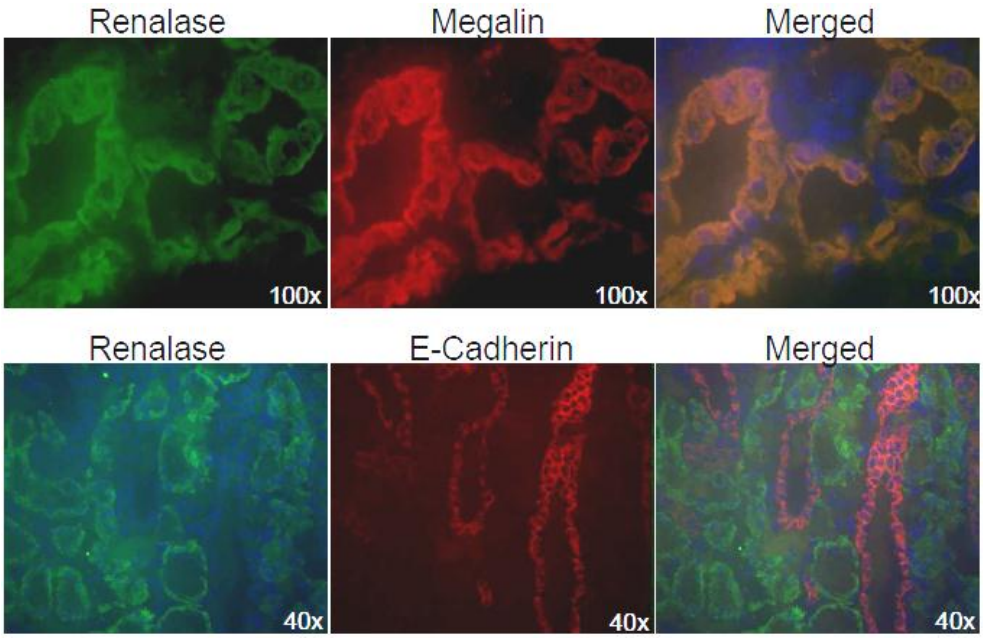

Figure 20. Renalase co-localizes with proximal tubules (Lee *et al.*, 2012 submitted). Pig kidney sections were co-stained with renalase antibody (green) and either with megalin (top) or E-cadherin (bottom). Nuclear staining in blue.

Cell fractionation approach was also used to further investigate the localization of renalase. The protein was found in all the fractions obtained by differential sedimentation, but these preliminary experiments need to be repeated in more stringent conditions because a significant extent of cross-contamination. Moreover, in order to disrupt the possible non-specific binding of renalase to membranes, additional washing step with NaCarbonate on NaCl revealed a possible interaction with integral membrane proteins.

Conclusions and Future Prospects

The important role that renalase seems to play in the control of cardiovascular functions, confirmed by many evidences, has led to a growing interest on this newly discovered protein. However, several questions still remain unanswered, in particular about its catalytic activity.

The major aim of this project was to provide a detailed biochemical and structural characterization of renalase, in order to elucidate the possible reaction it catalyzes and, thus, to better understand the mechanism of its physiological action.

The solution of the crystal structure of recombinant human renalase classifies it as a member of *p*-hydroxybenzoate hydroxylase superfamily (Milani *et al.*, 2011), sharing its general fold with MAO-like enzymes. The functional characterization of the protein, mainly focused on the analysis of its interaction with nicotinamide dinucleotides, confirmed that renalase catalyzes both NADH- and NADPH-dependent diaphorase reactions, as previously reported (Farzaneh-Far *et al.*, 2010). In addition, we provided evidence of direct hydride transfer (HT) from both NADH and NADPH to the enzyme FAD cofactor and of formation of a 1:1 complex with the oxidized forms of the nicotinamide dinucleotides. However, the exceedingly low k_{cat} and k_{cat}/K_m values observed in the steady-state reactions, confirmed by the very slow HT in the reductive half-reaction and the millimolar affinity of the enzyme for both NAD^+ and $NADP^+$, strongly suggest that nicotinamide dinucleotides are not actual renalase physiological substrates. Such conclusion is in line with the absence of an evident NAD(P) binding site in the three-dimensional structure of the protein.

The rapid reaction study of the oxidation of the renalase reduced flavin cofactor by O_2 at different pH values revealed that the reaction proceeded monotonically with no evidence of transient semiquinone and/or peroxide flavin intermediates, thus excluding the transfer of single electrons to O_2. The value of the second-order constant of the process, 20/40-fold higher than that involving free FAD (250 $M^{-1}s^{-1}$) but some order-of-magnitude lower than that observed in typical flavin oxidases, suggested that renalase might be either a lowly efficient oxidase or an aromatic hydroxylase. The latter hypothesis was excluded on the basis of a structural comparison between renalase and flavin monooxygenases belonging to the *p*-hydroxybenzoate hydroxylase superfamily.

Moreover, consistently with structural evidences that show that residue 37 is located in a surface loop far from the active site, we found no difference between the NAD(P)H-dependent diaphorase activities of the Asp and Glu variants of renalase, in contrast with previously reported data (Farzaneh-Far *et al.*, 2010).

We were also able to clarify the origin of the apparent differences in the catalytic properties between the spontaneously *in vivo* folded recombinant holo-renalase produced in our lab and the *in vitro* refolded, FAD-reconstituted protein prepared by Dr. Desir. The biochemical and structural characterization of the latter renalase preparation indicated that the refolded protein, although soluble, is unable to bind FAD with high affinity and, more importantly, that its supposed enzymatic activity was due to the presence in the preparation of significant amount of *E coli* flavin reductase as a contaminant.

Finally, immunofluorescence colocalization studies with E-cadherin and megaline in pig kidney clearly showed that renalase is exclusively localized in the proximal tubule epithelial cells. Furthermore, its subcellular localization, as determined by differential sedimentation, and its

cytoplasmic punctate distribution, observed by immunofluorescence in pig kidney tissue samples, strongly suggested that renalase associates to membrane organelles, which is suggestive of processing through an unconventional secretory pathway.

In conclusion, the detailed biochemical characterization of recombinant human renalase here reported is expected to represent a solid framework on whose basis novel working hypotheses about renalase molecular mechanism could be devised and future new experimental observations could be interpreted. Furthermore, the structural and functional data collected within this project converge in suggesting that renalase could most probably represent a flavin-dependent oxidase acting on a bulk substrate, different from a catecholamine and which has still to be identified. We are confident that with the current exponentially increasing number of research articles published by different research groups on this topic (22 out of the total 51 entries retrieved from PubMed with the keyword “renalase” have 2012 as publication year) the molecular mechanism of renalase will be elucidated soon. The structural information we have obtained, together with the *in vitro* approaches to the functional study of the renalase active site developed within this project, will then be invaluable to exploit renalase and/or the pathway to which it belongs as a target for novel drugs active on the cardiovascular system.

Supplementary Results

Rapid reaction study of renalase flavin cofactor reactivity with O_2

The general fold of renalase classifies it as a member of the flavoprotein superfamily sharing the *p*-hydroxybenzoate hydroxylase fold topology, which includes oxidases and monooxigenases. Both subgroups of enzymes use O_2 as oxidant in their physiological reactions, but while the former produces H_2O_2 without transient formation of flavin intermediates, the latter generates H_2O through the formation of a transient peroxide form of FAD. For this reason, the study of the reaction between reduced flavin cofactor ($FADH_2$) of renalase and O_2 could provide precious information about the nature of the reaction catalyzed by this flavoenzyme.

The FAD prosthetic group of recombinant human renalase was reduced through anaerobic stepwise photoreduction performed using the light/EDTA system. In particular, renalase reduction was achieved by one- electron donation from 5-carba-5-deazariboflavin semiquinone produced by light irradiation, with EDTA serving as the final electron source. Renalase was subjected to successive short periods of illumination until full reduction of the flavin was reached. Absorption spectra were recorded before and after each irradiation.

Reduced renalase was then reacted with O_2 at 25 °C by mixing the anaerobic protein solution with air-equilibrated 100 mM NaPi, 100 mM $Na_4P_2O_7$ buffers adjusted at diverse pH values (in the 5.5-10.5 range). The actual pH final values obtained after mixing, were experimentally determined (Table 5). Renalase and O_2 final concentrations in the reaction mixture were 14 µM and 125 µM, respectively.

nominal pH	5.5	6.5	7.5	8.5	9.5	10.5
actual pH	5.8	6.7	7.7	8.6	9.5	10.3

Table 5. pH values of the reaction mixtures determined before and after the mixing.

The rate of flavin oxidation was measured by monitoring the increase in absorbance at 454 nm (Figure 21). Absorbance values were fitted to the following exponential decay equation:

$$y = A_0 e^{-kt} + offset$$

to obtain rate the constants (Figure 22).

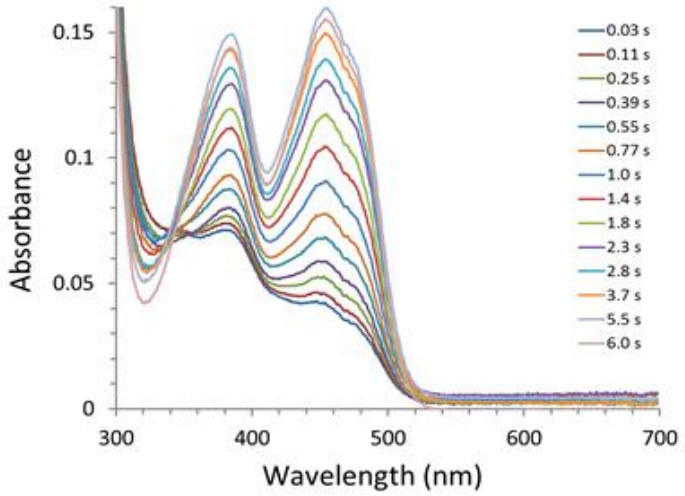

Figure 21. Absorption spectra recorded during the oxidation of the renalase flavin cofactor by O_2 at 25 °C in 100 mM NaPi, 100 mM $Na_4P_2O_7$, pH 10.3.

The reaction proceeded monotonically in all tested conditions with no evidence of transient flavin semiquinone and/or flavin peroxide formation, thus excluding single-electron transfer to O_2. Pseudo-first order constants, determined at different pH, are reported in Table 6 (Figure 23). As shown,

the rate of the process slightly decreases at basic pH values, with a maximum at pH 6.7.

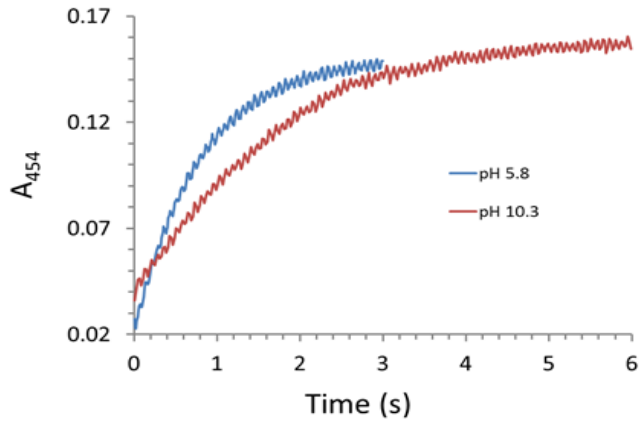

Figure 22. Absorbance traces at 454 nm recorded during the $FADH_2$ oxidation with O_2 by stopped-flow spectrophotometry.

pH	5.8	6.7	7.7	8.6	9.5	10.3
k_{app} (s^{-1})	1.25	1.28	1.02	0.83	0.69	0.57

Table 6. Pseudo-first order constants of $FADH_2$ oxidation at different pH values.

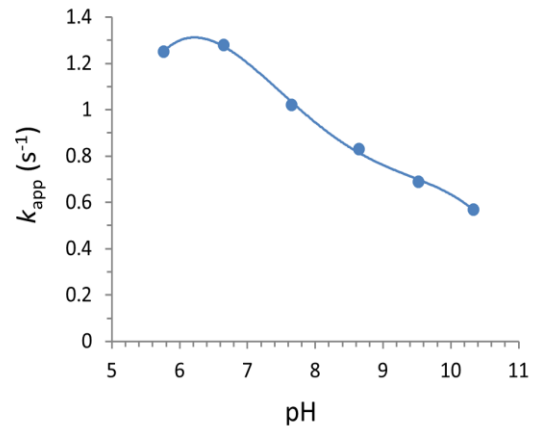

Figure 23. pH dependence of $FADH_2$ oxidation by O_2. Plot of the values of the rate constant of the flavin oxidation as a function of pH (after mixing).

Assuming that the process is bimolecular and considering the oxygen concentration in the reaction mixture, a second order constant value range from $4.56 \cdot 10^3$ $M^{-1}s^{-1}$ to $10.2 \cdot 10^3$ $M^{-1}s^{-1}$ was determined. Such rates are 20/40-fold higher than that reported for free FAD (250 $M^{-1}s^{-1}$), although they are lower than those of typical flavin oxidases (10^5-10^6 $M^{-1}s^{-1}$) (Gadda, 2012; Chaiyen *et al.*, 2012).

Taking into consideration that the binding of the not yet known substrate(s) of renalase could increase the rate of its reaction with O_2, these results suggest that renalase might be an oxidase converting O_2 in H_2O_2 and not a O_2^--producing enzyme, as reported in literature (Farzaneh-Far *et al.*, 2010).

Characterization of recombinant human renalase produced in Desir's lab

Since the catalytic properties of the spontaneously *in vivo* folded renalase produced in our lab markedly differed from those of the *in vitro* refolded, FAD-reconstituted protein produced in Desir's lab (Farzaneh-Far *et al.*, 2010), we received a sample of the latter protein for a detailed biochemical characterization.

The absorption spectrum of the refolded renalase sample revealed the presence of a large amount of free FAD, exceeding the protein molar concentration by a factor of ten.

To remove the FAD excess from the protein solution, the preparation was subjected to gel filtration (Figure 24). In the high molecular weight fraction, containing renalase, FAD was not detectable by spectrophotometry. This result suggested that the FAD cofactor was not steady bound to renalase, and was readily released by the protein during chromatography.

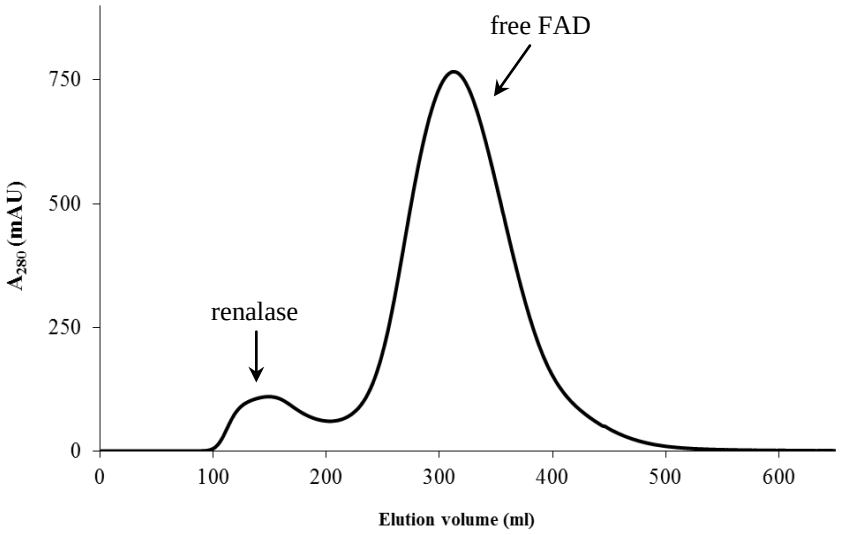

Figure 24. Gel filtration of recombinant human renalase prepared by Dr. Desir.

Furthermore, the protein fraction was found devoid of any NADH-oxidase activity. The activity was almost fully recovered when FAD was included in the assay mixture.

Since the protein preparation was found to be significantly contaminated by several other proteins, in order to improve its purification it was subjected to a chromatographic separation on a column of Ni Sepharose, in which the weak affinity of the protein for the resin was exploited to separate it from the contaminants (Pandini *et al.*, 2010). The spectral and SDS-PAGE analyses of the fractions of the chromatogram revealed the presence of free FAD and contaminants, but very low amount of renalase in the void volume (Figure 25). On the other hand, the fraction containing renalase, eluted at the expected volume, lacked any NADH-oxidase activity. Interestingly, this activity was found associated to the fraction containing free FAD and contaminants.

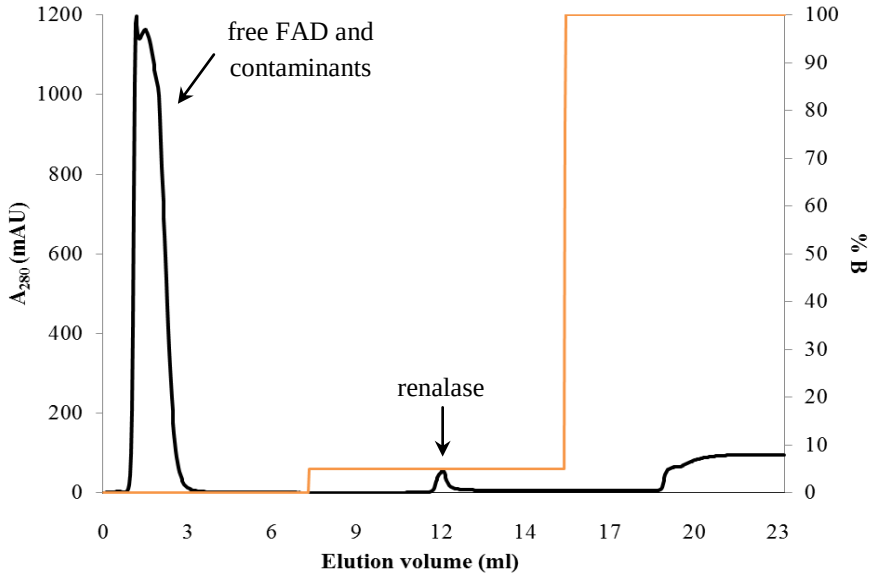

Figure 25. Purification of the renalase produced by Dr. Desir on Ni Sepharose.

To investigate the nature of the FAD-dependent NADH-oxidase activity observed in the renalase preparation produced by Dr. Desir, a preliminary determination of the enzyme specificity was performed with all possible combinations of NADH or NADPH as the reducing substrate, and FAD, flavin mononucleotide (FMN) or riboflavin (Rf) as the electron acceptor. Quite surprisingly, renalase was found able to catalyze the transfer of electrons from either NADH or NADPH to Rf, FMN and FAD (Table 7).

Electron donor substrate	Electron acceptor substrate	K_m (μM)	Vmax (ΔA_{340}/min)
NADH	Rf	0.40	72×10^{-3}
NADH	FMN	0.43	41×10^{-3}
NADH	FAD	0.17	14×10^{-3}
NADPH	Rf	2.7	120×10^{-3}
NADPH	FMN	1.4	21×10^{-3}
NADPH	FAD	n.d.	3×10^{-3}

Table 7. Apparent steady-state kinetic parameters of FAD-stripped Desir's recombinant protein preparation.

The relatively high values of K_m for the flavin derivatives indicated that they behave as substrates rather than prosthetic groups in the observed reaction, suggesting the enzyme catalyzing it could be a NAD(P)H-dependent flavin reductase. Moreover, the observed catalytic properties were surprisingly similar to those of the well-known *E. coli* flavin reductase (FRE) (Fontecave *et al.*, 1987).

In order to test the hypothesis that a contamination by FRE could be responsible of the NADH-dependent activity observed in the renalase preparation produced by Dr. Desir, in collaboration with Dr. Tedeschi the sample was analyzed by tandem mass spectrometry. The material was first subjected to SDS-PAGE to separate its protein components (Figure 26), then four bands in the molecular mass range expected for FRE were cut and

analyzed by mass spectrometry, after trypsin digestion. Interestingly, the amino acid sequences of the peptides analyzed confirmed the presence of FRE as a major component of bands A and B (Figure 27), while bands C and D contained renalase fragments, possible due to its partial degradation.

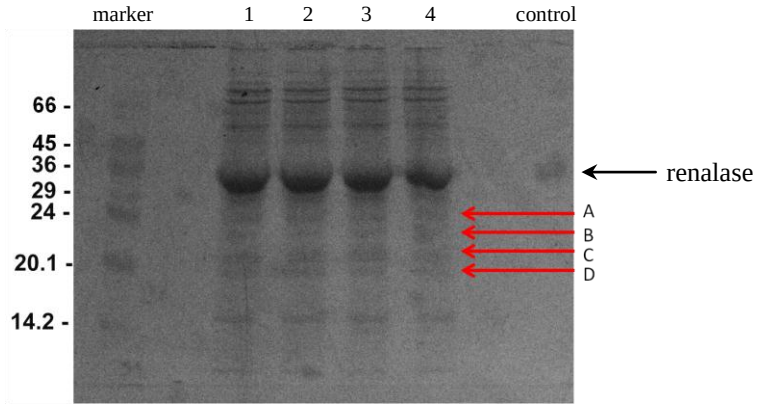

Figure 26. SDS-PAGE analysis of renalase sample prepared by Dr. Desir. Lanes 1-2-3-4, renalase samples after trichloroacetic acid (TCA) precipitation. Control, recombinant human renalase produced in our lab. Red arrows A-B-C-D represent the bands analyzed by peptide mass fingerprinting.

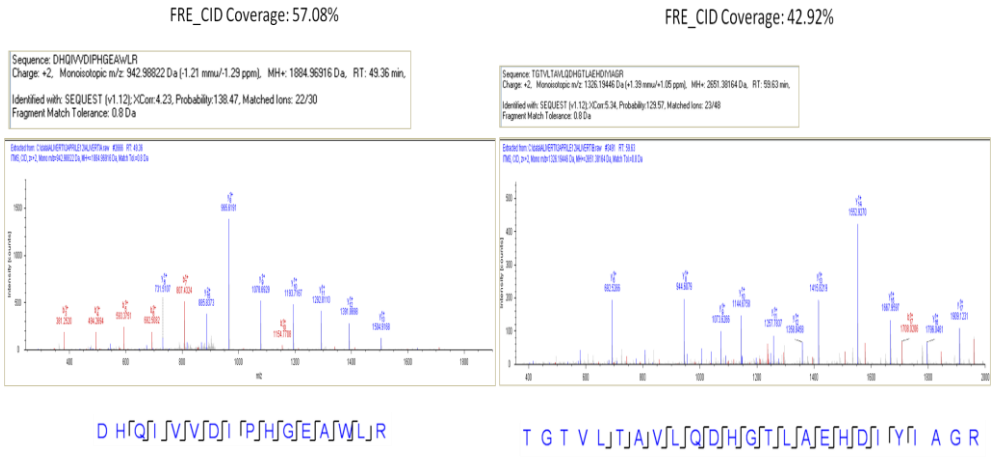

Figure 27. Spectra of the bands A (left) and B (right) obtained by tandem mass spectrometry. The amino acid sequences of the peptides are ascribable to FRE.

Our biochemical and structural characterization indicated that the *in vitro* refolded renalase produced by Dr. Desir doesn't stably bind the FAD cofactor and lacks NADH-dependent oxidase activity. Moreover, our data demonstrated that the NADH-dependent activity of the preparation is attributable to FRE, which was present as a major contaminant.

Tissue and subcellular localization of endogenous mammalian renalase

Renalase has been proposed to be secreted by kidney into the bloodstream and urine in response to stress conditions like hypertension, but the molecular mechanism regulating its basal or stimulated secretion is still unknown (Milani *et al.*, 2011). Structural evidences indicate the proposed secretion signal peptide could not be cleaved without the loss of the protein native conformation, suggesting that renalase trafficking would occur through an atypical secretory pathway.

The localization of endogenous renalase was initially studied by immunofluorescence microscopy in human immortalized HK-2 cells (human kidney 2 is a proximal tubular cell line derived from normal kidney). Monoclonal antibody 28-4, raised in rabbit, was used in combination with Alexa488-goat anti-rabbit secondary antibody. Renalase was clearly detected in the cells and seemed to be preferentially localized in the cytoplasm, where it showed a punctate distribution suggestive of an organelle association (Figure 28).

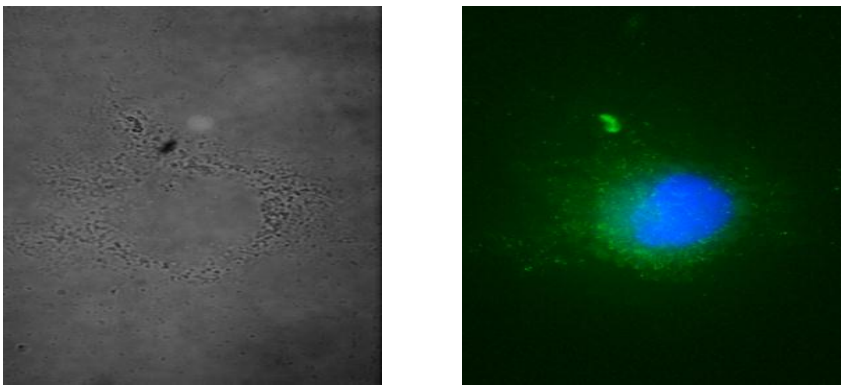

Figure 28. Renalase localization in HK-2 cells. Samples were imaged with a fluorescent microscope and photographed using a SPOT camera software. Left: phase; Right: immunofluorescence. HK-2 cells were stained with a renalase antibody (green). Nuclear staining in blue. Images were magnified 100X.

Similar studies were then performed in pig kidney tissue samples. Two monoclonal antibodies, 28-4 and 37-10 (both raised in rabbit), were used. Renalase localized to renal tubule epithelium, displaying the same punctate distribution observed in HK-2 cells (Figure 29).

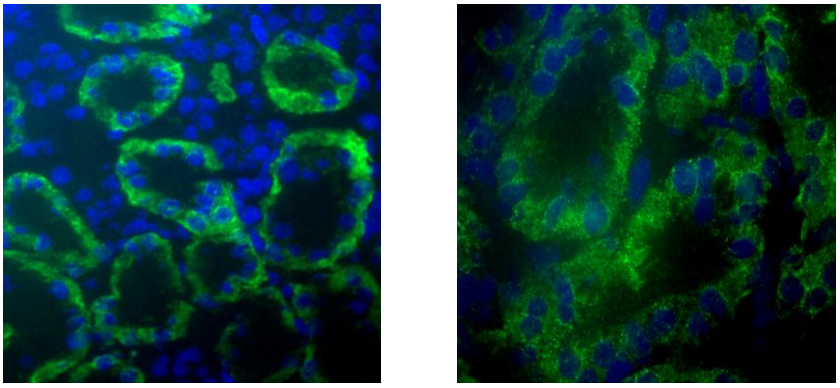

Figure 29. Renalase localization in pig kidney. Pig kidney sections were fixed, permeabilized and incubated with anti-renalase 28-4. Secondary antibody Alexa488-goat anti-rabbit (green) was then applied. Nuclear staining in blue. Left: 40X; Right: 100X.

Moreover, preliminary experiments carried in the absence of detergent suggested that a fraction of renalase could be associated to extracellular surface of plasma membrane (Figure 30).

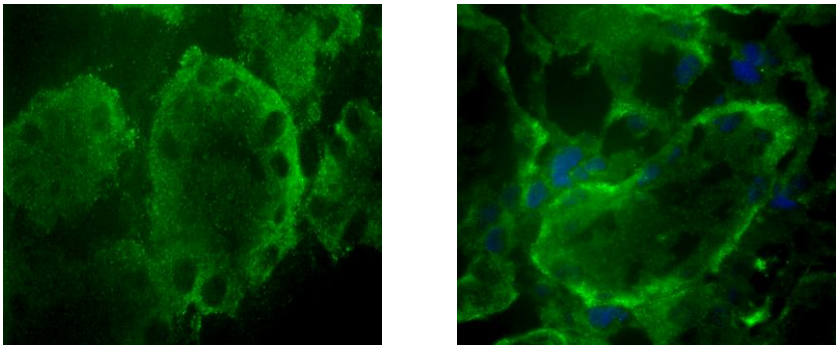

Figure 30. Renalase localization in pig kidney. Left: absence of detergent, 100X. Right: treatment with 0.1% triton X100, 100X. Endogenous renalase in green, nuclear staining in blue.

The same renalase cytoplasmic distribution was observed in mouse renal tubules. Moreover, as expected, no renalase was detected in renalase KO mouse kidney tissue (Figure 31).

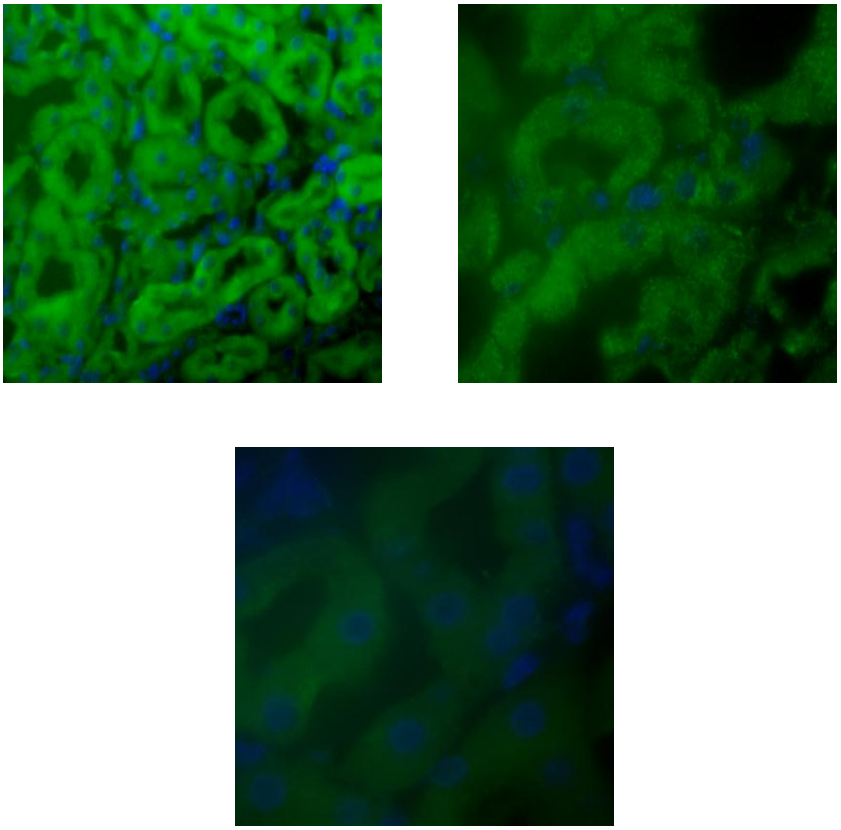

Figure 31. Renalase localization in mouse kidney. Monoclonal 28-4 anti-renalase was used in combination with Alexa488-goat anti-rabbit secondary antibody (green). Left and Right top: endogenous renalase in mouse kidney samples 40X and 100X, respectively. Central bottom: no protein was detected in renalase KO mouse kidney, 100X. Nuclear staining in blue.

In pig kidney, a cell fractionation approach was also used to investigate the localization of endogenous renalase. The centrifugation protocol yielded the following subcellular fractions:

PNS	500x*g*	10 min
P3	3,000x*g*	10 min
P15	15,000x*g*	10 min
P180	180,000x*g*	1 hr
P300	300,000x*g*	1 hr

PNS = heavy membranes, pieces of tissue and cells not disrupted
P3 = heavy lysosomes and mitochondria
P15 = lysosomes and peroxisomes
P180 = microsomes, ER and Golgi
P300 = small vesicles

Initial experiments, carried out by Western blot analysis, revealed the presence of renalase in all the fractions obtained by differential sedimentation (Figure 32). However the analysis of the distribution of several subcellular markers, i.e. calnexin (ER), TGN-38 (Golgi), lamin (nucleus), LC3 (autophagosomes), Lamp2B (lysosomes), Sec31 (ER to Golgi, COPII Coat), Rab7 (late endosomes) and Rab11 (recycling endosomes, mitochondria) revealed a significant extent of cross-contamination. Thus, further fractionation experiments needed to be performed under more stringent conditions.

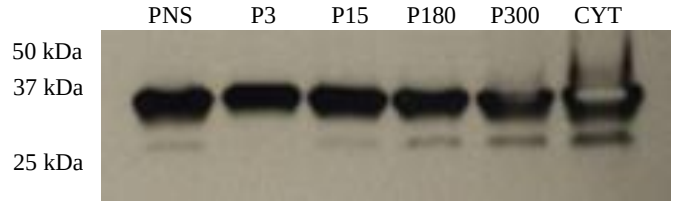

Figure 32. Western blot analysis of pig kidney fractions obtained after different centrifugation steps. Monoclonal 28-4 anti-renalase in combination with HRP-goat anti-rabbit secondary antibody was used to detect endogenous renalase.

In order to disrupt the possible non-specific binding of renalase to membranes, an additional washing step with Na_2CO_3 or NaCl was included. Interestingly, renalase was still present in the P3 fraction after 1 M Na_2CO

treatment (Figure 33), but not after incubation with 2.5 M NaCl, implying a possible specific interaction with integral membrane proteins.

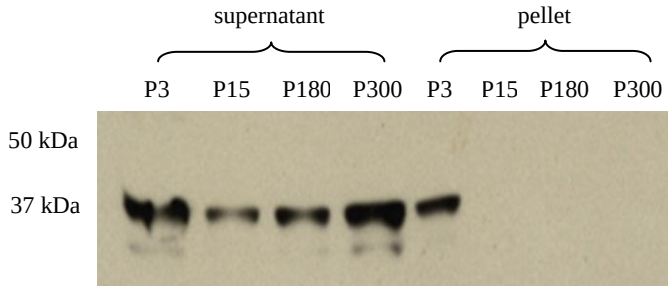

Figure 33. Western blot analysis of pig kidney fractions after 1 M Na_2CO_3 treatment. Monoclonal 28-4 anti-renalase in combination with HRP-goat anti-rabbit secondary antibody was used to detect endogenous renalase.

The subcellular localization of renalase and its cytoplasmic punctate distribution, strongly suggest that the protein could be associated to membranous organelles.

Appendix 2

State of the Art

During the PhD program, I was also involved in a side project focused on the elucidation of the role of the Y258 residue of *Plasmodium falciparum* ferredoxin-NADP$^+$ reductase (PfFNR) in the control of NADPH specificity.

P. falciparum (Figure 34) belongs to the phylum Apicomplexa, which consists of unicellular, obligate intracellular parasites and is responsible for the most deadly form of malaria in humans (Seeber *et al.*, 2008). Besides the nucleus, mitochondrion and endoplasmic reticulum, Apicomplexa exhibit a distinctive 'apical complex' (after which the phylum is named) that has been shown to be required for pathogen survival and represents a known site of action of antimalarial compounds.

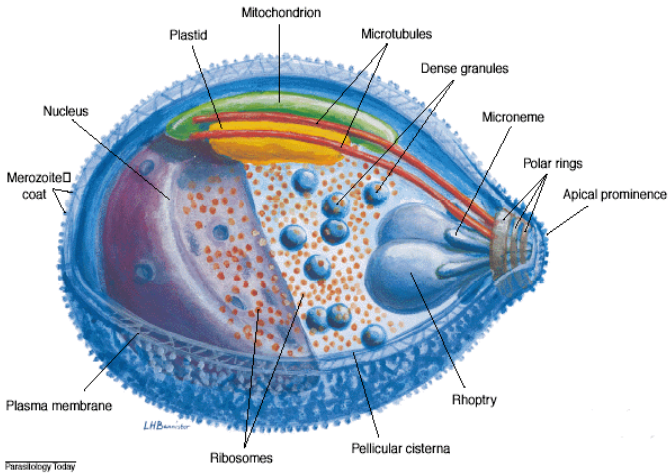

Figure 34. *Plasmodium falciparum* cell structure (Bannister *et al.*, 2003).

In the apicoplast (an organelle of the apical complex) of *P. falciparum* a ferredoxin-NADP$^+$ reductase has been identified. This protein is directly involved in the apicoplast metabolism, since it was demonstrated that the ferredoxin/ferredoxin-NADP$^+$ reductase redox system of *P. falciparum*

serves as the physiological electron donor for LytB, the enzyme that catalyzes the last step of the DOXP pathway of isoprenoids biosynthesis in apicoplast (Rorich *et al.*, 2005).

PfFNR is an enzyme belonging to dehydrogenase electron-transferases class of flavoproteins that contains flavin adenine dinucleotide (FAD) as prosthetic group, which is responsible for the catalytic properties of the holoenzyme. PfFNR is able to catalyze the exchange of reducing equivalents between the $NADP^+$/NADPH and the ferredoxin(Fe^{3+})/ferredoxin (Fe^{2+}) redox couples, in particular it promotes the transfer of two electrons from one molecule of NADPH to two molecules of ferredoxin:

$$2\ Fd(Fe^{3+}) + NADPH \rightleftharpoons 2\ Fd(Fe^{2+}) + NADP^+ + H^+$$

Compared to the typical plastidic FNRs, PfFNR exhibits most of their basic features except for a lower turnover number and a weaker ability to discriminate between NADH and NADPH (Balconi *et al.*, 2009). These functional differences result from critical details about how the plasmodial enzyme binds NADPH 2'-phosphate group (Figure 35).

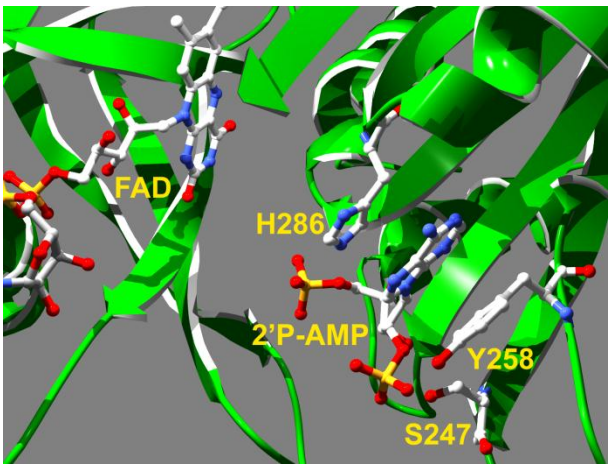

Figure 35. Three-dimensional structure of the PfFNR active site. Part of the cleft between the FAD and NADP binding domains is shown. FAD, the substrate analogue adenosine 2',5'-diphosphate (2'-PAMP), S247, Y258 and H286 are represented as ball-and-stick models.

Aim of the Project

The project was mainly focused on the role of two PfFNR residues that interact with the 2'-phosphate and the pyrophosphate groups of NADPH, Y258 and H286 respectively, in the modulation of the coenzyme specificity of this enzyme. In particular, Y258 provides the second aromatic ring (in addition to H286) to sandwich the adenine moiety of the coenzyme and also donates a H-bond to the 2'-phosphate group of NADPH (Figure 35). For this reason, the replacement of Y258 with a phenylalanine is expected to only disrupt the latter interaction leaving aromatic stacking unaffected.

Main Results

The study of the role of Y258 and H286 in catalysis was carried out by site-directed mutagenesis, generating two PfFNR variants carrying either the single Y258F and the double Y258F/H286Q replacement.

The effect of the mutations on the steady-state kinetic parameters of the PfFNR variants for the NAD(P)H-dependent activity was largely independent from the presence of histidine or glutamine at position 286 (Table 8). In particular, the Y258F replacement abolished the difference between the k_{cat}^{NADPH} and k_{cat}^{NADH} of the single and double mutant. Furthermore, the Y258F mutation had opposite effects on K_m^{NADPH} and K_m^{NADH}, increasing the former and lowering the latter. The combination of these effects led to a 50-fold decrease in the PfFNR specificity ratio and, interestingly, the effect of the two replacements displayed no additivity. Since k_{cat} is related to the rate of hydride transfer (HT) between the nicotinamide dinucleotide and the FAD prosthetic group in the enzyme-

cofactor complex, these data suggested that the Y258 hydroxyl could have an important role in optimizing the HT from NADPH to FAD.

Table 8. Steady-state kinetic parameters of the PfFNR variants for the NADPH- and NADH-$K_3Fe(CN)_6$ reductase reaction (Baroni, Pandini *et al.*, 2012).

PfFNR	k_{cat}^{NADPH} (s^{-1})	K_m^{NADPH} (μM)	k_{cat}/K_m^{NADPH} ($s^{-1}\,\mu M^{-1}$)	k_{cat}^{NADH} (s^{-1})	K_m^{NADH} (μM)	k_{cat}/K_m^{NADH} ($s^{-1}\,\mu M^{-1}$)	NADPH:NADH specificity ratio
wild type	125 ± 4	36 ± 6	3.5 ± 0.5	48 ± 2	720 ± 90	0.05 ± 0.005	70
H286Q	185 ± 3	57 ± 5	3.3 ± 0.3	100 ± 3	715 ± 80	0.15 ± 0.015	22
Y258F	50 ± 0.5	160 ± 16	0.3 ± 0.03	47 ± 1	260 ± 40	0.2 ± 0.04	1.5
Y258F/H286Q	53 ± 0.5	240 ± 17	0.2 ± 0.01	47 ± 1	360 ± 40	0.15 ± 0.015	1.3

The reductive half reaction of the enzyme variants was studied in detail by stopped-flow spectrophotometry, using either NADPH or NADH as reductant. The reaction of PfFNR with the nicotinamide dinucleotides led to the formation of a charge-transfer complex (CT) between NAD(P)H and FAD, observed as an increase in the absorption above 550 nm. The Y258F mutation lowered the k_{HT} for NADPH and abolished the accumulation of CT, without hampering HT from NADH to FAD. The PfFNR-Y258F/H286Q double mutant displayed the same kinetic properties of PfFNR-Y258F, confirming that the effects of the Y258F replacement completely overshadow those of the H286Q one. The k_{HT} values determined by rapid reaction kinetic (Table 9) matched very well the k_{cat} of both NADPH- and NADH-dependent reactions.

Table 9. Rate constants of hydride transfer from NADPH and NADH to FAD in PfFNR variants as determined by stopped-flow spectrophotometry (Baroni, Pandini *et al.*, 2012).

	k_{HT} (s^{-1})	
PfFNR form	NADPH	NADH
wild type	148 ± 2	65 ± 1
H286Q	240 ± 4	125 ± 7
Y258F	74 ± 2	83 ± 1
Y258F/H286Q	70 ± 4	80 ± 2

In order to verify the hypothesis that the decrease in the HT determined by Y258 hydroxyl deletion when NADPH, but not NADH, is the hydride donor might be the result of a destabilization of the catalytically competent conformation of bound NADPH (which in the wild-type enzyme is associated with the transient formation of the CT), both PfFNR variants were subjected to anaerobic photoreductions in the absence and presence of $NADP^+$. Compared to the wild-type, where a long-wavelength absorbing species representing CT was observed, no CT species were detected during the reduction of PfFNR-Y258F or PfFNR-Y258F/H286Q in the presence of $NADP^+$.

The contribution of Y258 to substrate recognition was further investigated by differential spectrometry, since it's well known that the binding of $NADP^+$ by FNRs perturbs the visible absorption spectrum of bound FAD cofactor (Deng *et al.*, 1999). Both PfFNR variants displayed lower affinity for $NADP^+$ in comparison to that of the wild-type form, with higher K_d values of enzyme-$NADP^+$ complexes (Table 10). More importantly, the difference spectra and the values of the differential extinction coefficient at 508 nm revealed that the removal of the Y258 hydroxyl group highly destabilized the nicotinamide-flavin interaction.

Table 10. Dissociation constants of the complex between the PfFNR variants and $NADP^+$, and intensities of the ligand-induced spectral perturbation of bound FAD (Baroni, Pandini *et al.*, 2012).

PfFNR form	K_d (μM)	$\Delta\varepsilon_{508}$ ($mM^{-1}\ cm^{-1}$)
wild type	60 ± 9^a	0.30 ± 0.01
H286Q	130 ± 10^a	1.14 ± 0.04
Y258F	170 ± 30	0.04 ± 0.002
Y258F/H286Q	130 ± 40	0.03 ± 0.002

Conclusions and Future Prospects

These data allowed us to conclude that the Y258 side chain favors the adoption of the catalytically competent conformation of the nicotinamide moiety of NADPH, enhancing the hydride transfer and, therefore, enzyme turnover. Moreover, the hydroxyl of this residue contributes to make the enzyme able to discriminate against NADH by keeping its K_m^{NADH} high.

Although *P. falciparum* FNR is less strictly NADPH-dependent than its homologues, the almost complete abolishment of coenzyme selectivity reported in this study had never been accomplished before through a single mutation.

References

1. Aliverti A., Pandini V., Pennati A., de Rosa M., Zanetti G. (2008). Structural and functional diversity of ferredoxin-$NADP^+$ reductase. *Arch. Biochem. Biophys.* 474, 283-291
2. Aliverti A., Pandini V., Zanetti G. (2004). Domain exchange between isoforms of ferredoxin-$NADP^+$ reductase produces a functional enzyme. *Biochim. Biophys Acta.* 1696, 93-101
3. Balconi E., Pennati A., Crobu D., Pandini V., Cerutti R., Zanetti G., Aliverti A. (2009). The ferredoxin-$NADP^+$ reductase/ferredoxin electron transfer system of *Plasmodium falciparum*. *FEBS J.* 276, 3825-3836
4. Ballou D.P., Entsch B., Cole L.J. (2005) Dynamics involved in catalysis by single-component and two-component flavin-dependent aromatic hydroxylases. *Biochem. Biophys. Res Commun.* 1, 590-598
5. Bannister L.H., Hopkins J.M., Dluzewski A.R., Margos G., Williams I.T., Blackman M.J., Kocken C.H., Thomas A.W., Mitchell G.H. (2003). *Plasmodium falciparum* apical membrane antigen 1 (PfAMA-1) is translocated within micronemes along subpellicular microtubules during merozoite development. *J. Cell Sci.* 116, 3825-3834
6. Baraka A., El Ghotny S. (2012). Cardioprotective effect of renalase in 5/6 nephrectomized rats. *J. Cardiovasc. Pharmacol. Ther.* 17, 412-416
7. Binda C., Newton-Vinson P., Hubalek F., Edmonson D.E., Mattevi A. (2002). Structure of human monoamine oxidase B, a drug target for the treatment of neurological disorders. *Nat. Struct. Biol.* 9, 22-26
8. Boomsma F., Bhaggoe U.M., van der Houwen A.M.B., van der Meiracker A.H. (2003). Plasma semicarbazide-sensitive amine oxidase in human (patho)physiology. *Biochim. Biophys. Acta.* 1647, 48-54

9. Boomsma F., Tipton K.F. (2007). Renalase, a catecholamine-metabolising enzyme? *J. Neural. Transm.* 114, 775-776
10. Buraczynska M., Zukowski P., Buraczynska K., Mozul S., Ksiazek A. (2011). Renalase gene polymorphisms in patients with type 2 diabetes, hypertension and stroke. *Neuromolecular Med.* 13, 321-327
11. Chayien P., Fraaije M.W., Mattevi A. (2012). The enigmatic reaction of flavins with oxygen. *Trends in Biochemical Sciences.* 37, 373-380
12. Cockcroft D.W., Gault M.H. (1976). Prediction of creatinine clearance from serum creatinine. *Nephron.* 16, 31-41
13. De Colibus L., Li M., Binda C., Lustig A., Edmonson D.E., Mattevi A. (2005). Three dimensional structure of human monoamine oxidase A (MAO-A): relation to the structure of rat MAO-A and human MAO-B. *PNAS.* 102, 12684-12689
14. Deng Z., Aliverti A., Zanetti G., Arakaki A.K., Ottado J., Orellano E.G., Calcaterra N.B., Ceccarelli E.A., Carrillo N., Karplus P.A. (1999). A productive $NADP^+$ binding mode of ferredoxin- $NADP^+$ reductase revealed by protein engineering and crystallographic studies. *Nat. Struct. Biol.* 6, 847-853
15. Desir G.V. (2007). Renalase is a novel renal hormone that regulates cardiovascular function. *J. Am. Soc. Hypertens.* 1, 99-103
16. Desir G.V., Li Y., Liu D., Wang P., Xu J., Giordano F. (2007). Downregulation of cardiac renalase expression in CKD, and protective effect of renalase in acute coronary syndrome. (Abstract F-PO206) *J. Am. Soc. Nephrol.* 18:149A
17. Desir G.V. (2008). Renalase deficiency in chronic kidney disease, and its contribution to hypertension and cardiovascular disease. *Curr. Opin. Nephrol. Hypertens.* 17, 181-185
18. Desir G.V., Xu J. (2008). Recombinant renalase. International patent WO 2008039690.

19. Desir G.V. (2009). Regulation of blood pressure and cardiovascular function by renalase. *Kidney Int.* 76, 366-370
20. Desir G.V., Tang L., Wang P., Li G., Velazquez H. (2010). Antihypertensive effect of recombinant renalase in Dahl salt sensitive (DSS) rats. (Abstract SA-PO2781) *J. Am. Soc. Nephrol.* 21:748A
21. Desir G.V., Wang P., Li G., Tang L., Velazquez H. (2010). Renalase belongs to a new class of catecholamines metabolizing enzymes. (Abstract PUB546) *J. Am. Soc. Nephrol.* 21:934A
22. Desir G.V. (2011). Role of renalase in the regulation of blood pressure and the renal dopamine system. *Curr. Opin. Nephrol. Hypertens.* 20, 31-36
23. Desir G.V., Tang L., Wang P., Li G., Sampaio-Maia B., Quelhas-Santos J., Pestana M., Velazquez H. (2012). Renalase lowers ambulatory blood pressure by metabolizing circulating adrenaline. *J. Am. Heart Assoc.* 1 (4), e002634
24. Desir G.V., Wang L., Peixoto A.J. (2012). Human renalase: a rewiew of its biology, function, and implications for hypertension. *J. Am. Soc. Hypertens.* [Epub ahead of print]
25. Ding J.X., Jiang L., Zhang Q.D., Liu W.H. (2009). Expression of renalase in the tubular epithelial cells is correlated with pathological phenotypes and blood pressure in a IgA nephropathy. (Abstract). *NDT Plus.* 2
26. Edmonson D.E., Binda C., Mattevi A. (2004). The FAD binding sites of human monoamine oxidases A and B. *Neurotoxicology.* 25, 63-72
27. Edmonson D.E., Binda C., Mattevi A. (2007). Structural insights into the mechanism of amine oxidation by monoamine oxidases A and B. *Arch. Biochem. Biophys.* 464, 269-276

28. Edmonson D.E., Binda C., Wang J., Upadhyay A.K., Mattevi A. (2009). Molecular and mechanistic properties of the membrane-bound mitochondrial monoamine oxidases. *Biochemistry.* 48, 4220-4230
29. Eikelis N., Hennebry S.C., Lambert G.W., Schlaich M.P. (2011). Does renalase degrade catecholamine? *Kidney Int.* 79, 1380.
30. Farzaneh-Far R., Desir G.V., Na B., Schiller N.B., Whooley M.A. (2010). A functional polymorphism in renalase (Glu37Asp) is associated with cardiac hypertrophy, dysfunction, and ischemia: data from the heart and soul study.
31. Fitzpatrick P.F. (2010). Oxidation of amines by flavoproteins. *Arch. Biochem. Biophys.* 493, 13-25
32. Fontecave M., Eliasson R., Reichard P. (1987). NAD(P)H:flavin oxidoreductase of *Escherichia coli*. A ferric ionic reductase participating in the generation of the free radical of ribonucleotide reductase. *J. Biol. Chem.* 262, 12325-12331
33. Fraaijie M.W., Mattevi A. (2000). Flavoenzymes: diverse catalysis with recurrent features. *TIBS.* 25, 126-132
34. Gadda G. (2012). Oxygen activation in flavoprotein oxidases: the importance of being positive. *Biochemistry.* 51(13), 2662-2669
35. Ghosh S.S., Gehr T.W.B., Sica D.A., Masilamani S., Ghosh S., Wang R., Mc Guire E., Sultan-Qurraie A. (2006). Effect of renalase inhibition on blood pressure. (Abstract TH-PO473J) *J. Am. Soc. Nephrol.* 17:208A
36. Go A.S., Chertow G.M., Fan D., McCulloch C.E., Hsu C.Y. (2004). Chronic kidney disease and the risk of death, cardiovascular events, and hospitalization. *N. Engl. J. Med.* 351, 1296-1305
37. Go A.S., Lo J.C. (2006). Epidemiology of non-dialysis requiring chronic kidney disease and cardiovascular disease. *Curr. Opin. Nephrol. Hypertens.* 15,296-302

38. Gu R., Lu W., Xie J., Bai J., Xu B. (2011). Renalase deficiency in heart failure model of rats – a potential mechanism underlying circulating norepinephrine accumulation. *PLoS One.* 6, e14633
39. Hennebry S.C., Eikelis N., Socratous F., Desir G.V., Lambert G., Schlaich M. (2010). Renalase, a novel soluble FAD-dependent protein, is synthesized in the brain and peripheral nerves. *Mol. Psychiatry.* 15, 234-236
40. Hynson R.M., Kelly S.M., Price N.C., Ramsay R.R. (2004). Conformational changes in monoamine oxidase A in response to ligand binding or reduction. *Biochim. Biophys. Acta.* 1672, 60-66
41. Kitamura M., Sagara T., Taniguchi M., Ashida M., Ezoe K., Kohno K., Kojima S., Ozawa K., Akutsu H., Kumagai I., Nakaya T. (1998). Cloning and expression of the gene encoding flavodoxin from *Desulfovibrio vulgaris*. *J. Biochem.* 123, 891-898
42. Koomans H.A., Blankestijn P.J., Joles J.A. (2004). Sympathetic hyperactivity in chronic renal failure: a wake-up call. *J. Am. Soc. Nephrol.* 15, 524-537
43. Joles J.A., Koomans H.A. (2004). Causes and consequences of increased sympathetic activity in renal disease. *Hypertension.* 43, 699-706
44. Joosten V., van Berkel W.J.H. (2007). Flavoenzymes. *Curr. Opin. Chem. Biol.* 11, 195-202
45. Levey A.S., Coresh J., Balk E., Kausz A.T., Levin A., Steffes M.W., Hogg R.J, Perrone R.D., Lau J., Eknoyan G. (2003). National Kidney Foundation practice guidelines for chronic kidney disease: evaluation, classification, and stratification. *Ann. Inter. Med.* 139, 137-147
46. Li G., Xu J., Wang P., Velazquez H., Li Y., Wu Y., Desir G.V. (2008). Catecholamines regulate the activity, secretion and synthesis of renalase. *Circulation.* 117, 1277-1282

47. Li M., Hubalek F., Newton-Vinson P., Edmonson D.E. (2002). High level expression of human liver monoamine oxidase A in *Pichia pastoris*: comparison with the enzyme expressed in *Saccharomyces cerevisiae*. *Protein expr. Purif.* 24, 152-162
48. Malyszko J., Zbroch E., Malyszko J.S., Koc-Zorawska E., Mysliwiec M. (2011) Renalase, a novel regulator of blood pressure, is predicted by kidney function in renal transplant recipients. *Transplantation Proceedings.* 43, 3004-3007
49. Massey V. (1995). Introduction: flavoprotein structure and mechanism. *FASEB J.* 9, 473-475
50. Massey V. (2000). The chemical and biological versatility of riboflavin. *Biochem. Soc. Trans.* 28, 283-296
51. Medvedev A.E., Veselovsky A.V., Fedchenko V.I. (2010). Renalase, a new secretory enzyme responsible for selective degradation of catecholamines: achievements and unsolved problems. *Biochemistry (Mosc).* 75, 951-958
52. Milani M., Balconi E., Aliverti A., Mastrangelo E., Seeber F., Bolognesi M., Zanetti G. (2007). Ferredoxin-$NADP^+$ reductase from *Plasmodium falciparum* undergoes $NADP^+$-dependent dimerization and inactivation: functional and crystallographic analysis. *J. Mol. Biol.* 367, 501-513.
53. Nickel W. (2010). Pathways of unconventional protein secretion. *Curr. Opin. Biotech.* 21, 621-626
54. Nickel W., Rabouille C. (2009). Mechanisms of regulated unconventional protein secretion. *Nat. Rev. Mol. Cell Biol.* 10, 148-155
55. O'Seaghdha C.M., Lyass A., Massaro J.M., Meigs J.B., Coresh J., D'Agostino R.B., Astor B.C., Fox C.S. (2012). A risk score for chronic kidney disease in the general population. *Am. J. Med.* 125, 270-277

56. Oberg B.P., McMenamin E., Lucas F.L., McMonagle E., Morrow J., Ikizler T.A., Himmelfarb J. (2004). Increased prevalence of oxidant stress and inflammation in patients with moderate to severe chronic kidney disease. *Kidney Int.* 65, 1009-1016
57. Pandini V., Ciriello F., Tedeschi G., Rossoni G., Zanetti G., Aliverti A. (2010). Synthesis of human renalase1 in *Escherichia coli* and its purification as a FAD-containing holoprotein. *Protein Expr. Pur.* 72, 244-253
58. Park J. (2012). Cardiovascular risk in chronic kidney disease: role of the sympathetic nervous system. *Cardiol. Res. Pract.* 2012: 319432
59. Pfeffer S.R. (2010). Unconventional secretion by autophagosome exocytosis. *J. Cell. Bio.* 4, 451-452
60. Przybylowski P., Malyszko J., Kozlowska S., Koc-Zorawska E., Mysliwiec M. (2011). Serum renalase depends on kidney function but not on blood pressure in heart transplant recipients. *Transplant Proc.* 43, 3888-3891
61. Quelhas-Santos J., Sampaio-Maia B., Simões-Silva L., Fernades-Cerquieira C., Pestana M. (2010). High-salt diet further decreases renal, cardiac and plasma renalase levels in a chronic kidney disease rat model. (Abstract SA017) *NDT Plus.* 3:32
62. Quelhas-Santos J., Serrao P., Soares-Silva I., Tang L., Sampaio-Maia B., Desir G.V. (2012). Effects of recombinant renalase on renal dopamine activity in the renalase knock out mouse model. (Abstract FP069) *NDT*. 27, 86
63. Rodriguez-Iturbe B., Correa-Rotter R. (2010). Cardiovascular risk factors and prevention of cardiovascular disease in patients with chronic renal disease. *Expert Opin. Pharmacother.* 11, 2687-2698

64. Röhrich R.C., Englert N., Troschke K., Reichenberg A., Hintz M., Seeber F., Balconi E., Aliverti A., Zanetti G., Köhler U., Pfeiffer M., Beck E., Jomaa H., Wiesner J. (2005). Reconstitution of an apicoplast-localized electron transfer pathway involved in the isoprenoid biosynthesis of *Plasmodium falciparum*. *FEBS Lett*. 579, 643-648
65. Schäfer T., Zentgraf H., Zehe C., Brügger B., Bernhagen J., Nickel W. (2004). Unconventional secretion of fibroblast growth factor 2 is mediated by direct translocation across the plasma membrane of mammalian cells. *J. Biol. Chem.* 279, 6244-6251
66. Schreuder H.A., Prick P.A, Wierenga R.K., Vriend G., Wilson K.S., Hol W.G., Drenth J. (1989). Crystal structure of the *p*-hydroxybenzoate hydroxylase-substrate complex refined at 1.9 Å resolution. Analysis of the enzyme-substrate and enzyme-product complexes. *J. Mol. Biol.* 208, 679-696
67. Seeber F., Limenitakis J., Soldati-Favre D. (2008). Apicomplexan mitochondrial metabolism: a story of gains, losses and retentions. *Trends Parasitol.* 24, 468-478
68. Setini A., Petrucci F., Senatori O., Nicotra A. (2005). Molecular characterization of monoamine oxidase in zebrafish (*Danio rerio*). *Comp. Biochem. Physiol. B Biochem. Mol. Biol.* 140, 153-161
69. Son S.Y., Ma J., Kondou Y., Yoshimura M., Yamashita E., Tsukihara T. (2008). Structure of human monoamine oxidase A at 2.2 Å resolution the control of opening the entry for substrates/inhibitors. *PNAS.* 105, 5739-5744
70. Stec A., Semczuk A., Furmaga J., Ksiazek A., Buraczynska M. (2011). Polymorphism of the renalase gene in end-stage renal disease patients affected by hypertension. *Nephrol. Dial. Transplant.* 0, 1-4
71. Strausberg R.L., Feingold E.A., Klausner R.D., Collins F.S. (1999). The mammalian gene collection. *Science.* 286, 455-457

72. Wang F., Wang N.S, Xing T., Cao Y, Xiang H.Y. (2009).The cloning and expression of renalase and the preparation of its monoclonal antibody. *J. Shanghai Jiaotong Univ.* 14, 376-379
73. Wang F., Wang N.S. Xing T. (2010). Construction of eukaryotic recombinant vector of renalase and its expression as a eukaryotic protein. *J. Shanghai Jiaotong Univ.* 15, 637-640
74. Wang F., Xing T., Wang N. (2011) Construction and DNA immunization of human renalase eukaryotic expression vector. *NDT Plus.* 4:221
75. Wang F., Xing T., Li J., Bai M., Hu R., Zhao Z., Tian S., Zhang Z., Wang N. (2012). Renalase's expression and distribution in renal tissue and cells. *PLoS One.* 10, e46442
76. Wang J., Qi S., Cheng W., Li L., Wang F., Li Y.Z., Zhang S.P. (2008). Identification, expression and tissue distribution of a renalase homologue from mouse. *Mol. Biol. Rep.* 35, 613-620
77. Wu Y., Xu J., Velazquez H., Wang P., Li G., Liu D., Sampaio-Maia B., Quelhas-Santos J., Russell K., Russell R., Flavell R.A., Pestana M., Giordano F., Desir G.V. (2011). Renalase deficiency aggravates ischemic myocardial damage. *Kidney Int.* 79, 853-860
78. Xu J., Li G., Wang P., Velazquez H., Yao X., Li Y., Wu Y., Peixoto A., Crowley S., Desir G.V. (2005). Renalase is a novel, soluble monoamine oxidase that regulates cardiac function and blood pressure. *J. Clin. Invest.* 115, 1275-1280
79. Xu J., Desir G.V. (2007). Renalase, a new renal hormone: its role in health and disease. *Curr. Opin. Nephrol. Hypertens.* 16, 373-378
80. Zhao Q., Fan Z., He J., Chen S., Li H., Zhang P., Wang L., Hu D., Huang J., Qiang B., Gu. (2007). Renalase gene is a novel susceptibility gene for essential hypertension: a two-stage association study in northern Han Chinese population. *J. Mol. Med.* 85, 877-885

Send Orders of Reprints at reprints@benthamscience.org

Current Pharmaceutical Design, **2013**, *19*, 000-000

Is Renalase a Novel Player in Catecholaminergic Signaling? The Mystery of the Catalytic Activity of an Intriguing New Flavoenzyme

Sara Baroni[1], Mario Milani[2], Vittorio Pandini[1], Giulio Pavesi[1], David Horner[1] and Alessandro Aliverti[1,*]

[1]*Dipartimento di Bioscienze, Università degli Studi di Milano, via Celoria 26, 20133 Milano, Italy;* [2]*CNR-Istituto di Biofisica, Università degli Studi di Milano, via Celoria 26, 20133 Milano, Italy*

Abstract: Renalase is a flavoprotein recently discovered in humans, preferentially expressed in the proximal tubules of the kidney and secreted in blood and urine. It is highly conserved in vertebrates, with homologs identified in eukaryotic and prokaryotic organisms. Several genetic, epidemiological, clinical and experimental studies show that renalase plays a role in the modulation of the functions of the cardiovascular system, being particularly active in decreasing the catecholaminergic tone, in lowering blood pressure and in exerting a protective action against myocardial ischemic damage. Deficient renalase synthesis might be the cause of the high occurrence of hypertension and adverse cardiac events in kidney disease patients. Very recently, recombinant human renalase has been structurally and functionally characterized *in vitro*. Results show that it belongs to the *p*-hydroxybenzoate hydroxylase structural family of flavoenzymes, contains non-covalently bound FAD with redox features suggestive of a dehydrogenase activity, and is not a catecholamine-degrading enzyme, either through oxidase or NAD(P)H-dependent monooxygenase reactions. The biochemical data now available will hopefully provide the basis for a systematic and rational quest toward the identification of the reaction catalyzed by renalase and of the molecular mechanism of its physiological action, which in turn are expected to favor the development of novel therapeutic tools for the treatment of kidney and cardiovascular diseases.

Keywords: Chronic kidney disease, end-stage renal disease, blood pressure, myocardial ischemia, sympathetic nervous system, catecholamines, oxidoreductase, nicotinamide dinucleotides.

1. INTRODUCTION

Renalase was discovered in 2005, through an *in silico* screen of the human genome aimed at identifying genes encoding previously uncharacterized proteins, predicted to be soluble and secreted, which yielded, among others, a gene preferentially expressed in the kidneys [1]. The hypothesis underlying this effort was that kidney endocrine functions possibly included still unknown signaling proteins [2-7]. Over the last six years, an increasing amount of clinical and experimental evidence has been accumulating supporting the idea that renalase is a primary player in the pathogenesis of the cardiovascular events that usually follow renal dysfunctions. While the link between renalase and the pathophysiology of the cardiovascular system seems now to be clear, the molecular mechanism underlying its actions is still obscure in most respects. Several excellent reviews have recently been published on the consequences of renalase deficiency in diabetes, hypertension, cardiac hypertrophy, myocardial ischemia, and stroke [8-13]. This article will mainly focus on the molecular and biochemical properties of mammalian renalase through a critical survey of the often contradictory results published to date on the possible catalytic properties of this protein, with the purpose of discriminating between solid achievements and the many inconsistent observations.

2. THE DISCOVERY OF RENALASE

Renalase was identified in 2005 by the research team of Gary V. Desir [1], and the story of its discovery is an instructive demonstration of the power of a rationally-designed data mining strategy in the post-genomic era [2,3]. The seminal idea that prompted the search of a still unknown signaling protein released by the kidneys was that traditional pathophysiological mechanisms were insufficient to fully account for the increased risk of cardiovascular adverse events in patients with chronic kidney disease [4,5,14]. Indeed, besides eliminating waste products and maintaining water and electrolyte homeostasis, the kidney also exerts well known endocrine functions (*e.g.* it secretes erythropoietin and calcitriol) and plays a pivotal role in the renin-angiotensin-aldosterone system by releasing the proteinase renin. However, in end stage renal disease, replacement therapy and renal transplant fail to fully restore the functions of the natural organ. Thus, Desir and coworkers concluded that it would be no surprise that "the current endocrine function of kidney was incomplete and that the organ might secrete additional proteins with important biological roles" [1]. To identify them, the Mammalian Gene Collection Project database was screened *in silico* for cDNA encoding proteins predicted to possess these three features: to be uncharacterized, to have a signal peptide for secretion and to lack transmembrane segments. This *a priori* selection yielded 114 hits out of 12,563 distinct open reading frames considered [1]. The candidate genes were then experimentally validated by Northern blot analysis and observing the actual secretion of their products. Just one open reading frame survived these *a posteriori* criteria, showing a robust expression in the kidney and producing a protein secreted in the medium when transiently expressed in mammalian cultured cells. Finally, the gene product, named renalase by its discoverers, was found in blood plasma and urine of healthy individuals. To date, various research groups have confirmed the presence of renalase in plasma, and solid evidence has accumulated that circulating renalase predominantly originates from the kidneys. However, its discovery has been at least partly serendipitous, since renalase tissue distribution is much wider than initially reported (see Chapter 4), and the peptide originally predicted to represent a secretion signal probably does not serve this role (see Chapter 6).

3. STRUCTURE OF THE RENALASE GENE

The human renalase gene (gene symbol: *RNLS*, formerly *C10orf59*) spans about 300,000 nucleotides from position 90,043,859 to 90,343,082 of the minus strand of chromosome 10 at q23.33. Mapping full-length cDNA sequences to the genome identifies eleven exons, which encode different splicing variants of the pro-

*Address correspondence to this author at the Dipartimento di Bioscienze, Università degli Studi di Milano, via Celoria 26, 20133 Milano, Italy; Tel: +39 0250314897; Fax: +39 0250314895;
E-mail: alessandro.aliverti@unimi.it

1381-6128/13 $58.00+.00

tein (Fig. 1). The main isoform (renalase 1, NP_001026879) is composed of 342 residues, with a theoretical molecular mass of 37,847 Da [7,8,15]. The orthologous mouse gene is annotated on chromosome 19C1 [16] and, as detailed in Chapter 7.1, it has been recently inactivated by homologous recombination, providing important experimental clues about its role in the modulation of the cardiovascular system [8,17].

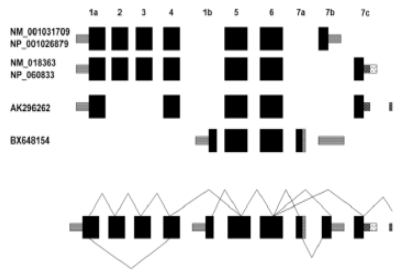

Fig. (1). Schematic representation of the structure of the human renalase gene and its major expression products. The schematic intron/exon organization of the known splicing variants of the *RNLS* transcripts is shown. On the right, the deduced amino acid sequence of the *RNLS* exons is reported.

The renalase gene and its main protein product are highly conserved in vertebrates, with amino acid sequence identity above 60% [7,16]. The evident homology between renalase and the vertebrate monoamine oxidase (MAO) A and B genes [1,15] (as well as the intermittent use of the term MAO C to describe the renalase gene product [16]) implicitly suggest a close evolutionary relationship between these three genes. However, neither comparative genomic nor phylogenetic analyses lend support to this hypothesis. The human MAO genes show high levels of overall colinearity and similarity to a family of prokaryotic MAOs (typified by the *aofH* flavin-containing MAO gene product of *Mycobacterium tuberculosis* H37Rv over 85% of its length). Renalase however, shares extensive colinearity with members of a distinct and widely distributed FAD dependent oxidoreductase family (*e.g.* 27% identity and 46% similarity with *Cyanothece* sp. ADN1670 over 95% of its length). Indeed, the human MAO A and renalase protein sequences share only 38% identity in the 10% of the renalase sequence that aligns well with the human MAO A polypeptide. These observations immediately suggest that, rather than deriving from a eukaryotic specific gene duplication, the ancestor of the MAO genes on one hand and renalase on the other were independently acquired by eukaryotes from prokaryotic forbearers.

Unfortunately, contemporaneous, cross kingdom phylogenetic analyses of MAO-like and renalase-like genes are impossible due to low numbers of unambiguously aligned residues. However, MAO-like genes are found in mycetozoa, many fungi, plants and some protists. Among non-metazoan eukaryotes, gene products displaying overall similarity with renalase are observed in plants and some stramenopiles but not in fungi (although the N-terminal region of renalase shows significant similarity to portions of fungal prenylcysteine lyase proteins). Phylogenetic reconstructions of selected MAO-like protein sequences lend moderate support to the monophyly of eukaryotic genes, but fail to identify a well-supported prokaryotic sister group, suggesting that such genes have been present within eukaryotes since their origin, but not affording insight into the nature of their prokaryotic donor. The evolutionary history of eukaryotic renalase genes is even less clear, with animal, plant and oomycete genes potentially deriving from independent acquisitions from prokaryotes. In any case, these considerations indicate that inferences regarding the role of renalase should be derived from studies of MAOs only with great caution as these amine-oxidase-like subfamilies are only distantly related to one another (not shown).

4. RENALASE ISOFORMS AND GENE EXPRESSION PATTERN

Different mRNA transcripts of *RNLS* have been detected and sequenced, highlighting the existence of protein variants originating from alternative splicing [8,18,19]. Besides the aforementioned renalase1 (NP_001026879), a second annotated protein isoform exists (renalase 2, NP_060833), with a slightly shorter polypeptide chain (315 residues) and a different sequence in its C-terminal region. The other two characterized *RNLS* transcripts (AK296262 and BX648154) encode much shorter deduced polypeptides (233 and 138, respectively). The comparison of the primary structures of the alternatively spliced renalase isoforms in the light of the crystal structure of renalase 1 [20] suggests that, while renalase 2 would probably be a compact globular protein similar to its larger isoform, the other two polypeptides would be unlikely to yield flavin-containing proteins, since they lack essential structural elements for FAD binding (see Chapter 6). Thus, the potential physiological significance of such shortest variants is uncertain. In the case of the mouse orthologous gene, two transcript isoforms are annotated: the first (NM_001146342) has intron-exon structure identical to human NP_001026879 and its translation product has been partly characterized [16]; the second lacks exons 2 and 3 (as does human transcript AK296262) (see Fig. 1), but encodes a protein whose deduced C-terminal region is identical to that of NP_001026879. This suggests that isoform sampling in human tissues is still incomplete, and further alternative transcripts might exist.

In the most comprehensive study on the pattern of *RNLS* expression published so far, autoptic human tissues samples known to express MAOs have been analyzed both by immunoblotting using an anti-renalase monoclonal antibody and by reverse transcriptase polymerase chain reaction [19]. In addition to kidney and myocardium [1], renalase was found in forearm vein and artery, renal vein and artery, ureter, median nerve, hypothalamus, pons, medulla oblongata, cerebellum, pituitary grand, cortex, and spinal cord [19]. In the kidneys, renalase was shown to be present in glomeruli and proximal tubules [1]. Widespread transcription of the human relanase gene is also confirmed by microarray data [21] and Whole Transcriptome Next-Generation Sequencing (RNA-Seq) [22]. Renalase 1 is the only isoform apparently detected in blood plasma and urine and it represents the major isoform in all tissues tested (kidney, heart, skeletal muscle, liver, testicle, hypothalamus, adrenal gland) [1,19]. Transcripts encoding renalase 2 and the two shortest variants (AK296262 and BX648154), although at lower levels than renalase 1 mRNA, were observed in all samples examined, while no renalase 2 transcript was detected in the hypothalamus [19]. A renalase concentration of 0.1 mg per gram wet tissue has been estimated in the kidneys by immunoblotting [10]. Data on the absolute concentration of renalase in human blood plasma have been explicitly reported only recently, as determined by ELISA, showing that it is about 4 μg/ml in healthy individuals, corresponding to 0.1 μM [23-28]. Murine renalase gene expression was observed by reverse transcriptase PCR in kidney, testicle, liver, heart, 12.5-days whole embryo, brain, and skeletal muscle [16].

Several hundred single nucleotide polymorphisms (SNPs) of *RNLS* are known, most of which are located in the flanking regions, within the introns or the untranslated regions of the gene and thus do not result in missense mutations, although they could possibly affect gene expression and mRNA splicing. The twenty-four SNPs resulting in amino acid replacements are shown in Table 1. Interestingly, most of the mutated residues are located on the molecular surface of renalase 1, at sites where the replacements are expected to have little impact on protein conformational stability. Several of

Table 1. Known Single Nucleotide Polymorphisms of the Renalase Gene that Result in Protein Amino acyl Substitutions

SNP accession no.	Experimental evidence[a]	Exon no.[a]	Base change	Amino acyl replacement
rs2296545	genomic	1a	C/G	Asp37/Glu37
rs147588689	cDNA	2	A/G	Arg75/Cys75
rs143513862	cDNA	3	C/T	Val85/Ile85
rs79981780	cDNA	3	C/T	Ile93/Val93
rs149825485	cDNA	3	C/G	Asp102/Glu102
rs140158928	cDNA	3	A/G	Ile111/Thr111
rs139294588	genomic	4	C/G	Gln134/His134
rs146646870	cDNA	4	C/T	Glu143/Lys143
rs77594193	genomic	4	A/G	Pro151/Leu151
rs41317260	genomic	4	A/C	Met161/Ile161
rs78525460	cDNA	5	G/T	Gln181/Lys181
rs112858030	genomic	5	A/G	Ser191/Phe191
rs183742907	genomic	5	A/C	Ala195/Ser195
rs116376263	cDNA	5	A/T	Asp207/Glu207
rs151245420	cDNA	5	C/T	Ser217/Gly217
rs191733133	genomic	5	C/T	Arg222/His222
rs188639368	genomic	5	A/G	Ile226/Thr226
rs143744963	genomic	5	C/T	Ile226/Val226
rs117446494	cDNA	5	C/T	Asn232/Ser232
rs148749882	cDNA	6	A/G	Ser235/Pro235
rs149300466	cDNA	6	A/G	Pro240/Ser240
rs138921267	cDNA	6	C/T	Val243/Met243
rs146268123	cDNA	6	A/G	Phe250/Leu250
rs148477675	cDNA	7b	A/G	Ala310/Val310

[a] Exon numbering as shown in Fig. 1.

the SNPs mapping in the interior of the renalase molecule maintain the hydrophobic character of the residue side chain, with the exceptions of Ile111Thr, Ala195Ser, Ile226Thr and Pro240Ser. The only allelic variant involving a residue interacting with FAD carries the Met161Ile replacement, in which the substitution of the side chain, which stacks on the FAD adenine ring, does not seem to put at risk the binding of the cofactor. As reported in Chapter 7.3, for a few *RNLS* SNPs (listed in Table **2**) the possible association of a specific allele or genotype to some pathological conditions has been studied (see Chapter 7.3).

Bioinformatics analysis, physiological and clinical evidence, and experimental data indicate that renalase is at least partially secreted. First of all, as mentioned above, renalase 1 was detected in body fluids such as blood plasma and urine [1,10,29,30]. Secondly, in patients suffering from chronic kidney disease and primary glomerulonephritis, as well as in animal model of kidney failure, extracellular renalase was absent or present at lower concentrations, indicating the kidneys as the main source of the secreted protein [1,30-32]. Finally, mammalian cells transfected with constructs expressing either human or mouse renalase were shown to secrete the protein into the culture medium [1,16]. However, as discussed in Chapter 6, it is unlikely that the N-terminal region of renalase, initially proposed as a secretion signal [1], could be processed by the conventional cell secretory pathway, because the cleavage of this peptide would dramatically destabilize the native conformation of the protein.

5. BIOCHEMICAL PROPERTIES OF RENALASE

5.1. Purification of Endogenous and Recombinant Renalase Forms

Any proposal about the mechanism of the physiopathological action of a newly discovered protein needs to be verified in the context of its functional and structural properties. In the case of renalase, the application of this general rule had to wait several years until sufficient amounts of stable recombinant holoprotein became available for biochemical characterization, which eventually led also to the characterization of its crystal structure. The only attempt to characterize endogenous human renalase was carried out

Table 2. Single Nucleotide Polymorphisms of the Renalase Gene Characterized for their Association with Pathological Conditions

SNP accession no.	Location[a]	Alleles	MAF[b]	Diseases and risk-associated allele	Ref.
rs2576178	5' flanking region	G/A	0.46	Essential hypertension (G); hypertension in end stage renal disease (G); type 2 diabetes (G)	[44,45,67]
rs2296545	Exon 1a	C/G Asp37/Glu37	0.44	Essential hypertension (C); hypertension in type 2 diabetes (C); cardiac hypertrophy, dysfunction and ischemia (C)	[33,44,45]
rs2765446	Intron 3-4	C/T	0.46	n. s.[c]	[44]
rs2437871	Intron 3-4	A/C	0.46	Type 2 diabetes (A)	[68]
rs11202776	Intron 4-5	C/T	0.12	n. s.[c]	[44]
rs1648512	Intron 5-6	A/G	0.32	n. s.[c]	[44]
rs10887800	Intron 5-6	A/G	0.50	Hypertension in end stage renal disease (G); stroke (G)	[45,67]
rs1035796	Intron 7a-7b	C/T	0.47	n. s.[c]	[44]
rs2114406	3' flanking region	A/G	0.22	n. s.[c]	[44]

[a] Intron number numbered according to adjacent exons as shown in Fig. 1. [b]MAF, minor allele frequency; [c]n. s., no significant correlation with the considered pathological conditions.

on the protein isolated from the urine of healthy volunteers [1]. Excreted renalase was purified by ammonium sulfate precipitation followed by immunoaffinity chromatography using antibodies against the recombinant protein. Unfortunately, essentially no biochemical characterization was performed on the purified material, except for electrophoretic analysis and catalytic activity assays (see Chapter 5.2). Thus, although SDS-PAGE provided a molecular mass (35,000 Da) slightly lower than that predicted for the full length 342-residue polypeptide (37,847 Da), the accuracy of the estimate did not allow definitive conclusions about the presence or absence of the signal peptide after post-translational processing of urine renalase. Even more surprisingly, the possible presence of a bound flavin cofactor was not verified in the purified protein [1].

The production of recombinant mammalian renalase in different hosts using various expression strategies has been described by four independent groups. Desir's group reported the production of two recombinant forms of human renalase in *Escherichia coli*. Initially, the protein was expressed as an N-terminal fusion with glutathione S-transferase (GST) and purified in soluble form by affinity chromatography on a Glutathione Sepharose column [1,17]. GST-renalase was used to raise anti-renalase polyclonal antibodies and to study its catalytic activity *in vitro*. Later, two recombinant allelic isoforms of human renalase were synthesized with no tag or fusion partners, extracted from *E. coli* inclusion bodies by chaotropic agents and refolded *in vitro* in the presence of FAD [17,33]. Wang and coworkers produced human renalase in *E. coli* as a fusion protein containing at the N-terminus the *pelB* leader sequence for localization in the cell periplasm, and a C-terminal His-tag. The abundant 38 *k*Da product was purified (although it was not specified whether under denaturing or non-denaturing conditions) and used for monoclonal antibody production [34]. Zhang's group reported the synthesis of *Mus musculus* renalase in *E. coli* as an N-terminal fusion with GST, with no purification attempt [16].

Recombinant renalase has also been produced in eukaryotic cells, although its isolation from this source has never been reported. Mouse renalase has been successfully synthetized in human embryonic kidney cells as a C-terminally enhanced green fluorescent protein (EGFP)-tagged fusion [16]. The expression of human renalase in insect cells by a baculovirus-based system was described, although many details of the cloning procedure are missing and no explanation is given of the very large apparent molecular mass of the expression product (85 *k*Da) [35]. The same authors also reported the synthesis of human renalase in embryonic kidney cells [36]. Finally, the production of human renalase in the yeast *Pichia pastoris* has been described in a patent by Desir and coworkers [37]. Gene expression was obtained using the pPICZα (Invitrogen) vector, which promotes its integration in the host genome and secretion of the resulting translation product in the growth medium, where it was detected immunochemically.

Despite the ability of renalase to incorporate a flavin nucleotide being an absolute prerequisite for its initially proposed enzymatic action, the actual presence of FAD or FMN in the mentioned recombinant renalase forms was not reported. Since the presence of flavin nucleotides is difficult to miss due to its intense yellow color, we suspect that no purification procedure yielded a stable flavoprotein. Using the pGEX-4T-2/mMAO-C plasmid kindly provided by Dr. Shu-Ping Zhang [16], we obtained the synthesis in *E. coli* of limited amounts of soluble mouse GST-renalase, which, after successful isolation by affinity chromatography, contained no flavin cofactor (Aliverti, unpublished results). Apparently, the only observation (reported in its first article on this subject) that led Desir to conclude that human renalase is a flavoprotein was that inclusion of 0.1 μM FAD in the bacterial culturing medium was required in order to isolate a recombinant protein that demonstrated oxidoreductase active [1]. This is an inconsistent observation, since it has long been known that FMN or FAD biosynthesis by *E. coli* is not a limiting factor in flavoprotein production, even when expression levels exceed 25 mg of target protein per gram of bacterial cells [38,39]. Indeed, Medvedev and coauthors clearly stated that a conclusive proof that renalase contains FAD was still lacking [9]. This proof was obtained in the same year, when after several expression trials in both *E. coli* [40] and *Saccharomyces cerevisiae* [Aliverti, unpublished results], we finally obtained limited amounts of highly purified human flavin-containing renalase spontaneously folded *in vivo* in the bacterial host [40]. Both Glu37 and Asp37 allelic isoforms of renalase were found to contain 1 mol FAD per mol protein, which, at variance with MAO enzymes, was tightly but not covalently bound to the apoprotein. The fluorescence of the bound cofactor was found completely quenched, and circular di-

chroism spectrophotometry indicated that its isoalloxazine ring is embedded in a highly asymmetrical environment, markedly different from that of MAOs [40]. Dynamic light scattering, far ultraviolet circular dichroism, sulfhydryl titration and mass spectrometry predicted a globular, highly packed conformation in solution, with no disulfide bonds and an α and β secondary structure content of 23% and 21-25%, respectively [40]. By thermal denaturation at low ionic strength and neutral pH, an apparent melting temperature of 54 °C was determined for recombinant renalase, indicating that its native conformation is particularly stable [Aliverti, unpublished results]. Under non-denaturing conditions, renalase was also very resistant to the action of a variety of proteases, indicating the absence of large flexible surface loops. The protein was digested only in the presence of urea at concentrations above 1.5 M, without detectable transient intermediate polypeptides, indicating a global native conformation stabilized by highly cooperative tertiary contacts [Aliverti, unpublished results]. Production of renalase in *E. coli* with either an N-terminal His-tag, C-terminal His-tag, or a N-terminal cleavable SUMO polypeptide did not affect its biochemical properties, suggesting that the recombinant protein was not altered in any way by the fusion strategy [40, Aliverti, unpublished results]. All the above indirect conclusions about the structural properties of renalase are in full agreement with the crystal structure of the protein (see Chapter 6).

5.2. Functional Properties of Renalase

Only two groups have published data on the biochemical *in vitro* properties of renalase to date. In their seminal 2005's paper, Desir and coworkers reported that both recombinant GST-renalase fusion and the natural protein isolated from urine possessed amine oxidase activity with a substrate preference profile different from those of either MAO A or MAO B [1]. Dopamine was described as the best renalase substrate, followed by epinephrine and then norepinephrine, whereas its activity towards other biogenic amines was negligible. Moreover, renalase activity was unaffected by clorgyline and pargyline, specific inhibitors of MAO A and B, respectively [1]. Based on this observations, mammalian renalase was proposed to represent a new type of MAO [1,7,15], which was later named MAO C [16], a term under which is currently classified in some databases. These conclusions were strongly questioned by Frans Boomsma and Keith F. Tipton [41], who pointed out that copper enzyme semicarbazide-sensitive amine oxidase is the only enzyme responsible for the degradation of catecholamines in mammalian blood plasma. The supposed activity of purified renalase, measured only as H_2O_2 production, might be due to catecholamine outoxidation, which is known to be relevant at pH above 7 in the absence of antioxidants. Alternatively, since the reaction was followed for just 0.25% of the expected total amine conversion, this activity might be due to the oxidation of contaminant(s) that are common in commercial catecholamines. Finally, they argued that, even if renalase were actually able to degrade biogenic amines, its reported turnover number is so low (> 0.25 min^{-1}) [1], that it would hardly affect blood catecholamine concentration [41].

Subsequently, Desir's group proposed a catecholamine-triggered activation mechanism for circulating renalase, which would exist in inactive form under normal condition [29]. These authors reported that, while amine oxidase activity is undetectable in rat plasma under basal conditions, a 2 min infusion with epinephrine or dopamine determined the rapid (<1 min) onset of renalase activity (assayed as H_2O_2 production specifically inhibited by an anti-renalase antibody) that lasted for several minutes. Since the plasma concentration of renalase did not follow the same time course, increasing only ca. 10 min after perfusion, they concluded that the rapid rise of amine oxidation activity was due to the conversion of an inactive prorenalase form to the functional enzyme. Consistent with this finding, they also observed that urine human renalase displays a much higher turnover rate than the plasma form. Since blood plasma was found to have a strong inhibitory effect on purified urine renalase, they concluded that circulating prorenalase might represents a resting enzyme form, possibly complexed with a specific inhibitor [8,18,29].

As reported in Chapter 5.1, recently we obtained a recombinant *in vivo*-folded FAD-containing human renalase. At variance with previous reports, we found that our protein, although eliciting the expected effects on blood pressure when injected into rats, was completely devoid of any amine oxidase activity [40]. At the same time, Desir and coauthors reasoned that, since the renalase sequence contains the dinucleotide binding motif GXGXXG, which is the hallmark of the Rossmann fold, it could bind either NAD or NADP [17,33,42]. Indeed, they found that *in vitro* refolded recombinant human renalase possesses NADH-oxidase activity, with a K_m^{NADH} of 15 ± 1 μM, and a V_{max} of 15 ± 0.1 nmol/min/mg, corresponding to a k_{cat} of 0.40 min^{-1} [17]. The enzyme was inactive towards NADPH. When epinephrine was included in the reaction mixture, it was degraded at a rate 18-fold faster than in the absence of NADH through a reaction that was abolished by superoxide dismutase but not by catalase. NADH-dependent epinephrine degradation by renalase displayed a $K_m^{epinephrine}$ of 17 ± 4 μM, and a V_{max} of 22 ± 0.1 nmol/min/mg, corresponding to a k_{cat} of 0.58 min^{-1} [42]. On these bases, the authors stated that renalase is a new type of FAD-containing, NADH-dependent, catecholamine degrading enzyme, although no explanation was given of how the same Rossmann fold domain could bind both FAD and NADH.

Serious doubts over the putative amine-degrading activity of renalase were again raised by Nina Eikelis and coauthors [43], who pointed out that: (i) the supposed renalase catecholamine-degrading rate was too low to be ascribed to a real enzyme activity, (ii) a structurally sound recombinant renalase produced by others did not metabolize catecholamines [40], and (iii) renalase gene inactivation was studied in a mouse strain (C57BL/6 [17]) that synthetized a shortened form of renalase, which lacks the FAD/NAD-binding motif, and thus expected to be enzymatically inactive. Desir replied that the renalase knock out was maintained in a mixed mouse background (129Sv/J and C5BL/6), where the former wild-type strain produces a full-length renalase, and the reason for the discrepancy between enzyme activity data obtained in different laboratories depends on the fact that Aliverti's group omitted NADH in the assays [43].

Another intriguing aspect of renalase function is the role played by the residue 37 side-chain in catalysis. As mentioned in Chapter 4, the *RNLS* rs2296545 G allele, encoding the Asp37 variant of renalase, was found to be associated with cardiovascular pathologies [33,44,45]. The catalytic properties of both Asp37 and Glu37 renalase isoforms were compared by studying their NADH-diaphorase activity, measured with the water-soluble salt 2-(4-iodophenyl)-3-(4-nitrophenyl)-5-(2,4-disulfophenyl)-2H-tetrazolium (WST-1) as an artificial electron acceptor. The Glu37Asp replacement determined an increase in K_m^{NADH} from 34 ± 4 to 820 ± 115 μM, and a decrease in V_{max} from 58 ± 1 to 25 ± 2 nmol/min/mg [33]. The effect of the conservative Glu37Asp mutation was interpreted on the basis of the critical role played by the corresponding residue in MAOs (Glu34 in MAO B) and other flavoenzymes sharing the same FAD-binding motif [17]. In such enzymes the Glu γ-carboxylate interacts with the adenosyl ribose moiety of bound FAD, controlling their catalytic properties, as demonstrated by the large impact of the Glu34Asp mutation on activity [46,47].

Very recently, we compared the functional properties of the Glu37 and Asp37 isoforms of recombinant *in vivo* folded renalase [20, Aliverti, unpublished results] and found no difference between them, in sharp contrast with the aforementioned report [33]. Moreover, we provided a solid confirmation that renalase slowly reacts with both NADH and NADPH, and weakly binds the oxidized forms of both dinucleotides. We found that renalase catalyzes NADH- and NADPH-dependent diaphorase reactions with various artificial electron acceptors (2-(4-iodophenyl)-3-(4-nitrophenyl)-5-

phenyl-2*H*-tetrazolium chloride (INT) being the preferred one), and determined the following steady-state kinetic parameters: k_{cat}^{NADH} = 0.14 min^{-1}, k_{cat}^{NADPH} = 0.26 min^{-1}, K_m^{NADH} = 18 μM, K_m^{NADPH} = 175 μM [20]. In addition to indicating that Glu37 has no role in the catalysis of these reactions, our steady-state kinetic data markedly differ from those published by Desir's group in showing that renalase is not strictly specific for NADH [20]. Moreover, we demonstrated that protein-bound FAD is involved in these reactions, showing its reduction at rates compatible with catalysis, when renalase is incubated under anaerobiosis with either NADH or NADPH. By differential spectrophotometry we determined that the dissociation constants of the protein for NAD^+, $NADP^+$ and 2-phospho-AMP were all in the range of 1-2 mM. Taken together, the very low turnover numbers, the low affinity for nucleotides, and the poor selectivity in discriminating among them, strongly suggest that renalase is not a NAD(P)*H*-dependent enzyme, and that the observed diaphorase activity indicates a physiologically irrelevant side reaction [20]. Finally, we showed that renalase slightly stabilizes the neutral form of FAD and that is able to form a sulfite adduct [20]. These observations indicate that the reactivity of the FAD prosthetic group of renalase dramatically differs from that of MAO A and B, allowing us to conclude, in agreement with the phylogenetic data (see Chapter 3), that renalase is not a MAO-like enzyme and likely is not even an oxidase.

6. THREE-DIMENSIONAL STRUCTURE OF RENALASE

The crystal structure of human renalase isoform 1 (PDB ID 3QJ4) was solved at 2.5 Å resolution by molecular replacement using a putative oxidoreductase from *Pseudomonas syringae* q888a4 (PDB ID 3KKJ) as starting model [20]. The renalase molecule has a compact, elongated, globular shape, with α and β secondary structure content of 26% and 25%, respectively. It is organized in two domains: one consisting of three non-adjacent polypeptide stretches, and the other by the two intervening segments. At the interface between the two domains, a wide and deep cleft runs perpendicularly to the longer axis of the molecule on the side opposite to the entrance of the active-site cavity described below. The FAD cofactor is buried within the interior of the molecule, with the exception of a few small regions, including part of the isoalloxazine ring, and is firmly, but not covalently bound to the protein through several H-bonds and other contacts. The first domain, as predicted by the presence of the dinucleotide binding motif, adopts the classical Rossman fold, which is used to bind the FAD prosthetic group [48], thus excluding the possibility that it could provide a NADH-binding site, as proposed by other authors [33]. The second domain, based mainly on an antiparallel five-stranded beta sheet surrounded by three helices and a β hairpin, is presumably involved in substrate binding. The overall fold unequivocally classifies renalase as a member of the *p*-hydroxybenzoate hydroxylase (PHBH) protein superfamily [49], which comprises several flavoenzymes catalyzing highly diverse reactions (Table **3**). The oxidases of this superfamily belong either to the L-amino acid oxidase or to the D-amino acid oxidase structural families, renalase more closely resembling the former enzymes, which encompass also MAOs. In comparison to most of its structural homologs, renalase lacks a third domain, which in PHBH is named the interface domain [50], and which participates in substrate binding in MAOs and polyamine oxidase [51]. Due to the absence of this structural element, the polar, positively charged cavity of 224 $Å^3$ that faces the *re* side of the flavin ring and presumably represents the active site is freely accessible to the solvent trough a large opening [20].

As renalase was claimed to degrade catecholamines by either oxidase or NADH-dependent reactions [1,33], these proposed catalytic activities have been considered in the light of its three-dimensional structure [20]. As shown in (Fig. **2**), the renalase active-site markedly differs from those of MAOs and related amine oxidases: the former lacks both the 'aromatic cage' that in the latter enzymes binds the substrate amine group and promotes its oxidation, and a lysine (Lys 305 and Lys296 in MAO A and MAO B, respectively) conserved in most of the oxidases of the superfamily [20]. These features refute the classification of renalase as a MAO, suggesting that probably it is not an oxidase at all. In principle, the observed NADH reactivity of renalase [33] is suggestive of a possible monooxygenase (*i.e.* hydroxylase) activity, substantiated by its structural similarity to PHBH, the prototype of flavin-dependent aromatic hydroxylases [52]. Such activity is compatible with the observed very slow reaction between renalase and NADH or NADPH [20], since in aromatic hydroxylases the reductive half-reaction (FAD reduction) is exceedingly slow in the absence of a hydroxylatable substrate [52]. Moreover, the lack of a typical NAD-binding site in renalase [20] is in line with this hypothesis, because PHBH binds NADPH at a site [53] that corresponds to the aforementioned interdomain cleft of renalase, which could play an equivalent role. However, control of FAD reduction and reactivity of the flavin-C4a-hydroperoxide intermediate is obtained in aromatic hydroxylases through large conformational transitions occurring during the catalytic cycle, in which the isoalloxazine ring oscillates, alternating between 'in' and 'out' conformations [52]. When the flavin adopts the 'in' conformation, its N5 atom is strictly protected from the solvent to avoid H_2O_2 release from the flavin peroxide, a reaction competing with substrate hydroxylation [52]. As reported elsewhere [20], the swing of the flavin ring to the 'out' position is precluded in renalase by the obstructing presence of the β18 strand and particularly by the Trp288 side-chain (Fig. **2**). Notably, in renalase the isoalloxazine N5 position is solvent exposed [20]. In addition to the Rossman fold GXGXXG signature, flavoprotein hydroxylases display two highly conserved consensus sequences: the 'GD' and the 'DG' motifs [54]. Whereas, the former polypeptide region participates in FAD binding and is conserved in renalase, the latter motif, critical for the interaction with the nicotinamide nucleotide, is absent. In particular, Gly160 and His162 of PHBH, which are very important for NADPH binding [54], in renalase are both replaced by Pro residues (Pro162 and Pro164), excluding the presence of a functional NAD(P)-binding site in this protein. These considerations, combined with the observation that the FAD structural environment is incompatible with the required chemistry (confirmed by the production of superoxide upon reaction with O_2 [33] instead of hydrogen peroxide as typical in hydroxylases [52]), led to the logical conclusion that renalase cannot be a monooxygenase. We proposed that the slow NAD(P)H-dependent activity of renalase is a side reaction arising from non-physiological access of the nucleotides to the flavin ring, driven by the positive charge of the wide active-site cavity [20].

As mentioned in Chapter 5.2, Glu37 was proposed to modulate the NADH-dependent activity of renalase by interacting with the FAD ribose moiety [17]. Structural data ruled out this hypothesis, by showing that Glu37 is part of a loop near the rim of the surface cleft [20], in agreement with our observation that the Glu37Asp replacement had no effect on the properties of the flavoprotein [20].

As reported in Chapter 4, a plausible N-terminal signal peptide for secretion (of 16-17 residues) was predicted in renalase [1], although SignalP 4.0 [55] assigns it just a borderline score. Inspection of the protein crystal structure shows that this region corresponds to the central β1 stand and half of the adjacent α1 helix that are integral part of the Rossmann fold [20] and whose removal would cause the collapse of the entire FAD-binding domain, as shown in (Fig. **3A**). This consideration tends to exclude that the 1-16 peptide represents a signal for secretion, or that it is cleaved during protein processing. To reconcile this inference with the observation that renalase is actually present in blood plasma, a non-conventional secretion mechanism must be invoked [56].

Finally, the availability of the three-dimensional structure of the isoform 1 (NP_001026879) of renalase allows the development of "educated guesses" about the possible structural features of the alternative splicing isoforms. Renalase 2 (NP_060833) originates

Table 3. Outline of the Structural Superfamily of *p*-hydroxybenzoate Hydroxylase.[a]

Superfamily	Family	Representative members	Flavin binding	Catalyzed reaction	Metabolic function	Ref.
PHBH	PHBH-like enzymes	PHBH	Noncovalent	Hydroxylation of *p*-hydroxybenzoate to yield protocatechuate	Catabolism of aromatic acids in *Pseudomonas*	[50]
		Monooxygenase PhzS	Noncovalent	Hydroxylation of 5-methyl-phenazine-1-carboxylate to yield pyocyanin	Pyocyanin biosynthesis in *Pseudomonas*	[73]
		Dihydroxypyridine hydroxylase	Noncovalent	Hydroxylation of 2,6-dihydroxypyridine to yield 2,3,6-trihydroxypyridine	Nicotine degradation in *Arthrobacter*	[74]
	L-amino acid oxidase-like enzymes	L-amino acid oxidase	Noncovalent	Oxidation of L-α-amino acids to the corresponding α-keto acids	Amino acid catabolism	[75]
		MAO	Covalent bond between FAD 8-methyl and Sγ of a Cys residue	Oxidation of monoamines to the corresponding aldehydes	Catabolism of catecholamines and other monoamines	[76]
		N,N-dimethylglycine oxidase	Covalent bond between FAD 8-methyl of and Nε of a His residue	Oxidative demethylation of N,N-dimethylglycine to yield sarcosine	Choline and 1-carbon metabolism	[77]
		Polyamine oxidase	Noncovalent	Oxidation of secondary amino groups of polyamines with hydrolysis of resulting imines	Spermidine and spermine catabolism	[78]
		Lysine-specific histone demethylase 1	Noncovalent	Oxidative demethylation of histone mono and dimethylated Lys residues	Regulation of gene expression by nucleosome demethylation	[79]
	D-amino acid oxidase-like enzymes	D-amino acid oxidase	Noncovalent	Oxidation of D-α-amino acids to the corresponding α-keto acids	Amino acid catabolism	[80]
		Monomeric sarcosine oxidase	Covalent bond between FAD 8-methyl and Sγ of a Cys residue	Oxidative demethylation of sarcosine to yield glycine	Choline and 1-carbon metabolism	[81]
		Glycine oxidase	Noncovalent	Oxidation of D-α-amino acids to the corresponding α-keto acids	Amino acid catabolism	[82]
	UDP-galactopyranose mutase-like enzymes	UDP-galactopyranose mutase	Noncovalent	Interconversion between UDP-galactopyranose and UDP-galactofuranose	Biosynthesis of cell wall precursors in Gram-negative bacteria, fungi and protozoa	[83]
		Poly-unsaturated fatty acid isomerase	Noncovalent	Double-bond isomerization of polyunsaturated fatty acid	Biosynthesis of conjugated linoleic acids	[84]

[a] This classification of the members of the PHBH superfamily is adapted from that of SCOP, Structural Classification of Proteins [85].

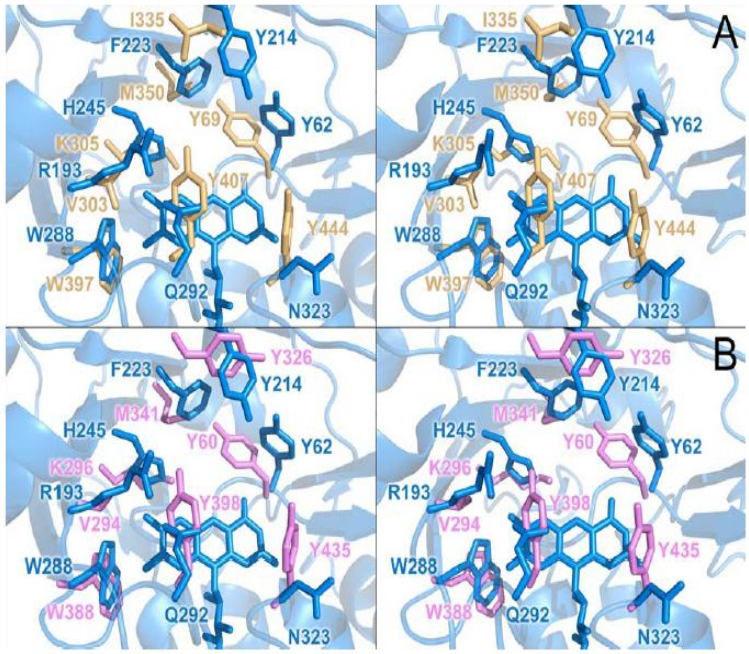

Fig. (2). Comparison between the active site of renalase and those of MAO A and MAO B. Stereo view of the putative active site of human renalase overlaid on those of MAO A (**panel A**) and MAO B (**panel B**). The FAD isoalloxazine ring and relevant amino acyl residues of renalase (PDB ID 3QJ4, chain A) are shown in blue (black in the printed version of the article), whereas the corresponding residues of MAO A (PDB ID 2BXR, chain A) and MAO B (PDB ID 1GOS, chain A), including the 'aromatic cage' (Tyr407 and Tyr444 in MAO A, and Tyr398 and Tyr435 in MAO B) are depicted in gold and pink, respectively (both white in the printed version of the article).

from alternative splicing between exons 6 and 7, causing a frame shift that alters the C-terminal sequence and makes the polypeptide chains 27 residue shorter through the introduction of a premature stop codon (Fig. **1**) [19]. This profoundly modifies the sequence of the region corresponding to the β hairpin β19-β20 and precisely deletes the two C-terminal helices η2 and α11 of isoform 1 [20], as outlined in (Fig. **3B**). These structural modifications are expected to make FAD more exposed in renalase 2 than in renalase 1 and to significantly affect the features of its active-site cavity. In comparison to renalase 1, the splicing isoform AK296262 lacks the polypeptide segments encoded by exons 2 and 3 (Fig. **1**). As a result, the surface exposed α4 helix of the FAD-binding domain and the β3-β4 hairpin and the β5-α2-α3-β6-β7 subregion of the substrate-binding domain are deleted [20]. The resulting protein would lack critical residues for the binding of the FAD isoalloxazine, suggesting that it would not be able to incorporate the cofactor and hence to be active as an oxidoreductase. In the variant BX648154 the FAD-binding domain is almost completely deleted, resulting in a polypeptide with unpredictable properties.

7. PHYSIOLOGICAL ROLES OF RENALASE AND THEIR IMPAIRMENT AS POSSIBLE PATHOGENIC MECHANISMS OF CARDIOVASCULAR DISEASES

Despite our appreciation of the probable molecular mechanism of its physiological activity, the nature of the catalyzed reaction, and the identity of its substrate(s) is very poor (see Chapter 5), there is quite solid and constantly accumulating evidence of the important roles played by renalase in the control of blood pressure and heart function. Since its discovery, two key observations were made about renalase pathophysiological actions: 1) its concentration in blood plasma is dramatically lowered in subjects suffering from severe kidney disease; and 2) the parenteral administration of the recombinant protein has a hypotensive effect in rats [1]. For clarity, the proofs of the relationship between renalase and cardiovascular system pathophysiology will be subdivided here in experimental, clinical and epidemiological aspects.

7.1 Experimental Evidence of Renalase Action on the Cardiovascular and Sympathetic Systems

The finding by Desir's group that intravenous injection of recombinant renalase in healthy rats decreases, in dose-dependent manner, systolic, diastolic, and mean arterial pressure, as well as heart rate and contractility [1] has been partially confirmed by us [40]. In addition, it was later shown that subcutaneous administration of the protein has a profound effect on blood pressure and heart rate in an animal model of hypertension (Dahl salt-sensitive and 5/6 nephrectomized rats; [10,57]. Very interestingly, using an isolated heart model of acute coronary syndrome, perfusion with recombinant renalase was shown to exert a strong protective effect against ischemia, preserving ventricular function and reducing myocardial necrosis and infarct size [58]. A major breakthrough in the identification of renalase physiological role has been the inactivation of the *RNLS* gene in mouse by homologous recombination [17]. In com-

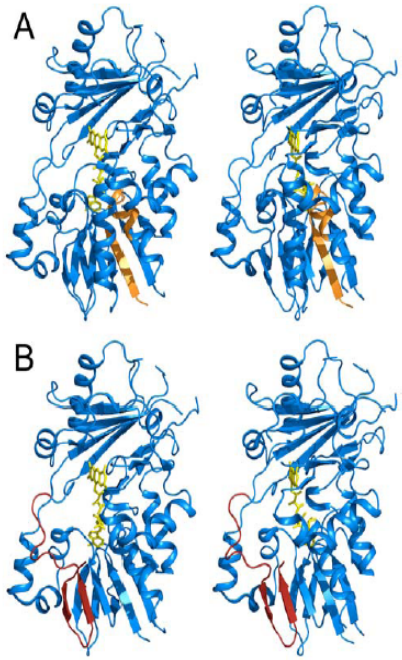

Fig. (3). Putative renalase signal peptide and structural differences between renalase 1 and 2. Ribbon model of the three-dimensional structure of human renalase (PDB ID 3QJ4, chain **A**). **Panel A**, Crystal structure of renalase 1, showing the 1−16 N-terminal peptide, proposed to represent a secretion signal, in orange (light grey in the printed version of the article). **Panel B**, Hypothetical model of renalase 2 (NP_060833), in which the shorter C-terminal peptide encoded by exon 7c replaces the longer one encoded by exon 7b (see Fig. **1**). Renalase 2 is predicted to lack the α11 helix of renalase 1 and to present a different amino acid sequence in the region highlighted in red (grey in the printed version of the article), which includes β19 and β20 strands.

parison to littermates, KO mice displayed 25% lower body mass, tachycardia, hypertension, and higher circulating norepinephrine levels, while markers of endothelial function were unaffected. Moreover, gene inactivation was found to greatly increase the extent of myocardial damage following induced ischemia on isolated heart, an effect that was fully prevented by renalase infusion [17]. Since *RNLS* KO was also shown to be associated to a markedly decreased NAD^+/NADH ratio in the myocardium, it was proposed that the cardioprotective effect of renalase might be mediated by the control of both sympathetic activity and redox potential of the NAD^+/NADH couple, which in turn is expected to affect energy metabolism and sirtuin-1 signaling [17]. However, the exceedingly low turnover of renalase measured in NADH-dependent reactions *in vitro* (see Chapter 5.2) would exclude direct effects on NADH and/or NAD^+ concentrations *in vivo*. Very recently, using an animal model of chronic kidney disease, *i.e.* 5/6 nephrectomized rats, Baraka and El Ghotny showed that prolonged renalase administration after the chirurgic procedure significantly controlled the plasma noradrenaline rise induced by nephrectomy, ameliorating the resulting cardiovascular complications, including hypertension, myocardial fibrosis and cardiac hypertrophy [59].

A link between renalase and catecholamine metabolism emerges from several studies. Downregulation of *RNLS* expression in healthy mice by antisense phosphorothioate oligonucleotides was found to produce both a rise in blood pressure and an increased sensitivity to norepinephrine injection [8,60]. In various rat models of chronic kidney disease, lower concentrations of renalase in kidneys, heart and blood were always accompanied by increased levels of epinephrine and norepinephrine in plasma and heart [30,32,61,62]. Furthermore, some of these studies together with other investigations on rodent models showed that renalase levels inversely correlate with the concentration of dopamine, which has hypotensive and cardioprotective actions at variance with other catecholamines [63], in kidneys and urine [32,64]. The known natriuretic action of dopamine and its recently proposed participation in the modulation of phosphate tubular reabsorption have also suggested a role for renalase in the control of sodium and phosphate ions homeostasis [64].

7.2. Clinical Evidence for Renalase Actions on the Cardiovascular and Excretory Systems

The involvement of renalase in the renal dopaminergic system was substantiated by a clinical report on eight kidney transplant recipients, showing a correlation between the increase in dopamine concentration and the decline of renalase excretion in urine [65]. Other reports highlighted the involvement of renalase in different forms of hypertension. First, in a study on neurogenic hypertensive subjects, where noradrenaline spillover from adrenergic nerves was significantly increased, renalase secretion by the kidneys was undetectable in most patients [66]. Furthermore, biopsies from twenty-three patients affected by IgA nephropathy, the most common form of primary glomerulonephritis, displayed decreased renalase levels in tubular epithelial cells, correlating with both pathology chronicity indexes and hypertension [31]. Recent studies on the impact of kidney and heart transplantation on the level of circulating renalase led to the unexpected finding that plasma renalase concentration increases after organ implantation and the degree of increase correlates with the severity of kidney failure in the allograft recipients [23-25]. The same authors also investigated in chronic kidney disease patients the impact of hemodialysis and peritoneal dialysis on blood serum renalase They concluded that impairment of renal function correlates with increased renalase levels [26-28], which was found up to 10-fold higher in anuric patients that underwent bilater nephrectomy in comparison to healthy subjects [26]. Finally, it was reported that stroke and hypertensions were associated to lower serum renalase concentrations in a hemodialysis population [27].

7.3. Epidemiologic Data Implying Renalase Gene Polymorphisms as Disease Risk Factors

To date, four independent genetic studies have highlighted a correlation between four individual *RNLS* SNPs and the propensity to develop specific pathological conditions in different populations, as summarized in Table **2**. In the first such study, carried out on 1317 hypertensive and 1269 normotensive subjects recruited from the International Collaborative Study of Cardiovascular Disease in Asia (InterASIA), *RNLS* was shown to represent a susceptibility gene for essential hypertension in the northern Han Chinese population [44]. In particular, the G and the C alleles of the rs2576178 and rs2296545 SNPs, respectively, displayed significant higher frequencies in the pathological group. Genotyping suggested a codominant model for the expression of both risk-associated alleles [44]. The association of rs2576178, which maps in the 5' flanking region of the renalase transcript, with hypertension was confirmed by a case-control study on 400 Caucasian end-stage renal disease patients of Polish origin under dialysis [67]. The same survey also found a significant correlation of the G allele of the rs10887800, mapping in intron 6, with increased incidence of hypertension. A similar study, carried out on 900 type 2 diabetic patients and control

individuals from a population of Polish origin found a significant correlation between the rs2576178 G allele and type 2 diabetes, and a strong association of the rs10887800 G allele with stroke in hypertensive individuals, regardless of their diabetic status [45]. Interestingly, *RNLS* was recognized as a novel gene responsible for type-2 diabetes by a genome wide association scan in the Amish population, which identified rs2437871 as a disease-linked SNP [68]. Among the *RNLS* SNPs considered in the above studies, rs2296545 is the only resulting in variants of the encoded protein, which differs for the presence of a Glu (G allele) or an Asp (C allele) residue at position 37. The homozygous CC genotype was recently shown to be associated with cardiac hypertrophy, ventricular dysfunction, poor exercise capacity and higher susceptibility to induced ischemia [33], through genotyping 590 Caucasian individuals from the Heart and Soul Study [69],

8. CONCLUDING REMARKS

As foreseen by Eberhard Ritz, who, soon after the discovery of renalase, wrote that "it is easy to predict that in the near future this novel endocrine product of the kidney will be intensely investigated experimentally and in renal patients" [2], this protein has been the subject of several studies that, over the last seven years, have considerably strengthened its connection with the physiopathology of the cardiovascular and excretory systems. Moreover, the involvement of renalase in the modulation of the catecholaminergic system has become increasingly clear. Thus, human renalase is now regarded as a new player in the control of blood pressure and heart function, whose modulation could lead to promising new pharmacological treatments of various cardiovascular dysfunctions [3,8,13,23,24,70,71]. Renalase has been proposed as a drug for replacement therapy in end stage renal disease [12,17,59,70,72], as early biomarker of acute kidney ischemia [10] and essential hypertension [8], as well as prognostic factor for stroke [27,45], and even as possible target for the therapy of psychiatric disorders caused by altered catecholaminergic signaling in the central nervous system [19]. Obviously, development of effective tools for pharmacological intervention requires the mechanism of renalase action to be known at the molecular level. Unfortunately, this is not the case yet, since the supposed catalytic activity of renalase as a catecholamine-degrading enzyme has recently been proved wrong by the detailed biochemical characterization of the recombinant human protein [20,40]. However, the structural and functional data on renalase should provide the basis for a systematic and rational quest toward the identification of its substrates and the catalyzed reaction.

CONFLICT OF INTEREST

The authors confirm that this article content has no conflicts of interest.

ACKNOWLEDGEMENTS

We are grateful to Dr. Shu-Ping Zhang for generously providing us plasmid pGEX-4T-2/mMAO-C for the expression in *E. coli* of mouse renalase.

LIST OF ABBREVIATIONS

MAO	=	Monoamine oxidase
GST	=	Glutathione S-transferase
SNP	=	Single nucleotide polymorphism
PHBH	=	*p*-hydroxybenzoate hydroxylase

REFERENCES

[1] Xu J, Li G, Wang P, Velazquez H, *et al.* Renalase is a novel, soluble monoamine oxidase that regulates cardiac function and blood pressure. J Clin Invest 2005; 115: 1275-80.

[2] Ritz E. Kidney and Blood Pressure - The Story Unfolds. J Am Soc Nephrol 2005; 16: 2521-23.

[3] Luft FC. Renalase, a catecholamine-metabolizing hormone from the kidney. Cell Metab 2005; 1: 358-60.

[4] Santos SF, Peixoto AJ. Hypertension in dialysis. Curr Opin Nephrol Hypertens 2005; 14: 111-8.

[5] Go AS, Lo JC. Epidemiology of non-dialysis-requiring chronic kidney disease and cardiovascular disease. Curr Opin Nephrol Hypertens 2006;15 :296-302.

[6] Amann K, Wanner C, Ritz E. Cross-talk between the kidney and the cardiovascular system. J Am Soc Nephrol. 2006; 17: 2112-9.

[7] Xu J, Desir GV. Renalase, a new renal hormone: its role in health and disease. Curr Opin Nephrol Hypertens 2007; 16: 373-8.

[8] Desir GV. Regulation of blood pressure and cardiovascular function by renalase. Kidney Int 2009; 76: 366-70.

[9] Medvedev AE, Veselovsky AV, Fedchenko VI. Renalase, a new secretory enzyme responsible for selective degradation of catecholamines: achievements and unsolved problems. Biochemistry (Mosc) 2010; 75: 951-8.

[10] Desir GV. Role of renalase in the regulation of blood pressure and the renal dopamine system. Curr Opin Nephrol Hypertens 2011; 20: 31-6.

[11] Desir GV. Novel insights into the physiology of renalase and its role in hypertension and heart disease. Pediatr Nephrol 2012; 27: 719-25.

[12] Malyszko J, Malyszko JS, Mikhailidis DP, Rysz J, Zorawski M, Banach M. Hypertension and kidney disease: is renalase a new player or an innocent bystander? J Hypertens 2012; 30: 457-62.

[13] Zbroch E, Małyszko J, Małyszko J, Zórawski MJ, Myśliwiec M. Kidney and hypertension: is there a place for renalase? Pol Arch Med Wewn 2012; 122: 174-9.

[14] Haase-Fielitz A, Haase M, Bellomo R, *et al.* Decreased catecholamine degradation associates with shock and kidney injury after cardiac surgery. J Am Soc Nephrol 2009; 20: 1393-403.

[15] Desir GV. Renalase is a novel renal hormone that regulates cardiovascular function. J Am Soc Hypertens 2007; 1: 99-103.

[16] Wang J, Qi S, Cheng W, *et al.* Identification, expression and tissue distribution of a renalase homologue from mouse. Mol Biol Rep 2008; 35: 613-20.

[17] Wu Y, Xu J, Velazquez H, *et al.* Renalase deficiency aggravates ischemic myocardial damage. Kidney Int. 2011;79: 853-60.

[18] Desir GV. Renalase deficiency in chronic kidney disease, and its contribution to hypertension and cardiovascular disease. Curr Opin Nephrol Hypertens 2008; 17: 181-5.

[19] Hennebry SC, Eikelis N, Socratous F, Desir G, Lambert G, Schlaich M. Renalase, a novel soluble FAD-dependent protein, is synthesized in the brain and peripheral nerves. Mol Psychiatry 2010; 15: 234-6.

[20] Milani M, Ciriello F, Baroni S, *et al.* FAD-binding site and NADP reactivity in human renalase: a new enzyme involved in blood pressure regulation. J Mol Biol 2011; 411: 463-73.

[21] Roth RB, Hevezi P, Lee J, *et al.* Gene expression analyses reveal molecular relationships among 20 regions of the human CNS. Neurogenetics 2006; 7: 67-80.

[22] Wang ET, Sandberg R, Luo S, *et al.* Alternative isoform regulation in human tissue transcriptomes. Nature 2008; 456: 470-6.

[23] Malyszko J, Zbroch E, Malyszko JS, Koc-Zorawska E, Mysliwiec M. Renalase, a novel regulator of blood pressure, is predicted by kidney function in renal transplant recipients. Transplant Proc 2011; 43: 3004-7.

[24] Przybylowski P, Malyszko J, Kozlowska S, Malyszko J, Koc-Zorawska E, Mysliwiec M. Serum renalase depends on kidney function but not on blood pressure in heart transplant recipients. Transplant Proc 2011; 43: 3888-91.

[25] Zbroch E, Małyszko J, Małyszko J, Koc-Żórawska E, Myśliwiec M. Renalase, kidney function and markers of endothelial dysfunction in renal transplant recipients. Pol Arch Med Wewn 2012; 122: 40-4.

[26] Zbroch E, Malyszko J, Malyszko JS, Koc-Zorawska E, Mysliwiec M. Renalase, a novel enzyme involved in blood pressure regulation, is related to kidney function but not to blood pressure in hemodialysis patients. Kidney Blood Press Res 2012; 35: 395-9.

[27] Malyszko J, Koc-Zorawska E, Malyszko JS, *et al.* Renalase, stroke, and hypertension in hemodialyzed patients. Ren Fail 2012; PMID: 22583169.

[28] Zbroch E, Malyszko J, Malyszko J, Koc-Zorawska E, Mysliwiec M. Renalase in peritoneal dialysis patients is not related to blood pressure, but to dialysis vintage. Perit Dial Int 2012; 32: 348-51.

[29] Li G, Xu J, Wang P, *et al.* Catecholamines regulate the activity, secretion, and synthesis of renalase. Circulation 2008; 117: 1277-82.

[30] Gu R, Lu W, Xie J, Bai J, Xu B. Renalase deficiency in heart failure model of rats - a potential mechanism underlying circulating norepinephrine accumulation. PLoS One 2011; 6: e14633.

[31] Quelhas-Santos J, Fernandes-Cerqueira C, Moreira-Rodrigues M, Sampaio-Maia B, Pestana M. Expression of renalase in a ¾ nephroctomy rat model. NDT Plus 2009; 2.

[32] Ding J-X, Jiang L, Zhang Q-D, Liu, W-H Expression of renalase in the tubular epithelial cells is correlated with pathological phenotypes and blood pressure in a IgA nephropayhy. NDT Plus 2009; 2.

[33] Farzaneh-Far R, Desir GV, Na B, Schiller NB, Whooley MA. A functional polymorphism in renalase (Ghu37Asp) is associated with cardiac hypertrophy, dysfunction, and ischemia: data from the heart and soul study. PLoS One 2010; 5: e13496.

[34] Wang F, Wang N-S, Xing T, Cao Y, Xiang H-Y. The Cloning and Expression of Renalase and the Preparation of Its Monoclonal Antibody. J Shanghai Jiaotong Univ 2009; 14: 376-9.

[35] Wang F, Wang N-S, Xing T. Construction of Eukaryotic Recombinant Vector of Renalase and Its Expression as a Eukaryotic Protein. J Shanghai Jiaotong Univ 2010; 15: 637-40.

[36] Wang F, Xing T, Wang N. Construction and DNA immunization of human renalase eukaryotic expression vector. NDT Plus 2011; 4: 221.

[37] Desir GV, Xu J, inventors; Desir GV, Xu J, Yale University, assignees. Recombinant Renalase. International patent WO 2008039690. 2008 Apr.

[38] Kitamura M, Sagara T, Taniguchi M, *et al.* Cloning and expression of the gene encoding flavodoxin from *Desulfovibrio vulgaris* (Miyazaki F). J Biochem 1998; 123: 891-8.

[39] Aliverti A, Pandini V, Zanetti G. Domain exchange between isoforms of ferredoxin-NADP$^+$ reductase produces a functional enzyme. Biochim Biophys Acta 2004; 1696: 93-101.

[40] Pandini V, Ciriello F, Tedeschi G, Rossoni G, Zanetti G, Aliverti A. Synthesis of human renalase1 in Escherichia coli and its purification as a FAD-containing holoprotein. Protein Expr Purif 2010; 72: 244-53.

[41] Boomsma F, Tipton KF. Renalase, a catecholamine-metabolising enzyme? J Neural Transm 2007; 114: 775-6.

[42] Desir GV, Wang P, Li G, Tang L, Velazquez H. Renalase Belongs to a New Class of Catecholamines Metabolizing Enzymes. J Am Soc Nephrol 2010; 21: 934A.

[43] Eikelis N, Hennebry SC, Lambert GW, Schlaich MP. Does renalase degrade catecholamines? Kidney Int 2011; 79: 1380.

[44] Zhao Q, Fan Z, He J, *et al.* Renalase gene is a novel susceptibility gene for essential hypertension: a two-stage association study in northern Han Chinese population. J Mol Med 2007; 85: 877-85.

[45] Buraczynska M, Zukowski P, Buraczynska K, Mozul S, Ksiazek A. Renalase gene polymorphisms in patients with type 2 diabetes, hypertension and stroke. Neuromolecular Med 2011; 13: 321-7.

[46] Edmondson DE, Binda C, Mattevi A. The FAD binding sites of human monoamine oxidases A and B. Neurotoxicology 2004; 25: 63-72.

[47] Kwan SW, Lewis DA, Zhou BP, Abell CW. Characterization of a dinucleotide-binding site in monoamine oxidase B by site-directed mutagenesis. Arch Biochem Biophys 1995; 316: 385-91.

[48] Dym O, Eisenberg D. Sequence-structure analysis of FAD-containing proteins. Protein Sci 2001; 10: 1712-28.

[49] Fraaije MW, Mattevi A. Flavoenzymes: diverse catalysts with recurrent features. Trends Biochem Sci 2000; 25: 126-32.

[50] Schreuder HA, Prick PA, Wierenga RK, *et al.* Crystal structure of the *p*-hydroxybenzoate hydroxylase-substrate complex refined at 1.9 Å resolution. Analysis of the enzyme-substrate and enzyme-product complexes. J Mol Biol 1989; 208: 679-96.

[51] Fitzpatrick PF. Oxidation of amines by flavoproteins. Arch Biochem Biophys 2010; 493: 13-25.

[52] Palfey BA, McDonald CA. Control of catalysis in flavin-dependent monooxygenases. Arch Biochem Biophys 2010; 493: 26-36.

[53] Wang J, Ortiz-Maldonado M, Entsch B, Massey V, Ballou D, Gatti DL. Protein and ligand dynamics in 4-hydroxybenzoate hydroxylase. Proc Natl Acad Sci USA 2002; 99: 608-13.

[54] Eppink MH, Schreuder HA, Van Berkel WJ. Identification of a novel conserved sequence motif in flavoprotein hydroxylases with a putative dual function in FAD/NAD(P)H binding. Protein Sci 1997; 6: 2454-8.

[55] Petersen TN, Brunak S, von Heijne G, Nielsen H. SignalP 4.0: discriminating signal peptides from transmembrane regions. Nat Methods 2011; 8: 785-6.

[56] Nickel W, Rabouille C. Mechanisms of regulated unconventional protein secretion. Nat Rev Mol Cell Biol 2009; 10: 148-55.

[57] Desir GV, Tang L, Wang P, Li G, Velazquez H. Antihypertensive Effect of Recombinant Renalase in Dahl Salt Sensitive (DSS) Rats. J Am Soc Nephrol 2010; 21: 748A.

[58] Desir GV, Li Y, Liu D, Wang P, Xu J, Giordano F. Downregulation of Cardiac Renalase Expression in CKD, and Protective Effect of Renalase in Acute Coronary Syndrome. J Am Soc Nephrol 2007; 18: 149A.

[59] Baraka A, El Ghotny S. Cardioprotective effect of renalase in 5/6 nephrectomized rats. J Cardiovasc Pharmacol Ther 2012; PMID: 22626958.

[60] Ghosh SS, Gehr TWB, Sica DA, *et al.* Effect of Renalase Inhibition on Blood Pressure. Am Soc Nephrol 2006; 17: 208A.

[61] Ghosh SS, Krieg RJ, Sica DA, Wang R, Fakhry I, Gehr T. Cardiac hypertrophy in neonatal nephrectomized rats: the role of the sympathetic nervous system. Pediatr Nephrol 2009; 24: 367-77.

[62] Quelhas-Santos J, Sampaio-Maia B, Simões-Silva L, Fernandes-Cerqueieira C, Pestana M. High-salt diet further decreases renal, cardiac and plasma renalase levels in a chronic kidney disease rat model. NDT Plus 2010; 3: iii32.

[63] Felder RA, Sanada H, Xu J, *et al.* G protein-coupled receptor kinase 4 gene variants in human essential hypertension. Proc Natl Acad Sci USA 2002; 99: 3872-7.

[64] Weinman EJ, Biswas R, Steplock D, *et al.* Increased renal dopamine and acute renal adaptation to a high-phosphate diet. Am J Physiol Renal Physiol 2011; 300: F1123-9.

[65] Santos J, Cerqueira C, Silva I, *et al.* Inverse Relationship between urinary renalase levels and renal dopaminergic activity in kidney transplant recipients. NDT Plus 2010; 3: iii27.

[66] Socratous F, Eikelis N, Hennebry S, Schlaich MP. Altered renalase secretion in neurogenic human hypertension. Hypertension 2009; 53: 1117.

[67] Stec A, Semczuk A, Furmaga J, Ksiazek A, Buraczynska M. Polymorphism of the renalase gene in end-stage renal disease patients affected by hypertension. Nephrol Dial Transplant 2011; PMID: 21617193.

[68] Rampersaud E, Damcott CM, Fu M, *et al.* Identification of novel candidate genes for type 2 diabetes from a genome-wide association scan in the Old Order Amish: evidence for replication from diabetes-related quantitative traits and from independent populations. Diabetes 2007; 56: 3053-62.

[69] Ruo B, Rumsfeld JS, Hlatky MA, Liu H, Browner WS, Whooley MA. Depressive symptoms and health-related quality of life: the Heart and Soul Study. JAMA 2003; 290: 215-21.

[70] Schlaich MP, Socratous F, Hennebry S, *et al.* Sympathetic activation in chronic renal failure. J Am Soc Nephrol 2009; 20: 933-9.

[71] Paulis L, Unger T. Novel therapeutic targets for hypertension. Nat Rev Cardiol 2010; 7: 431-41.

[72] Unger T, Paulis L, Sica DA. Therapeutic perspectives in hypertension: novel means for renin-angiotensin-aldosterone system modulation and emerging device-based approaches. Eur Heart J 2011; 32: 2739-47.

[73] Greenhagen BT, Shi K, Robinson H, *et al.* Crystal structure of the pyocyanin biosynthetic protein PhzS. Biochemistry 2008; 47: 5281-9.

[74] Treiber N, Schulz GE. Structure of 2,6-dihydroxypyridine 3-hydroxylase from a nicotine-degrading pathway. J Mol Biol 2008; 379: 94-104.

[75] Pawelek PD, Cheah J, Coulombe R, Macheroux P, Ghisla S, Vrielink A. The structure of L-amino acid oxidase reveals the substrate trajectory into an enantiomerically conserved active site. EMBO J 2000; 19: 4204-15.

[76] De Colibus L, Li M, Binda C, Lustig A, Edmondson DE, Mattevi A. Three-dimensional structure of human monoamine oxidase A (MAO A): relation to the structures of rat MAO A and human MAO B. Proc Natl Acad Sci USA 2005; 102: 12684-9.

[77] Leys D, Basran J, Scrutton NS. Channelling and formation of 'active' formaldehyde in dimethylglycine oxidase. EMBO J 2003; 22(16): 4038-48.

[78] Binda C, Coda A, Angelini R, Federico R, Ascenzi P, Mattevi A. A 30-angstrom-long U-shaped catalytic tunnel in the crystal structure of polyamine oxidase. Structure. 1999; 7: 265-76.

[79] Stavropoulos P, Blobel G, Hoelz A. Crystal structure and mechanism of human lysine-specific demethylase-1. Nat Struct Mol Biol 2006; 13: 626-32.

[80] Mattevi A, Vanoni MA, Todone F, *et al*. Crystal structure of D-amino acid oxidase: a case of active site mirror-image convergent evolution with flavocytochrome b2. Proc Natl Acad Sci USA 1996; 93: 7496-501.

[81] Trickey P, Wagner MA, Jorns MS, Mathews FS. Monomeric sarcosine oxidase: structure of a covalently flavinylated amine oxidizing enzyme. Structure 1999; 7: 331-45.

[82] Mörtl M, Diederichs K, Welte W, *et al*. Structure-function correlation in glycine oxidase from *Bacillus subtilis*. J Biol Chem 2004; 279: 29718-27.

[83] Partha SK, van Straaten KE, Sanders DA. Structural basis of substrate binding to UDP-galactopyranose mutase: crystal structures in the reduced and oxidized state complexed with UDP-galactopyranose and UDP. J Mol Biol 2009; 394: 864-77.

[84] Liavonchanka A, Hornung E, Feussner I, Rudolph MG. Structure and mechanism of the Propionibacterium acnes polyunsaturated fatty acid isomerase. Proc Natl Acad Sci USA 2006; 103: 2576-81.

[85] Andreeva A, Howorth D, Chandonia J-M, *et al*. Data growth and its impact on the SCOP database: new developments. Nucl Acids Res 2008; 36: D419-25.

Received: September 13, 2012 **Accepted: October 30, 2012**

BIOCHEMISTRY
including biophysical chemistry & molecular biology

Article

pubs.acs.org/biochemistry

A Single Tyrosine Hydroxyl Group Almost Entirely Controls the NADPH Specificity of *Plasmodium falciparum* Ferredoxin-NADP$^+$ Reductase

Sara Baroni, Vittorio Pandini, Maria Antonietta Vanoni, and Alessandro Aliverti*

Department of Biomolecular Sciences and Biotechnology, Università degli Studi di Milano, via Celoria 26, 20133 Milano, Italy

ABSTRACT: *Plasmodium falciparum* ferredoxin-NADP$^+$ reductase (FNR) is a FAD-containing enzyme that, in addition to be a promising target of novel antimalarial drugs, represents an excellent model of plant-type FNRs. The cofactor specificity of FNRs depends on differences in both k_{cat} and K_m values for NADPH and NADH. Here, we report that deletion of the hydroxyl group of the conserved Y258 of *P. falciparum* FNR, which interacts with the 2′-phosphate group of NADPH, selectively decreased the k_{cat} of the NADPH-dependent reaction by a factor of 2 to match that of the NADH-dependent one. Rapid-reaction kinetics, active-site titrations with NADP$^+$, and anaerobic photoreduction experiments indicated that this effect may be the consequence of destabilization of the catalytically competent conformation of bound NADPH. Moreover, because the Y258F replacement increased the K_m for NADPH 4-fold and decreased that for NADH 3-fold, it led to a drop in the ability of the enzyme to discriminate between the coenzymes from 70- to just 1.5-fold. The impact of the Y258F change was not affected by the presence of the H286Q mutation, which is known to enhance the catalytic activity of the enzyme. Our data highlight the major role played by the Y258 hydroxyl group in determining the coenzyme specificity of *P. falciparum* FNR. From the general standpoint of engineering the kinetic properties of plant-type FNRs, although *P. falciparum* FNR is less strictly NADPH-dependent than its homologues, the almost complete abolishment of coenzyme selectivity reported here has never been accomplished before through a single mutation.

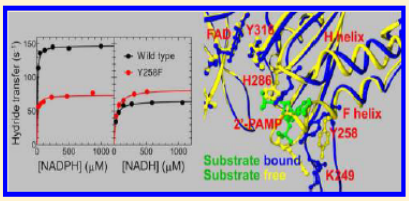

Plant-type ferredoxin-NADP$^+$ reductases (FNRs) are FAD-containing enzymes that catalyze the reversible exchange of reducing equivalents between the NADP$^+$/NADPH and the ferredoxin(Fe^{3+})/ferredoxin(Fe^{2+}) redox couples.[1−3] The prototype of FNRs is represented by the enzyme form responsible for NADPH regeneration in oxygenic photosynthesis. Whereas the strict relatives of the photosynthetic enzyme, the so-called "plastidic-type" FNRs, show remarkably similar properties, a divergent branch of plant-type FNRs, dubbed the "bacterial-type" FNRs, displays a greater variety of structural features, catalytic properties, and metabolic functions.[1] Furthermore, the structural module formed by the two-domain assembly of plant-type FNR has been recognized as the hallmark of the FNR protein superfamily,[4] which comprises enzymes that are highly medically relevant such as cytochrome P450 reductase,[5] Nox-family NADPH oxidases,[6] and nitric oxide synthases.[7]

Plastidic-type FNRs are usually highly specific for NADP$^+$ or NADPH [NADP(H)], displaying significantly higher values of both k_{cat}/K_m and k_{cat} for this coenzyme than for NAD$^+$ or NADH [NAD(H)].[2] The structural determinants of such coenzyme specificity have been extensively investigated, but a full understanding of the underlying mechanism(s) has not been developed. As expected, most of the difference in the binding energies of NADP(H) and NAD(H) relies on the specific interactions that FNR establishes with the 2′-phosphate group of the physiological coenzyme.[8] However, the FNR specificity significantly depends on k_{cat}, which is limited by the degree of access of the nicotinamide ring of the coenzyme to the active site, where hydride transfer (HT) between the nicotinamide and the flavin rings occurs.[2] Thus, other protein regions subtly affect discrimination against NAD(H). Such additional specificity determinants are amino acyl residues interacting with the substrate pyrophosphate group[9] and the C-terminal tyrosine, whose side chain functions as a gate to protect the *re* face of the flavin.[10,11]

In addition to higher plants, algae, and cyanobacteria, plastidic-type FNRs have been found in Apicomplexa,[12] a phylum of parasites that includes the malaria- and toxoplasmosis-causing agents, and in the bacterium *Leptospira interrogans*, which causes leptospirosis in humans and other mammals.[13] Apicomplexan FNR colocalizes with a plant-type ferredoxin in the apicoplast, a phylum-specific organelle, phylogenetically related to algal plastids. *Plasmodium falciparum* FNR (PfFNR) exhibits most of the basic features of typical plastidic FNRs but diverges from them by displaying a low turnover number and a much weaker ability to discriminate between NADPH and NADH.[14,15] These functional differences result from a few critical details in the way the plasmodial

Received: January 18, 2012
Revised: April 20, 2012
Published: April 20, 2012

enzyme binds the 2′-phosphate group of NADPH.[14] The resulting peculiar interactions of PfFNR with the adenylate moiety of NADPH have been shown to be instrumental for the covalent dimerization of the enzyme under oxidizing conditions, which could be a physiological mechanism for turning off the enzyme activity in vivo.[15] Possibly, during the evolution of PfFNR, a trade-off has occurred between high specificity for the nicotinamide nucleotide substrate and a redox-based regulation mechanism. As a result, in PfFNR coenzyme specificity is controlled by a reduced set of enzyme–NADPH interactions as compared to those for other plastidic-type FNRs.[14] This greater simplicity makes PfFNR an ideal model for studying the events at the basis of NADP(H) recognition in the FNR protein family. Moreover, because this enzyme is a potentially excellent candidate as a target for novel antiplasmodial drugs,[16,17] a detailed understanding of its catalytic cycle is expected to contribute to the fight against malaria.

Here, we show that two PfFNR residues, namely, Y258 and H286, which interact with the 2′-phosphate and the pyrophosphate groups of NADPH, respectively (Figure 1),

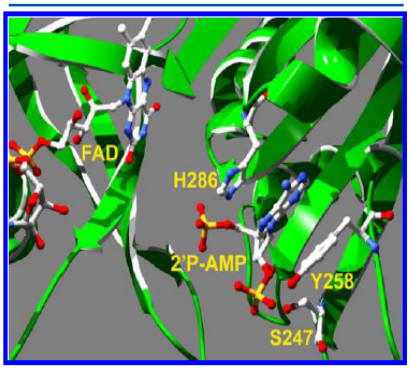

Figure 1. Three-dimensional structure of the PfFNR active site. Part of the cleft between the FAD-binding and NADP-binding domains is shown, with FAD, the substrate analogue adenosine 2′,5′-diphosphate (2′-PAMP), S247, Y258, and H286 represented as ball-and-stick models (PDB entry 2OK7, chain A). The distance between the oxygen atom of the Y258 side chain and the closest atom of the 2′-phosphate group of 2′-PAMP in the six protein molecules of the asymmetric unit has a mean value of 2.65 Å and a standard deviation of 0.13 Å.

have nonadditive roles in modulating the coenzyme specificity of this enzyme. Remarkably, removal of the Y258 hydroxyl group almost completely abolishes the ability of PfFNR to discriminate between NADPH and NADH, a result never accomplished before for any plant-type FNR through a single mutation.

MATERIALS AND METHODS

Materials. $NADP^+$, NADPH, and NADH were purchased from Sigma-Aldrich. All other chemicals were of the highest commercially available grade.

Site-Directed Mutagenesis. The base changes required for Y258F replacement were introduced into both pET-PfFNR[15] and pET-PfFNR-H286Q[18] using the QuikChange Lightning Site-Directed Mutagenesis Kit (Stratagene, Agilent Technologies Italia, Cernusco sul Naviglio, Milan, Italy) with the following pair of complementary mutagenic oligonucleotides (base changes underlined): 5′-TCAGATGCAACAAGTTTTT**TT**GTGCAAGATGAAATTTACAAAAGG-3′ and 5′-CCTTTTGTAAATTTCATCTTGCAC**AA**AAAACTTGTTGCATCTGA-3′.

The resulting plasmids, carrying the single mutation and the double mutation, were named pET-PfFNR-Y258F and pET-PfFNR-Y258F/H286Q, respectively, and their inserts were fully sequenced to verify the presence of the desired base changes and to rule out unwanted mutations.

Protein Overproduction and Purification. Wild-type and mutant PfFNR forms were overproduced in *Escherichia coli* Rosetta(DE3) and purified as previously reported.[18]

Spectral Analyses. Absorption spectra were recorded on a model 8453 diode-array (Agilent Technologies Italia) or a double-beam Cary 100 (Varian, Agilent Technologies Italia) spectrophotometer. The extinction coefficients of the mutant PfFNRs were determined on the basis of the amount of FAD released following sodium dodecyl sulfate treatment.[19] Spectrophotometric active-site titrations with $NADP^+$ were conducted at 16 °C in 50 mM Tris-HCl (pH 7.6), as reported previously.[18] To determine the K_d values of the $NADP^+$ complexes of the PfFNR variants carrying the Y258F replacement, which yielded low-intensity spectral perturbation upon ligand binding, the first derivative of their difference spectra ($d\Delta A/d\lambda$) was calculated to substantially improve the signal-to-noise ratio. Anaerobic photoreduction of the FAD prosthetic group of PfFNR forms was performed with the deazariboflavin/EDTA system[20] at 15 °C. The enzymes were diluted to ~15 μM in 50 mM HEPES-NaOH (pH 7.0) containing 10% glycerol, 15 mM EDTA, and 1.5 μM 5-carba-5-deazariboflavin. When present, $NADP^+$ was at a 1.2 molar ratio with respect to the enzyme.

Steady-State Kinetics. NADPH-dependent and NADH-dependent $K_3Fe(CN)_6$ activity assays were performed at 25 °C in 100 mM Tris-HCl (pH 8.2), as previously described.[18] To estimate the steady-state kinetic parameters of the enzyme forms, the concentrations of the electron donor (either NADPH or NADH) and of $K_3Fe(CN)_6$ were independently varied. All variants displayed a susceptibility to inhibition by the ferricyanide ion similar to that exhibited by the wild-type enzyme.[14] Because $K_3Fe(CN)_6$ was found to be saturating as a substrate at all concentrations tested, initial velocity data were fit to eq 1 by nonlinear regression analysis using GraFit version 5.0 (Erithacus Software Ltd., Horley, Surrey, U.K.):

$$v_0 = (k_{cat}[\text{PfFNR}]_T[\text{NAD(P)H}])/[(1+[\text{I}]/K_i)K_m + [\text{NAD(P)H}]] \quad (1)$$

where $[\text{PfFNR}]_T$ is the total concentration of the enzyme form considered, [NAD(P)H] is the concentration of either NADPH or NADH, which is considered the sole variable substrate, [I] represents the concentration of the competitive inhibitor $K_3Fe(CN)_6$, and K_i is the inhibition constant.

Rapid-Reaction Kinetics. Wild-type or mutant PfFNRs (17–19 μM, after mixing) were reacted with either NADPH or NADH (0.025–2 mM, after mixing) at 25 °C in 50 mM HEPES-NaOH (pH 7.0) under anaerobic conditions, using an SF-61 DX2 diode-array stopped-flow spectrophotometer (Hi-Tech Scientific, Bradford-upon-Avon, U.K.). For each shot, a set of 300 spectra within the 300–700 nm wavelength range was recorded over reaction times ranging from 0.5 to 7 s.

Table 1. Steady-State Kinetic Parameters of the PfFNR Variants for the NADPH− and NADH−$K_3Fe(CN)_6$ Reductase Reactions[a]

PfFNR	k_{cat}^{NADPH}[b] (s^{-1})	K_m^{NADPH} (μM)	k_{cat}/K_m^{NADPH} ($s^{-1}\ \mu M^{-1}$)	k_{cat}^{NADH}[b] (s^{-1})	K_m^{NADH} (μM)	k_{cat}/K_m^{NADH} ($s^{-1}\ \mu M^{-1}$)	NADPH:NADH specificity ratio[c]
wild type	125 ± 4[d]	36 ± 6[d]	3.5 ± 0.5[d]	48 ± 2	720 ± 90	0.05 ± 0.005	70
H286Q	185 ± 3[d]	57 ± 5[d]	3.3 ± 0.3[d]	100 ± 3	715 ± 80	0.15 ± 0.015	22
Y258F	50 ± 0.5	160 ± 16	0.3 ± 0.03	47 ± 1	260 ± 40	0.2 ± 0.04	1.5
Y258F/H286Q	53 ± 0.5	240 ± 17	0.2 ± 0.01	47 ± 1	360 ± 40	0.15 ± 0.015	1.3

[a]The inhibitory effect of $K_3Fe(CN)_6$, which acts on PfFNR as a competitive inhibitor with respect to both NADPH and NADH,[14] was taken into account in the calculation of the kinetic parameters, as described in Materials and Methods. [b]k_{cat} values are expressed as moles of NADPH or NADH oxidized per mole of active site (FAD) per second. [c]Coenzyme specificity expressed as the ratio of k_{cat}/K_m^{NADPH} to k_{cat}/K_m^{NADH}. [d]Data taken from ref 18.

Absorbance traces were fit to exponential decay equations using KinetAsyst version 3.0 (Hi-Tech Scientific). In agreement with our previous report,[18] absorbance traces were biphasic, displaying the same rate constant values over the entire wavelength range considered. The slow phase, which accounted only for minor spectral changes, occurred at a rate that was independent of reductant concentration and was too low to represent a process involved in catalysis. The apparent rate constants of the fast phase (k_{app}) at different NADH or NADPH concentrations were calculated by averaging the values obtained by fitting the absorbance traces from at least three shots. To estimate the rate of HT (k_{HT}), the k_{app} values at different NADPH or NADH concentrations were fit to the equation of a hyperbole and its upper limit was extrapolated.

RESULTS AND DISCUSSION

The two PfFNR variants carrying either the single Y258F and double Y258F/H286Q replacement were synthesized in the bacterial host at levels comparable to that of the wild-type enzyme and were purified with similar yields, indicating that the Y258F mutation does not markedly affect the folding process or the stability of the native conformation of the protein. Similarly, the amino acyl replacement induced no alteration of the absorbance spectrum of the flavoenzyme, so that the same extinction coefficient of 10 $mM^{-1}\ cm^{-1}$ at 454 nm[14] could be used to quantify all the PfFNR forms studied here.

The reactivity toward NADPH of PfFNR variants carrying different replacements at position 286 was previously studied in detail and reported elsewhere.[18] Because that study indicated that H286 plays a role in orienting the NMN moiety during HT and because such a steering effect is known to affect coenzyme specificity in plastidic-type FNRs, we measured the NADH-dependent activity of the PfFNR-H286Q, PfFNR-H286K, PfFNR-H286A, and PfFNR-H286L variants, previously produced.[18] As expected, the specificity of all variants was significantly impaired with respect to that of the wild-type enzyme. However, only for PfFNR-H286Q could reliable kinetic data be obtained, the NADH-dependent activity of the other variants being too low for accurate measurements. As shown in Table 1, while the H286Q mutation hardly affected the K_m values for either NADPH or NADH, it significantly increased both k_{cat}^{NADPH} and k_{cat}^{NADH}. As a consequence of the stronger effect on k_{cat}^{NADH}, PfFNR-H286Q was found to be 3.2-fold less specific for the pyridine nucleotide than the wild-type enzyme. This result is in keeping with the previous report of a similar effect obtained by mutating the corresponding site in *Anabaena* FNR.[9] For these reasons, the contribution to the specificity of H286 was not further studied by the detailed analysis of additional H286 mutants.

NADPH/NADH specificity of PfFNR ultimately relies on interactions between the protein and the 2′-phosphate group of NADPH. Y258, which provides the second aromatic ring, in addition to H286, to sandwich the adenine moiety of the coenzyme, also donates a H-bond to the 2′-phosphate group of NADPH (Figure 1). Replacement of Y258 with a phenylalanine is expected to disrupt the latter interaction while leaving aromatic stacking unaffected. Thus, the Y258F substitution was introduced into both wild-type PfFNR and its H286Q variant. As shown in Table 1, the effect of the mutation on the steady-state kinetic parameters of PfFNR was largely independent of the presence of histidine or glutamine at position 286. In particular, the Y258F replacement abolished the difference between the k_{cat}^{NADPH} and k_{cat}^{NADH} of the single and double mutants, decreasing their k_{cat}^{NADPH} values to match almost exactly that of wild-type PfFNR for NADH. Furthermore, the Y258F mutation had opposite effects on K_m^{NADPH} and K_m^{NADH}, significantly increasing the former and lowering the latter. The combination of these effects led to a 50-fold decrease in the PfFNR specificity ratio, i.e., the ratio between the k_{cat}/K_m of each enzyme form for the two coenzymes, which dropped to a mere 1.3−1.5 (Table 1). Interestingly, the effect of H286Q and Y258F replacements displayed no additivity. Rather, the Y258F substitution fully abolished the enhancing effect the H286Q replacement had on the k_{cat} values of PfFNR.

Steady-state kinetic data (Table 1) suggested that the Y258 hydroxyl of PfFNR could have an important role in optimizing the HT from NADPH to FAD. This finding was not unexpected, because, as mentioned in the introductory section, the preference of plastidic-type FNRs for NADPH over NADH relies on both lower K_m and higher k_{cat} values for the former dinucleotide.[2,8] Because k_{cat} is related to the rate of HT between the nicotinamide nucleotide and the FAD prosthetic group in the enzyme−cofactor complex,[15] we studied in detail the reductive half-reaction of the enzyme forms by stopped-flow spectrophotometry, using both NADPH and NADH as the reductant. Experimental conditions matched those used in our previous studies of the reaction of PfFNR and its H286 mutants with NADPH,[15,18] allowing direct comparisons. Like other well-characterized members of plastidic-type FNRs,[2] the reaction of PfFNR with NADPH led to the formation of a charge-transfer complex (CT) between NADPH and FAD, which could be observed as an increase in the absorption above 550 nm, which was completed in the dead time of the instrument (2−3 ms). This process was followed by the bleaching of the flavin corresponding to the reduction of the prosthetic group, which occurred in a biphasic fashion. The fast phase, accounting for most of the total absorbance change, corresponds to HT; the slow one, which took place at a rate not

compatible with catalysis, most probably represents a rearrangement of the reaction product.[18] Notably, a clear positive correlation between the extent of CT accumulation during the reaction of the various enzyme forms with NADPH and the k_{HT} value was observed.[18] In particular, PfFNR-H286Q displayed both an increased amount of transient CT formation and a higher k_{HT} for NADPH with respect to those of the wild-type enzyme (Figures 2 and 3). Here, we report for the first time the pre-steady-state characterization of the reaction of PfFNR forms with NADH. In agreement with steady-state data, the wild-type enzyme reacted with NADH showing a k_{HT} that is 44% of that determined with NADPH, with no significant CT formation (Figures 2 and 3 and Table 2). PfFNR-H286Q displayed a k_{HT} for NADH 2-fold higher than that of PfFNR, although such a large increase was not paralleled by formation of a significant amount of CT during the reaction. The Y258F mutation lowered the k_{HT} for NADPH to 50% of that of the wild type (Table 2) and abolished the accumulation of CT (Figures 2 and 3). Interestingly, the Y258F mutation did not hamper HT from NADH to FAD; on the contrary, it seemed to slightly increase the k_{HT} for NADH, in comparison to that of the wild-type enzyme (Table 2). The PfFNR-Y258F/H286Q double mutant displayed kinetic properties in all respects identical to those of PfFNR-Y258F (Figure 3 and Table 2), confirming that the effects of the Y258F replacement completely overshadow those of the H286Q one. As we showed elsewhere,[15] the k_{cat} of the NADPH–$K_3Fe(CN)_6$ reductase reaction catalyzed by PfFNR matches very well the k_{HT} value determined by stopped-flow spectrophotometry. Here we confirm that the turnover rate under saturating conditions is limited by the HT step, as shown by the nearly identical effects that the mutations introduced into PfFNR had on the k_{cat} and k_{HT} values of both NADPH- and NADH-dependent reactions (Tables 1 and 2).

Rapid-reaction kinetics strongly suggested that the decrease in the HT rate determined by Y258 hydroxyl deletion when NADPH, but not NADH, is the hydride donor might be the result of a specific destabilization of the catalytically competent conformation of bound NADPH, which in the wild-type and H286Q enzymes is associated with the transient formation of the CT between NADPH and FAD. To further confirm this conclusion, we subjected PfFNR-Y258F and PfFNR-Y258F/H286Q to anaerobic photoreduction in the absence and presence of $NADP^+$ in comparison with PfFNR and PfFNR-H286Q. In the absence of the ligand, the FAD prosthetic group of all PfFNR variants underwent reduction to the hydroquinone form in a similar fashion, with the accumulation of very small amounts of the FAD neutral semiquinone during the process (not shown). In the late stages of the photoreduction conducted in the presence of $NADP^+$, a long-wavelength absorbing species was observed in the case of the wild-type enzyme, representing a CT species (Figure 4A). We have previously shown that the amount of CT was slightly but significantly higher in the case of PfFNR-H286Q than in the case of the wild-type enzyme.[18] On the other hand, as clearly shown in panels B and C of Figure 4, no CT species were detected during the reduction of PfFNR-Y258F or PfFNR-Y258F/H286Q in the presence of $NADP^+$.

To further investigate the contribution of Y258 to substrate recognition, we studied the interaction of the PfFNR forms with $NADP^+$ by differential spectrophotometry. It is well-known that binding of $NADP^+$ to FNR perturbs the visible absorption spectrum of bound FAD,[10] and that the positive

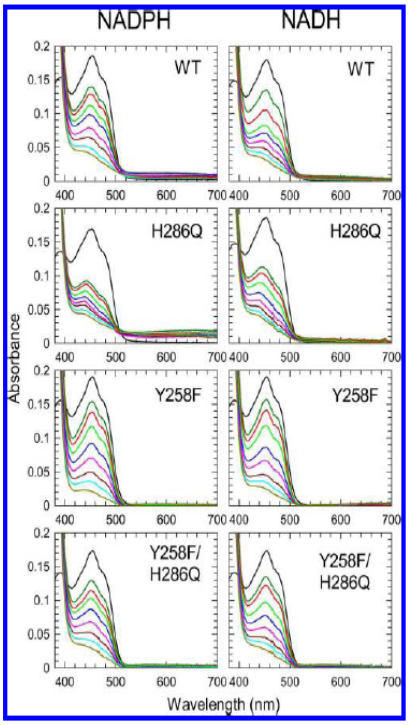

Figure 2. Spectra recorded by stopped-flow spectrophotometry during the anaerobic reduction of PfFNR forms by NADPH and NADH. PfFNR forms (17–19 μM) were reacted with 500 μM NADPH (left) or NADH (right) at 25 °C under anaerobiosis in 50 mM HEPES-NaOH (pH 7.0). In each panel, the spectrum of the oxidized PfFNR form is colored black while those recorded at increasing reaction times after mixing are depicted in different colors. NADPH: WT, 1 (dark green), 2 (red), 5 (light green), 7 (blue), 11 (magenta), 17 (brown), 61 (aqua), and 1000 ms (olive); H286Q, 0.74 (dark green), 2.2 (red), 3.7 (light green), 6.7 (blue), 11 (magenta), 32 (brown), 110 (aqua), and 450 ms (olive); Y258F, 1 (dark green), 3 (red), 7 (light green), 13 (blue), 21 (magenta), 41 (brown), 105 (aqua), and 600 ms (olive); Y258F/H286Q, 2 (dark green), 5 (red), 9 (light green), 15 (blue), 25 (magenta), 51 (brown), 165 (aqua), and 600 ms (olive). NADH: WT, 3 (dark green), 9 (red), 17 (light green), 23 (blue), 33 (magenta), 53 (brown), 115 (aqua), and 600 ms (olive); H286Q, 2 (dark green), 5 (red), 9 (light green), 19 (blue), 57 (magenta), 145 (brown), 275 (aqua), and 600 ms (olive); Y258F, 1 (dark green), 3 (red), 7 (light green), 15 (blue), 25 (magenta), 63 (brown), 155 (aqua), and 600 ms (olive); Y258F/H286Q, 1 (dark green), 3 (red), 9 (light green), 15 (blue), 25 (magenta), 51 (brown), 131 (aqua), and 600 ms (olive). Spectra of panels NADPH-WT and NADPH-H286Q are taken from ref 18 and are shown here for comparison.

peak around 500 nm in the difference spectrum (Figure 5A) is induced by the stacking between the $NADP^+$ nicotinamide and the FAD isoalloxazine.[11] Thus, the spectrophotometric titration of PfFNR with $NADP^+$ provides both the K_d of the resulting complex and a semiquantitative evaluation of the extent of occupancy of the enzyme active site by the nicotinamide ring of

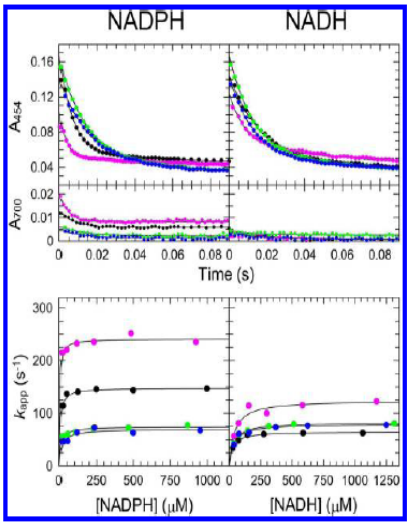

Figure 3. Time course and dependence by the concentration of NADPH and NADH of the reductive half-reaction of PfFNR forms, as studied by stopped-flow spectrophotometry. Enzyme forms (17−19 μM) were reacted at 25 °C, under anaerobiosis, in 50 mM HEPES-NaOH (pH 7.0) with NADPH and NADH at concentrations ranging from ≈25 μM to >1 mM after mixing. The top panels shows the absorbance at 454 and 700 nm recorded during the reaction of PfFNR (black), PfFNR-H286Q (magenta), PfFNR-Y258F (green), and PfFNR-Y258F/H286Q (blue) with NADPH (left) or NADH (right). The bottom panels show plots of the observed rate constant of the fast phase of the reaction (k_{app}) as a function of the concentration of NADPH (left) or NADH (right). Data from the four enzyme forms are reported in the same colors used in the top panels. Fitting the data sets with the equation of a rectangular hyperbola yielded the limit values for k_{app} (which provide the estimates of the corresponding k_{HT} values) reported in Table 2.

Table 2. Rate Constants of Hydride Transfer from NADPH and NADH to FAD in PfFNR Variants As Determined by Stopped-Flow Spectrophotometry

	k_{HT} (s^{-1})	
PfFNR form	NADPH	NADH
wild type	148 ± 2[a]	65 ± 1
H286Q	240 ± 4[a]	125 ± 7
Y258F	74 ± 2	83 ± 1
Y258F/H286Q	70 ± 4	80 ± 2

[a]Data taken from ref 18.

the ligand. As shown in Figure 5B, all mutant PfFNRs displayed a significantly lower affinity for $NADP^+$ in comparison to that of the wild-type protein, with the K_d values of the enzyme−$NADP^+$ complexes increased 2- or 3-fold (Table 3). More interestingly, as deduced from the comparison of the difference spectra displayed in Figure 5A and from the values of the differential extinction coefficient of the enzyme−$NADP^+$ complexes reported in Table 3, removal of the Y258 hydroxyl group highly destabilized the nicotinamide−flavin interaction. Such destabilization occurred even when the Y258F mutation

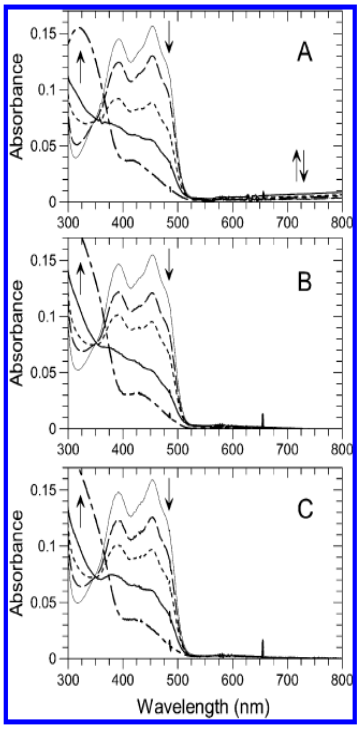

Figure 4. Anaerobic photoreduction of the FAD prosthetic group of PfFNR variants in the presence of $NADP^+$. Spectra of anaerobic mixtures of ≈15 μM PfFNR (A), PfFNR-Y258F (B), and PfFNR-Y258F/H286Q (C) in the presence of a slight excess of $NADP^+$ in 50 mM HEPES-NaOH (pH 7.0) recorded before (thin solid line) and after increasing irradiation times with visible light (different line styles). Arrows indicate the direction of the spectral changes observed during the experiment. Spectra were not corrected for the contribution of 5-deazariboflavin present in the mixtures.

was introduced into the PfFNR-H286Q variant, where the ring stacking interaction is stronger than in the case of PfFNR.

Taken as a whole, these data allow us to conclude that the Y258 side chain favors the adoption of the catalytically competent conformation of the NMN moiety of NADPH, enhancing HT and, therefore, enzyme turnover. In addition to productively interacting with NADPH, thus making it a good substrate, the side chain of Y258 also actively discriminates against NADH, by keeping K_m^{NADH} high. The structural basis of the latter effect can be rationalized considering that in the unbound PfFNR the side chain of Y258 is H-bonded to that of K249.[14] Whatever substrate is bound, either NADPH or NADH, this H-bond is severed because of the reported induced-fit reorganization of the substrate binding site.[14] However, while the binding energy lost by breaking the H-bond with K249 is compensated by the new interaction beween Y258 and NADPH, this compensation is not possible in the case of NADH, which lacks the 2′-phosphate group.

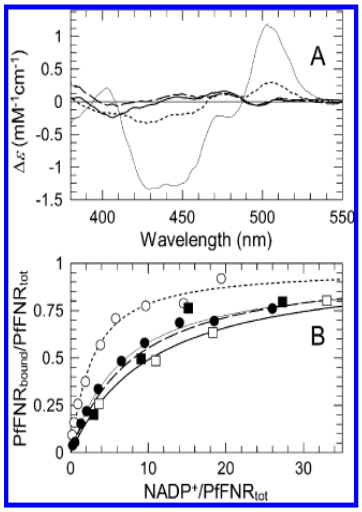

Figure 5. Binding of $NADP^+$ by PfFNR variants as studied by difference spectrophotometry. Spectrophotometric titrations of PfFNR forms with $NADP^+$ in 50 mM Tris-HCl (pH 7.6) at 15 °C. Data for the titrations of PfFNR and PfFNR-H286Q were taken from ref 17 and are displayed for comparison. (A) Difference spectra of enzyme–$NADP^+$ complexes computed by extrapolation to infinite $NADP^+$ concentration, for PfFNR (dotted line), PfFNR-H286Q (thin solid line), PfFNR-Y258F (thick solid line), and PfFNR-Y258F/H286Q (dashed line). (B) Progress of the titration of PfFNR (○), PfFNR-H286Q (●), PfFNR-Y258F (□), and PfFNR-Y258F/H286Q (■). Each curve was obtained by nonlinear fitting of the data with the theoretical equation for 1:1 binding.

Table 3. Dissociation Constants of the Complexes between the PfFNR Variants and $NADP^+$ and Intensities of the Ligand-Induced Spectral Perturbation of Bound FAD

PfFNR form	K_d (μM)	$\Delta\varepsilon_{508}$ (mM^{-1} cm^{-1})
wild type	60 ± 9[a]	0.30 ± 0.01
H286Q	130 ± 10[a]	1.14 ± 0.04
Y258F	170 ± 30	0.04 ± 0.002
Y258F/H286Q	130 ± 40	0.03 ± 0.002

[a]Data taken from ref 18.

What is the possible structural explanation of the effect of the interaction between PfFNR Y258 and NADPH 2′-phosphate on k_{cat}^{NADPH}? As in the other plastidic-type FNRs, PfFNR mainly interacts with the adenylate moiety of NADP(H). Indeed, the adenine, the 2′-phosphate, and the 5′-phosphate groups provide most contact sites.[2] The overlay of the crystal structures of ligand-free and 2′-PAMP-bound PfFNR displayed in Figure 6 clearly shows that the binding of this ligand, which mimics the adenylate half of the coenzyme, in addition to determining the unfolding of two turns of the αF helix, induces a large (2 Å) shift of the αH helix (residues 288–298), which moves away from FAD.[14] The N-terminal side of αH helix points toward the carboxylate of the C-terminal Y316, whose side chain stacks onto the *re* face of the flavin ring. Therefore, it is conceivable that the helix shift relieves some steric pressure from the latter residue, favoring the displacement of its phenolic side chain by

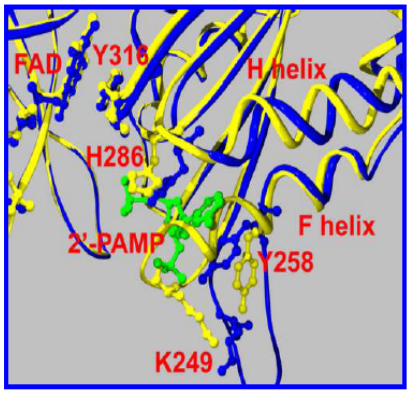

Figure 6. Induced-fit conformational changes induced by binding of 2′-PAMP to PfFNR. The crystal structures of ligand-free (PDB entry 2OK8, chain A) and 2′-PAMP-bound (PDB entry 2OK7, chain A) PfFNR are colored yellow and blue, respectively. Relevant amino acyl residues and ligands are represented as ball-and-stick models. 2′-PAMP is colored green.

the incoming nicotinamide ring of the bound coenzyme. H286 is located at a strategic site (i.e., in the loop connecting the β10 strand to the αH helix) to drive such helix movement when NADPH occupies its binding site. In our hypothesis, the adenylate moiety of the substrate acts as a lever on the αH helix: when the 2′-phosphate group of the ligand is anchored to the S247 and Y258 side chains, the interactions of the 5′-phosphate and adenine groups with H286 induce the above-described αH helix shift, which allows the nicotinamide ring of the coenzyme to access the active site.

The PfFNR specificity ratio of 70 (Table 1) is orders of magnitude lower than the corresponding value of 180000, reported for its homologue of *Toxoplasma gondii*,[21] a parasite related to *Plasmodium*. Thus, it is worth discussing the possible reasons for the poor selectivity of PfFNR for NADPH. As we previously reported, an obvious structural basis for the limited specificity of PfFNR is the lack of positively charged side chains interacting with the 2′-phosphate group of NADPH.[14] We have also shown that PfFNR undergoes a $NADP^+$-triggered dimerization process that results in enzyme inactivation in the presence of oxidizing agents, such as H_2O_2, which lock the homodimer via the formation of an intersubunit disulfide bridge.[15] The formation of the inactive homodimer is favored by NADP(H) binding in two ways, namely, (i) by promoting the unfolding of the αF helix in each subunit, which removes a major steric obstacle to dimerization, and (ii) by leading to the formation of two ionic interactions between the 2′-phosphate of the ligand molecules and the side chains of K287 and K292 of each opposite subunit.[14] The absence of ionic bonds involving the 2′-phosphate within the same subunit is thus functional to the inactivation process, where two NADP(H) molecules are sandwiched at the intersubunit interface of the dimer.[14] The low coenzyme specificity of PfFNR in comparison to those of its orthologs may well be due to specific metabolic features of the plasmodial apicoplast. Unfortunately, the actual concentrations of NADH and NADPH in the organelle are not available, and although some plasmodial apicoplast enzymes are thought to be highly NADH- or NADPH-specific,[22−24] a

comprehensive kinetic characterization with both coenzymes has been reported for none of them. In the absence of more convincing explanations, it is tempting to hypothesize that the loss of specificity might represent the price paid by PfFNR to gain a regulation mechanism of its catalytic activity. The rationale behind the ability of PfFNR to be turned off by oxidants could reside in the need for the parasite to save NADPH to cope with reactive oxygen species under oxidative stress conditions.[25]

CONCLUSION

Through the interpretation of our results in light of the crystal structure of PfFNR, we have provided a sound picture of the structural bases of the coenzyme specificity of this enzyme. The obvious question is whether this model can be extended to interpret coenzyme specificity in the other plastidic-type FNRs. At first glance, the answer is negative. Indeed, PfFNR is the only member of this group of enzymes known to undergo a large conformational change upon coenzyme binding.[2] Furthermore, H286 is not conserved in nonplasmodial FNRs. However, the bulky, aliphatic residue that in other plastidic-type FNRs replaces it (usually a leucine) similarly interacts with the adenine moiety of the ligand and contributes to coenzyme specificity.[9] In pea leaf FNR, it has been experimentally shown that binding of 2′-PAMP, which mimics the NADP(H) adenylate moiety, favors the interaction of analogues of the nicotinamide ring with the active site.[26] This induced-fit effect has been proposed to be mediated by a conformational transition involving the loop that in PfFNR includes C284, G285, and H286, which is in contact with the C-terminal tyrosine that controls access to the active site.[26] Small conformational changes in this loop have actually been observed in *Anabaena* FNR upon $NADP^+$ binding by X-ray crystallography.[27] Moreover, the comparison among free and $NADP^+$-bound forms of *Anabaena* FNR (PDB entries 1QUE, 1QUF, and 1GJR)[27] shows that binding of $NADP^+$ (resulting in complexes where the adenylate moiety occupies the expected binding site, but the NMN portion of the ligand adopts conformations incompatible with HT) also induces small rearrangements also in the 267−279 α helix, which corresponds to the αH helix of PfFNR. A similar comparison between the crystal structures of free (PDB entry 1FNB) and 2′-PAMP-bound (PDB entry 1FND) spinach leaf FNR[28] shows that also in this protein ligand binding induces a small 0.3−0.4 Å shift in the same α helix (residues 276−290). Thus, although this phenomenon is particularly marked in the case of PfFNR, our results strongly support the notion that the k_{cat} component of the coenzyme specificity of plastidic-type FNRs is based on induced-fit conformational changes of variable extents, in which structural alterations of the loop that includes H286 and the shift of the α helix pointing toward the C-terminus of the protein play a significant role.

AUTHOR INFORMATION

Corresponding Author

*Department of Biomolecular Sciences and Biotechnology, Università degli Studi di Milano, via Celoria 26, 20133 Milano, Italy. Phone: +39 02 50314897. Fax: +39 02 50314895. E-mail: alessandro.aliverti@unimi.it.

Notes

The authors declare no competing financial interest.

ACKNOWLEDGMENTS

We are grateful to Dr. Laura Marangoni for valuable technical assistance in performing some of the experiments here reported.

ABBREVIATIONS

FNR, ferredoxin-$NADP^+$ reductase (EC 1.18.1.2); NADP(H), $NADP^+$ or NADPH; NAD(H), NAD^+ or NADH; HT, hydride transfer; PfFNR, *P. falciparum* FNR; 2′-PAMP, adenosine 2′,5′-diphosphate; k_{app}, apparent first-order rate constant; k_{HT}, rate constant of HT; NMN, nicotinamide mononucleotide; CT, charge-transfer complex; PDB, Protein Data Bank.

REFERENCES

(1) Ceccarelli, E. A., Arakaki, A. K., Cortez, N., and Carrillo, N. (2004) Functional plasticity and catalytic efficiency in plant and bacterial ferredoxin-NADP(H) reductases. *Biochim. Biophys. Acta 1698*, 155−165.

(2) Aliverti, A., Pandini, V., Pennati, A., de Rosa, M., and Zanetti, G. (2008) Structural and functional diversity of ferredoxin-$NADP^+$ reductases. *Arch. Biochem. Biophys. 474*, 283−291.

(3) Medina, M. (2009) Structural and mechanistic aspects of flavoproteins: Photosynthetic electron transfer from photosystem I to $NADP^+$. *FEBS J. 276*, 3942−3958.

(4) Karplus, P. A., Daniels, M. J., and Herriott, J. R. (1991) Atomic structure of ferredoxin-$NADP^+$ reductase: Prototype for a structurally novel flavoenzyme family. *Science 251*, 60−66.

(5) Laursen, T., Jensen, K., and Møller, B. L. (2011) Conformational changes of the NADPH-dependent cytochrome P450 reductase in the course of electron transfer to cytochromes P450. *Biochim. Biophys. Acta 1814*, 132−138.

(6) Sumimoto, H. (2008) Structure, regulation and evolution of Nox-family NADPH oxidases that produce reactive oxygen species. *FEBS J. 275*, 3249−3277.

(7) Stuehr, D. J., Tejero, J., and Haque, M. M. (2009) Structural and mechanistic aspects of flavoproteins: Electron transfer through the nitric oxide synthase flavoprotein domain. *FEBS J. 276*, 3959−3974.

(8) Medina, M., Luquita, A., Tejero, J., Hermoso, J., Mayoral, T., Sanz-Aparicio, J., Grever, K., and Gomez-Moreno, C. (2001) Probing the determinants of coenzyme specificity in ferredoxin-$NADP^+$ reductase by site-directed mutagenesis. *J. Biol. Chem. 276*, 11902−11912.

(9) Tejero, J., Martínez-Julvez, M., Mayoral, T., Luquita, A., Sanz-Aparicio, J., Hermoso, J. A., Hurley, J. K., Tollin, G., Gómez-Moreno, C., and Medina, M. (2003) Involvement of the pyrophosphate and the 2′-phosphate binding regions of ferredoxin-$NADP^+$ reductase in coenzyme specificity. *J. Biol. Chem. 278*, 49203−49214.

(10) Deng, Z., Aliverti, A., Zanetti, G., Arakaki, A. K., Ottado, J., Orellano, E. G., Calcaterra, N. B., Ceccarelli, E. A., Carrillo, N., and Karplus, P. A. (1999) A productive $NADP^+$ binding mode of ferredoxin-$NADP^+$ reductase revealed by protein engineering and crystallographic studies. *Nat. Struct. Biol. 6*, 847−853.

(11) Piubelli, L., Aliverti, A., Arakaki, A. K., Carrillo, N., Ceccarelli, E. A., Karplus, P. A., and Zanetti, G. (2000) Competition between C-terminal tyrosine and nicotinamide modulates pyridine nucleotide affinity and specificity in plant ferredoxin-$NADP^+$ reductase. *J. Biol. Chem. 275*, 10472−10476.

(12) Vollmer, M., Thomsen, N., Wiek, S., and Seeber, F. (2001) Apicomplexan parasites possess distinct nuclear-encoded, but apicoplast-localized, plant-type ferredoxin-$NADP^+$ reductase and ferredoxin. *J. Biol. Chem. 276*, 5483−5490.

(13) Nascimento, A. S., Catalano-Dupuy, D. L., Bernardes, A., de Oliveira Neto, M., Santos, M. A., Ceccarelli, E. A., and Polikarpov, I. (2007) Crystal structures of *Leptospira interrogans* FAD-containing ferredoxin-$NADP^+$ reductase and its complex with $NADP^+$. *BMC Struct. Biol. 7*, 69.

(14) Milani, M., Balconi, E., Aliverti, A., Mastrangelo, E., Seeber, F., Bolognesi, M., and Zanetti, G. (2007) Ferredoxin-NADP$^+$ reductase from *Plasmodium falciparum* undergoes NADP$^+$-dependent dimerization and inactivation: Functional and crystallographic analysis. *J. Mol. Biol. 367*, 501−513.
(15) Balconi, E., Pennati, A., Crobu, D., Pandini, V., Cerutti, R., Zanetti, G., and Aliverti, A. (2009) The ferredoxin-NADP$^+$ reductase/ferredoxin electron transfer system of *Plasmodium falciparum*. *FEBS J. 276*, 3825−3836.
(16) Röhrich, R. C., Englert, N., Troschke, K., Reichenberg, A., Hintz, M., Seeber, F., Balconi, E., Aliverti, A., Zanetti, G., Köhler, U., Pfeiffer, M., Beck, E., Jomaa, H., and Wiesner, J. (2005) Reconstitution of an apicoplast-localised electron transfer pathway involved in the isoprenoid biosynthesis of *Plasmodium falciparum*. *FEBS Lett. 579*, 6433−648.
(17) Seeber, F., Aliverti, A., and Zanetti, G. (2005) The plant-type ferredoxin-NADP$^+$ reductase/ferredoxin redox system as a possible drug target against apicomplexan human parasites. *Curr. Pharm. Des. 11*, 3159−3172.
(18) Crobu, D., Canevari, G., Milani, M., Pandini, V., Vanoni, M. A., Bolognesi, M., Zanetti, G., and Aliverti, A. (2009) *Plasmodium falciparum* ferredoxin-NADP$^+$ reductase His286 plays a dual role in NADP(H) binding and catalysis. *Biochemistry 48*, 9525−9533.
(19) Aliverti, A., Curti, B., and Vanoni, M. A. (1999) Identifying and quantitating FAD and FMN in simple and in iron-sulfur-containing flavoproteins. *Methods Mol. Biol. 131*, 9−23.
(20) Massey, V., and Hemmerich, P. (1977) A photochemical procedure for reduction of oxidation-reduction proteins employing deazariboflavin as catalyst. *J. Biol. Chem. 252*, 5612−5614.
(21) Pandini, V., Caprini, G., Thomsen, N., Aliverti, A., Seeber, F., and Zanetti, G. (2002) Ferredoxin-NADP$^+$ reductase and ferredoxin of the protozoan parasite *Toxoplasma gondii* interact productively *in vitro* and *in vivo*. *J. Biol. Chem. 277*, 48463−48471.
(22) Krauth-Siegel, R. L., Müller, J. G., Lottspeich, F., and Schirmer, R. H. (1996) Glutathione reductase and glutamate dehydrogenase of *Plasmodium falciparum*, the causative agent of tropical malaria. *Eur. J. Biochem. 235*, 345−350.
(23) Kapoor, M., Dar, M. J., Surolia, A., and Surolia, N. (2001) Kinetic determinants of the interaction of enoyl-ACP reductase from *Plasmodium falciparum* with its substrates and inhibitors. *Biochem. Biophys. Res. Commun. 289*, 832−837.
(24) Pillai, S., Rajagopal, C., Kapoor, M., Kumar, G., Gupta, A., and Surolia, N. (2003) Functional characterization of β-ketoacyl-ACP reductase (FabG) from *Plasmodium falciparum*. *Biochem. Biophys. Res. Commun. 303*, 387−392.
(25) Kehr, S., Sturm, N., Rahlfs, S., Przyborski, J. M., and Becker, K. (2010) Compartmentation of redox metabolism in malaria parasites. *PLoS Pathog. 6*, e1001242.
(26) Paladini, D. H., Musumeci, M. A., Carrillo, N., and Ceccarelli, E. A. (2009) Induced fit and equilibrium dynamics for high catalytic efficiency in ferredoxin-NADP(H) reductases. *Biochemistry 48*, 5760−5768.
(27) Hermoso, J. A., Mayoral, T., Faro, M., Gómez-Moreno, C., Sanz-Aparicio, J., and Medina, M. (2002) Mechanism of coenzyme recognition and binding revealed by crystal structure analysis of ferredoxin-NADP$^+$ reductase complexed with NADP. *J. Mol. Biol. 319*, 1133−1142.
(28) Bruns, C., and Karplus, P. A. (1995) Refined crystal structure of spinach ferredoxin reductase at 1.7 Å resolution: Oxidized, reduced and 2′-phospho-5′-AMP bound states. *J. Mol. Biol. 247*, 125−145.

doi:10.1016/j.jmb.2011.06.010 J. Mol. Biol. (2011) 411, 463–473

Contents lists available at www.sciencedirect.com

Journal of Molecular Biology

journal homepage: http://ees.elsevier.com.jmb

FAD-Binding Site and NADP Reactivity in Human Renalase: A New Enzyme Involved in Blood Pressure Regulation

Mario Milani[1,2], Francesco Ciriello[1], Sara Baroni[1], Vittorio Pandini[1], Giulia Canevari[1,3], Martino Bolognesi[1,2] and Alessandro Aliverti[1]*

[1]*Dipartimento di Scienze Biomolecolari e Biotecnologie, Università degli Studi di Milano, via Celoria 26, 20133 Milan, Italy*

[2]*CNR-Istituto di Biofisica, Università degli Studi di Milano, via Celoria 26, 20133 Milan, Italy*

[3]*Department of Chemical Core Technologies, Nerviano Medical Sciences, Oncology, Viale Pasteur 10, Nerviano 20014, Italy*

Received 19 April 2011;
received in revised form
6 June 2011;
accepted 7 June 2011
Available online
14 June 2011

Edited by M. Guss

Keywords:
chronic kidney disease;
end-stage renal disease;
hypertension;
phosphate excretion;
flavoprotein structure

Renalase is a recently discovered flavoprotein that regulates blood pressure, regulates sodium and phosphate excretion, and displays cardioprotectant action through a mechanism that is barely understood to date. It has been proposed to act as a catecholamine-degrading enzyme, via either O_2-dependent or NADH-dependent mechanisms. Here we report the renalase crystal structure at 2.5 Å resolution together with new data on its interaction with nicotinamide dinucleotides. Renalase adopts the *p*-hydroxybenzoate hydroxylase fold topology, comprising a Rossmann-fold-based flavin adenine dinucleotide (FAD)-binding domain and a putative substrate-binding domain, the latter of which contains a five-stranded anti-parallel β-sheet. A large cavity (228 $Å^3$), facing the flavin ring, presumably represents the active site. Compared to monoamine oxidase or polyamine oxidase, the renalase active site is fully solvent exposed and lacks an 'aromatic cage' for binding the substrate amino group. Renalase has an extremely low diaphorase activity, displaying lower k_{cat} but higher k_{cat}/K_m for NADH compared to NADPH. Moreover, its FAD prosthetic group becomes slowly reduced when it is incubated with NADPH under anaerobiosis, and binds NAD^+ or $NADP^+$ with K_d values of ca 2 mM. The absence of a recognizable NADP-binding site in the protein structure and its poor affinity for, and poor reactivity towards, NADH and NADPH suggest that these are not physiological ligands of renalase. Although our study does not answer the question on the catalytic activity of renalase, it provides a firm framework for testing hypotheses on the molecular mechanism of its action.

*Corresponding author. E-mail address: alessandro.aliverti@unimi.it.

Abbreviations used: FAD, flavin adenine dinucleotide; MAO, monoamine oxidase; EDTA, ethylenediaminetetraacetic acid; INT, 2-(4-iodophenyl)-3-(4-nitrophenyl)-5-phenyl-2*H*-tetrazolium chloride; WST1, 2-(4-iodophenyl)-3-(4-nitrophenyl)-5-(2,4-disulfophenyl)-2*H*-tetrazolium sodium salt; HT, hydride transfer; MR, molecular replacement; PHBH, *p*-hydroxybenzoate hydroxylase; PDB, Protein Data Bank.

Introduction

Renalase was identified in a 2005 study that focused on new links between chronic kidney diseases and their cardiovascular complications.[1] The human renalase gene (*RNLS*) is located on chromosome 10 and includes 10 exons.[2] Various isoforms arising from alternative splicing have been reported, two of which (renalase1 and renalase2) are annotated in genome databases (GenBank accession numbers NP_001026879 and NP_060833, respectively). *RNLS* is expressed in the kidneys, heart, skeletal muscle, brain, and small intestine;[3] the main product (renalase1) has been detected also in blood, plasma, and urine.[2] End-stage renal disease is associated with lowered plasma renalase1 levels, indicating that the kidneys are the source of the circulating protein.[1] Renalase has also been proposed as an early biomarker of acute kidney ischemia.[4] Intravenous administration of renalase1 was found to decrease blood pressure and heart rate in normal rats,[1] while its subcutaneous injection had an intense and prolonged anti-hypertensive effect on an animal model of salt-sensitive hypertension,[4,5] and its perfusion was found to have a heart-protective effect on a cardiac ischemia mouse model.[2] Furthermore, *RNLS* gene inactivation in mouse resulted in increased sympathetic activity, tachycardia, and hypertension.[6] Two allelic variants of renalase displaying similar frequencies in the human population, carrying Glu or Asp at position 37, are known. The Asp variant was found to correlate significantly with an increased risk of developing essential hypertension and cardiac syndromes.[7,8] It has been proposed that renalase could modulate the intrarenal dopamine system, affecting sodium and phosphate excretion.[4,5,9] In a rat model of chronic heart failure, lowered blood renal flow is associated with decreases in kidney renalase synthesis and norepinephrine clearance.[10]

Despite its potential impact on the treatment of some of the "big killer" diseases in the developed world, an understanding of renalase action at the molecular level has not been reached yet. Stemming from its sequence similarity to flavin-dependent monoamine oxidases (MAOs), it has been suggested that renalase could be a catecholamine-degrading flavoenzyme.[1,11,12] Evidence has been provided for two possible catalytic mechanisms: O_2-dependent direct oxidation of amine substrate (as in the case of MAOs) or its NADH-dependent degradation, mediated by superoxide radical generation.[8] However, the turnover rate of renalase seems too low to fully justify its physiological effects; moreover, the actual presence of a catecholamine-degrading activity in blood plasma, other than that supported by semicarbazide-sensitive amine oxidase, has been excluded by Boomsma and Tipton.[13] (For two recent comprehensive reviews on renalase, the reader is referred to Desir[4] and Medvedev *et al.*[14]) Renalase is highly conserved in mammals, but orthologs are present in protists (*Phytophthora infestans* T30-4; 27% sequence identity), cyanobacteria (*Cyanothece* sp.; 28% identity), and bacteria (*Spirosoma linguale*; 26% identity), suggesting different biological functions associated with similar folds and possibly similar catalyzed reactions (see Fig. 5a).

With the aim of elucidating its catalytic mechanism, we produced an *in vivo* folded form of human renalase1 in *Escherichia coli*.[15] The recombinant protein was found to contain noncovalently bound flavin adenine dinucleotide (FAD), thus providing the first direct evidence that it is a flavoprotein. Here we present a further step towards the elucidation of its structure–function relationships by reporting its three-dimensional structure solved at 2.5 Å resolution. These data, together with kinetic and nucleotide binding studies, provide new hints on the active-site structural organization in this intriguing enzyme.

Results

Redox properties and reactivity of the renalase FAD prosthetic group

Since we report here solely on the properties of human renalase1, we use the term "renalase" throughout this article to indicate this specific isoform, unless otherwise stated. To shed light onto renalase enzymatic activity, we investigated the stability and protonation state of the semiquinone form of its FAD cofactor, which are important criteria for flavoprotein classification.[16,17] Anaerobic renalase solutions were subjected to stepwise photoreduction at different pH values, and the resulting absorption spectra were recorded. As shown in Fig. 1, the bound FAD could be readily reduced by the light/ethylenediaminetetraacetic acid (EDTA)/deazariboflavin system and was reoxidized to yield the original spectrum when the solution was exposed to air. More interestingly, at acidic pH, a significant amount of a species displaying a broad absorption band in the 550–650 nm region, identifiable as neutral flavin semiquinone, was formed during reduction. Above pH 7, the FAD blue semiquinone was undetectable (Fig. 1, inset), without clear evidence of accumulation of its red anionic form. This behavior varies from what is observed for both MAO-A and MAO-B, as well as for their homolog from *Aspergillus niger* (MAO-N, containing a noncovalently bound FAD), which strongly stabilizes the FAD anionic semiquinone.[18,19]

FAD reactivity with sulfite is a distinct key criterion for flavoenzyme classification, since a high stability of the sulfite–isoalloxazine adduct usually correlates with a high O_2 reactivity.[20]

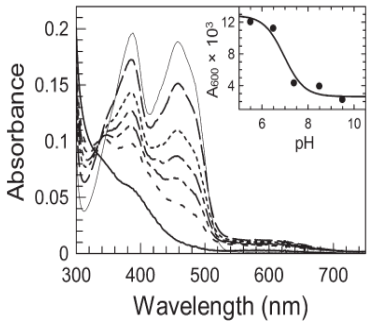

Fig. 1. Anaerobic photoreduction of renalase at different pH values. Progress of protein-bound FAD reduction as recorded on ca 18 μM renalase in 10 mM phosphate–NaOH/10 mM pyrophosphate–NaOH (pH 6.5). The different traces represent the spectra recorded before (continuous thin line) and after (different line styles) each successive illumination period, until a full reduction had been obtained (continuous thick line). The inset shows the maximal intensity reached at 600 nm in titrations carried out at different pH values. The interpolating line corresponds to the theoretical curve for the protonation of a single group with a pK_a of 7.0 ± 0.3.

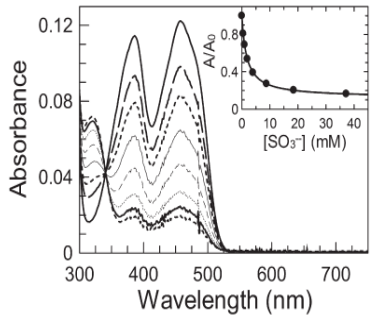

Fig. 2. Titration of renalase with SO_3^{2-} anion. Spectra of renalase in the visible region recorded before (continuous line) and after successive additions of $NaSO_3$ (final concentration: 0.5 mM, 1.0 mM, 2.0 mM, 3.9 mM, 8.8 mM, 18 mM, and 37 mM) showing the progressive bleaching of bound FAD. The inset reports the progress of FAD–sulfite adduct formation measured as the ratio between A_{457} measured in the presence of increasing $NaSO_3$ concentrations and its initial value. The curve represents the theoretical equation for a 1:1 stoichiometry, whose fit to the experimental data yielded a K_d of 1.8 ± 0.2 mM.

Renalase was found to react with sodium sulfite, yielding a complex with a K_d of 1.8 ± 0.2 mM (Fig. 2). The reaction was found to be very slow, with complex formation and dissociation constants of 0.056 ± 0.007 min^{-1} and 0.025 ± 0.003 min^{-1} mM^{-1}, respectively. Again, these results suggest both that renalase is not a typical oxidase and that it differs dramatically from MAOs, which do not react at all with sulfite due to the hydrophobicity of their active sites.[21]

Reactivity of renalase to nicotinamide dinucleotides

Renalase has been reported to catalyze slow O_2 reduction in the presence of NADH yielding the superoxide radical.[8] Since such NADH oxidase reaction suggests the possibility that renalase could be either a dehydrogenase or a monooxygenase, we studied in detail both its NADH-dependent and its NADPH-dependent diaphorase activities using various artificial electron acceptors such as 2-(4-iodophenyl)-3-(4-nitrophenyl)-5-phenyl-2*H*-tetrazolium chloride (INT), 2-(4-iodophenyl)-3-(4-nitrophenyl)-5-(2,4-disulfophenyl)-2*H*-tetrazolium sodium salt (WST1), and $K_3Fe(CN)_6$. The recombinant form of renalase that we have previously produced in *E. coli*[15] corresponds to its Asp37 variant. Since this variant has been reported to possess a lower catalytic activity than the Glu37 form,[8] we have introduced the Asp37Glu replacement in the protein by site-directed mutagenesis. The two variants of renalase displayed indistinguishable catalytic properties *in vitro*. As the Asp37 variant yielded crystals suitable for X-ray analysis, we focus here on the properties of this form.

Renalase displayed a low but measurable catalytic activity only *versus* INT and WST1, with the former substrate being the preferred one. Plots of the steady-state kinetic data for the INT reductase reactions are shown in Fig. 3. The steady-state kinetic parameters (Table 1) show that renalase is slightly but significantly more specific for NADH than for NADPH, although it displays a higher k_{cat} value with the latter cosubstrate. The reductive half-reaction of the catalytic cycle (i.e., the reduction of protein-bound FAD by either NADH or NADPH) was investigated under anaerobic conditions. Both nucleotides were able to transfer reducing equivalents to the renalase prosthetic group. Apparent first-order rate constants (k_{red}) for the hydride transfer (HT) of $(1.5 \times 10^{-2}) \pm (2 \times 10^{-4})$ min^{-1} and $(2.7 \times 10^{-2}) \pm (1 \times 10^{-4})$ min^{-1} were obtained for 1 mM NADH (k_{red}^{NADH}) and NADPH (k_{red}^{NADPH}), respectively.

In order to further investigate the interaction of the protein with nicotinamide dinucleotides, we performed spectrophotometric titrations of renalase with both NAD^+ and $NADP^+$. As shown in Fig. 4, renalase clearly interacts with both dinucleotides, forming complexes whose remarkably strong difference absorption spectra are very similar. Titrations follow the

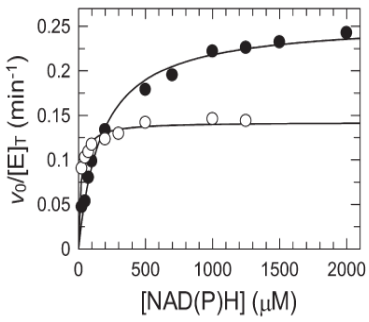

Fig. 3. Catalytic activity of renalase on NADH and NADPH. The steady-state rates of the NADH–INT (○) and NADPH–INT (●) reductase reactions catalyzed by renalase, monitored at 37 °C in 50 mM Tris–HCl (pH 7.2), are plotted as a function of reductant concentration.

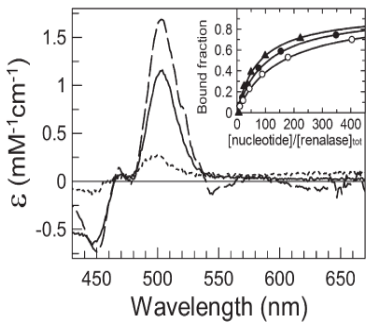

Fig. 4. Interaction of renalase with NADP$^+$, NAD$^+$, and 2′-P-AMP. Approximately 20 μM renalase was titrated with either NADP$^+$, NAD$^+$, or 2′-P-AMP at 25 °C in 50 mM Tris–HCl (pH 7.4). The difference spectra extrapolated under the ligand-saturating conditions of the complexes of renalase with NADP$^+$ (continuous line), NAD$^+$ (broken line), and 2′-P-AMP (dotted line) are shown as extinction coefficients. In the inset, the progress of the fractional amount of complexed protein is plotted as a function of NADP$^+$ (filled circles), NAD$^+$ (empty circles), or 2′-P-AMP (triangles) concentration. The curves represent the theoretical equation for a 1:1 stoichiometry, whose fit to the data yielded K_d values of 1.6±0.1 mM, 2.2±0.1 mM, and 1.2±0.3 mM, respectively.

theoretical curve expected for a 1:1 stoichiometry (Fig. 4, inset). The K_d values of the complexes of renalase with NAD$^+$ and NADP$^+$ were 2.2±0.1 mM and 1.6±0.1 mM, respectively. Interestingly, 2′-P-AMP titration yielded a similar K_d value (1.2±0.3 mM) but a far less intense difference spectrum (Fig. 4), implying that the adenylate portion of NADP$^+$ provides much of the binding energy, while the nicotinamide moiety plays a main role in the perturbation of the isoalloxazine environment. However, titration of renalase with up to 6 mM 5′-AMP did not result in any spectral change, suggesting that a single phosphate group in the ligand is not sufficient to provide enough binding energy and/or the ability to perturb isoalloxazine upon binding.

Renalase crystal structure

The crystal structure of renalase was solved through a composite molecular replacement (MR) approach and refined at 2.5 Å resolution (R/R_{free}=21.7/26.0%; see Table 2); two renalase molecules are hosted per asymmetric unit. The two independent molecules (molecules A and B) display very similar overall conformations, with a pairwise root-mean-square deviation (RMSD) of 0.41 Å calculated over 330 C^{α} pairs. A contained contact region (467 Å^2) is observed

Table 1. Kinetic parameters of renalase for the NADH-dependent and NADPH-dependent INT reductase reactions

Cosubstrate	k_{cat} (min^{-1})	K_m (μM)	k_{cat}/K_m (min^{-1} μM^{-1})
NADH	0.14	18	$(7.8\times10^{-3})\pm(1.2\times10^{-3})$
NADPH	0.26	175	$(1.5\times10^{-3})\pm(1.4\times10^{-4})$

INT–diaphorase activities of renalase were assayed at 37 °C in the presence of a fixed concentration (100 μM) of INT.

Table 2. Crystallographic data collection and structure refinement statistics

Data collection statistics	
Space group	$P2_1$
Unit cell parameters	
a, *b*, *c* (Å)	53.8, 86.6, 93.2
α, γ, β (°)	90, 90, 95.3
Resolution (Å)	48.4–2.5
Mosaicity (°)	1.0
Number of unique reflections	25,082 (3770)
Completeness (%)	84.7 (87.5)
Redundancy	1.8 (1.8)
R_{merge} [a] (%)	8.8 (49.5)
Average $I/\sigma(I)$	5.8 (1.9)
Refinement statistics	
R-factor [b] (%)	21.7
R_{free} [c] (%)	26.0
RMS bond lengths (Å)	0.008
RMS bond angles (°)	1.14
Ramachandran plot	
Residues in the most favored regions (%)	89.3
Residues in additionally allowed regions (%)	10.0

Values in parentheses are for the highest resolution shell.
[a] $R_{merge}=\Sigma|I-(I)|/\Sigma I\times100$, where I is the intensity of a reflection and (I) is its average intensity.
[b] R-factor $=\Sigma||Fo-Fc||/\Sigma|Fo|\times100\%$.
[c] R_{free} for cross-validation was calculated with 5% of reflections that were selected at random and were not included in the refinement.

between the two molecules, in keeping with the monomeric character of renalase in solution, shown by previous gel-filtration and dynamic light-scattering studies.[15] The refined electron density allowed us to model all the protein amino acids, with the exception of a few amino acids that are localized in the substrate-binding domain [i.e., Ser25 (chain A), Lys99-Glu100 (chains A and B), Asp140 (chain B), Ser150 (chain B), Glu201 (chain B), Lys205-Ile206 (chain A), Ser236 (chain B)-Glu237 (chains A and B), and Cys300 (chain B)].

The renalase molecule displays a bean-like elongated shape, with the longer axis being about 60 Å and with the shorter axis being 35 Å. The two lobes of the bean host the FAD-binding domain (amino acids 1–42, 109–189, and 294–341; Fig. 5b, red) and the putative substrate-binding domain (amino acids 43–108 and 190–294; Fig. 5b, blue and green), respectively. The two domains are bent, forming a wide and deep cleft at the center of the protein that, like a belt, runs perpendicularly to the protein's longest axis. Such crevice (positively charged) crosses the protein surface opposite to the partially exposed isoalloxazine ring. The FAD molecule is buried within the protein, except for part of the isoalloxazine ring (see the text below), a small portion of the adenine ring, and part of the adenosine ribose near the pyrophosphate bridge (located next to the mentioned cleft). The FAD-binding domain architecture is based on a Rossmann fold (as in the glutathione reductase family)[22] composed of a six-stranded central β-sheet (with $\beta_3\beta_2\beta_1\beta_4\beta_6\beta_5$ topology), surrounded by six α-helices and by an additional three-stranded mixed β-sheet. The putative substrate-binding domain consists of an anti-parallel five-stranded β-sheet surrounded by three α-helices and one β-hairpin. Moreover, it includes a small subdomain (amino acids 62–108), projecting helix α3 toward the FAD-binding domain (Fig. 5b, green).

The general fold of renalase classifies it as a member of the flavoprotein superfamily sharing the *p*-hydroxybenzoate hydroxylase (PHBH) fold topology, which includes both oxidase and nonoxidase enzymes.[23] Most PHBH-like enzymes catalyzing the oxidation of amines belong to one of two possible structural groups: the MAO family and the D-amino acid oxidase family.[24] Renalase is structurally more similar to MAO-like enzymes than to D-amino-acid-oxidase-like enzymes. A search for proteins that are structurally homologous to renalase, performed through the DALI server†, yielded a putative protoporphyrinogen oxidase [Protein Data Bank (PDB) ID: 3LOV; Z-score of 28.9, residue identity of 19%], in addition to L-amino acid oxidase, a Lys-specific histone demethylase, and an amine oxidase (PDB IDs: 2JB2, 2UXX, and 2BXR, respectively).

†http://ekhidna.biocenter.helsinki.fi/dali_server/

With the exception of histone demethylase, the main feature common to all the protein structures highlighted by DALI as structurally similar to renalase is the presence of an additional stretch of 110–140 amino acids that is entirely absent in renalase (Fig. 6a, left). This structural element corresponds to an additional domain that would be inserted between strand β7 and strand β8 of the renalase substrate-binding domain. Multiple alignment shows that the regions flanking such 'missing' domain are not conserved (Fig. 5a). Interestingly, one of the short segments disordered in the renalase crystal structure corresponds exactly to the insertion point of the 'missing' domain (Lys99-Glu100). The functional roles played by this domain in the renalase homologs are markedly different: in protoporphyrinogen oxidase, it is a membrane-binding domain, while in L-amino acid oxidase, it is a helical domain responsible for protein dimerization. On the contrary, in MAOs and polyamine oxidase, it is an integral part of the substrate-binding domain.

FAD binding

Nineteen residues are directly involved in FAD binding, six of which establish electrostatic or polar interactions with the cofactor (Fig. 6b). Only two of the latter interactions involve side-chain atoms (conserved residues Thr12 and Arg42 linked to the FAD pyrophosphate), with the others being due to main-chain atoms. Access to the dimethylbenzene moiety of the isoalloxazine ring is blocked by the conserved Trp288, while the cofactor pyrimidine ring is quite solvent exposed (Fig. 6a, right), establishing hydrogen bonds with the main-chain atoms of Tyr62 and Phe324 and displaying van der Waals interactions with Ala59.

Putative substrate-binding site

The absence of the 'missing' domain in renalase (see the text above) results in the presence of a wide surface concavity that is the entry site for the enzyme main core cavity, where the FAD cofactor is hosted (Fig. 6a, right). As a consequence, the putative enzyme active site is solvent exposed, as underscored by the presence of five water molecules above the isoalloxazine ring. The active-site cavity has a volume of about 224 $Å^3$ and can be roughly divided into two hemispheres: one composed of aromatic residues and the other composed of polar residues, centered on the isoalloxazine ring. The aromatic hemisphere (roughly above the isoalloxazine pyrimidine ring) is characterized by residues Tyr62 (mostly conserved), Tyr214, and Phe223 (aromaticity conserved), with the two Tyr residues being mutually hydrogen bonded (mean of the two subunits, 2.7 ± 0.2 Å). The polar hemisphere is lined by Gln292, Arg193, His245 (mostly conserved), and Arg222, and displays an overall positive charge

Fig. 5. Amino acid sequence and three-dimensional structure of human renalase. (a) Multiple alignment of human renalase with orthologs from different organisms: *Mus musculus* (110671808; 73% identity), *Danio rerio* (50540280; 60% identity), *Acyrthosiphon pisum* (193575653; 34% identity), and *Cyanothece* sp. (307154671; 28% identity). Partially conserved residues are boxed, with invariant residues highlighted in red. Secondary structure elements are indicated above the renalase sequence. (b) Renalase overall three-dimensional structure with secondary structure elements as highlighted in (a). The FAD-binding domain is shown in red, the substrate-binding domain is shown in blue, and the 62–108 subdomain is shown in green.

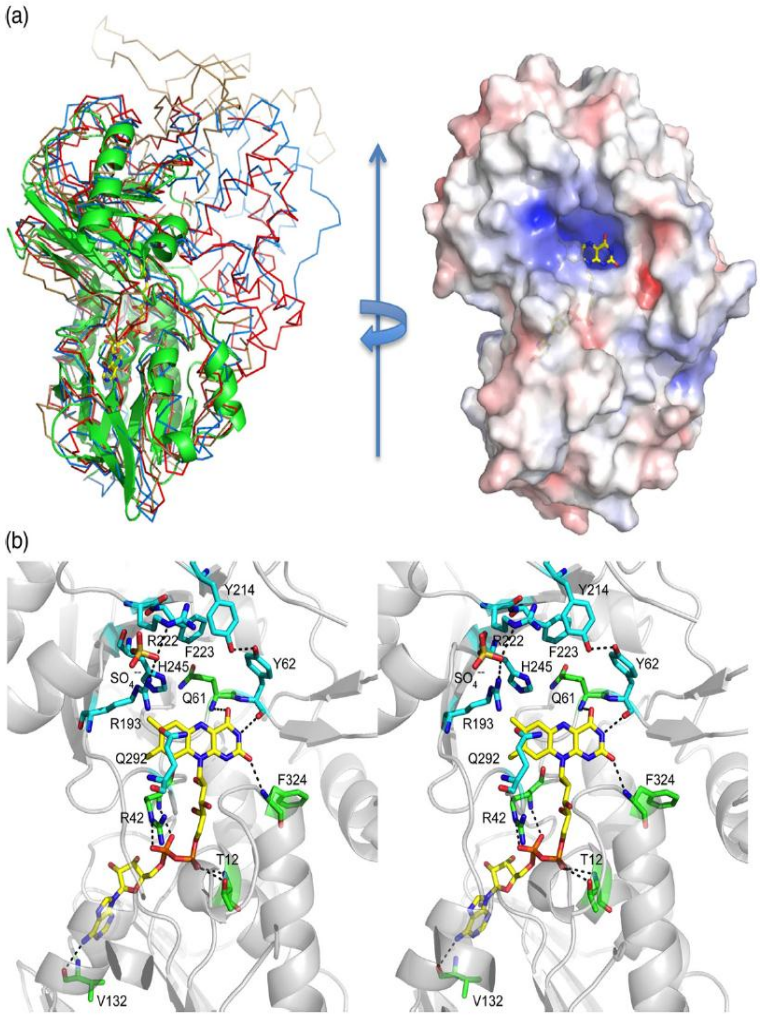

Fig. 6. Protein–FAD interactions and active-site cavity of renalase. (a) The overlay of the three-dimensional structure of renalase on the structures of its most similar homologs is displayed on the left. The renalase molecule is shown as a green ribbon, with the FAD prosthetic group displayed as a wire frame in CPK colors. The C^{α} traces of *Exiguobacterium* sp. protoporphyrinogen oxidase (PDB ID: 3LOV; blue; RMSD of 2.7 Å for 286 C^{α}), *Rhodococcus opacus* L-amino acid oxidase (PDB ID: 2JB2; brown; RMSD of 2.5 Å for 292 C^{α}), and *Homo sapiens* MAO (PDB ID: 2BXR; red; RMSD of 3.0 Å for 283 C^{α}) are also shown to highlight the location of the third domain that is not present in renalase. The molecular surface of renalase, colored according to its potential (rotated by 90° with respect to (a)), is displayed on the right. The entry of the active-site cavity, showing the pyrimidine side of the isoalloxazine ring of FAD, is clearly visible. (b) Stereo view of the proposed renalase active-site region, showing FAD, the residues exchanging hydrogen bonds with FAD (green carbon atoms), the main residues lining the cavity above the isoalloxazine ring (blue carbon atoms), and the ordered sulfate ion bound at the border of the active-site cavity.

(Fig. 6b). The water molecules found in the cavity bridge between the two sides, but their locations are not conserved in the two renalase chains, suggesting that the site is suited for accommodating polar compounds. A sulfate anion, hydrogen bonded to Thr247 and electrostatically compensated for by Arg193 and Arg222, is present in both asymmetric unit renalase molecules at the external border of the polar cavity (Fig. 6b). Since renalase has been proposed to represent a new form of MAO,[1,11] a structural comparison with the active site of the latter enzyme is useful. The overlay of the three-dimensional structure of renalase with those of MAO-A, MAO-B, and polyamine oxidase led to the observation that the position of the active-site cavity is highly conserved in all these enzymes. However, residues critical for the catalysis of amine oxidation are not maintained in renalase. In particular, Lys296 (MAO-B numbering) is replaced by His245, and the so-called 'aromatic cage' (formed by Tyr398 and Tyr435 in MAO-B)[25,26] is absent in renalase, where the two aromatic residues are replaced by Gln292 and Asn323 (Fig. 6b).

Discussion

The functional part of the study on renalase described here had two main purposes: (i) to assess the prosthetic group key chemical features that allow flavoprotein classification, and (ii) to analyze the interaction of renalase with nicotinamide dinucleotides, as conceivable cosubstrates of the enzyme. Concerning the first question, here we show that renalase provides a mild stabilization of the neutral form of the flavin semiquinone and that the renalase-bound FAD forms a sulfite adduct, although slowly and with low affinity. Both features do not classify renalase as a MAO-like enzyme. Moreover, lack of stabilization for the FAD anionic semiquinone and the previous observation that renalase reacts with O_2, producing the superoxide anion rather than hydrogen peroxide,[8] indicate that renalase is probably not even an oxidase.

As far as the second question is concerned, we confirm that renalase catalyzes both NADH-dependent and NADPH-dependent diaphorase reactions, as recently reported by Farzaneh-Far *et al.*[8] In addition, we provide evidence for direct HT from both NADH and NADPH to the enzyme and for a 1:1 complex formation with the oxidized dinucleotides and a NADP analog. However, the exceedingly low k_{cat} and k_{cat}/K_m values observed in the steady-state reactions, confirmed by a very slow HT in the reductive half-reaction and the millimolar affinity of the enzyme for both NAD^+ and $NADP^+$, strongly suggest that NADH and NADPH are not renalase physiological substrates. Such conclusion is in line with the absence of an evident NADP-binding site in the three-dimensional enzyme structure. Since PHBH, which shares the same general fold of renalase, is known to bind NADPH (unconventionally) at the protein surface in a groove crossing the FAD cavity,[27,28] we employed molecular modeling to assess whether renalase could accommodate NADPH in a similar way. Our structural comparisons indicate that FAD is much more deeply buried inside renalase than inside PHBH, making the putative NADPH-binding site sterically blocked in renalase. Thus, whereas NADPH can access the FAD isoalloxazine ring of PHBH with limited conformation changes, a similar NADPH binding mode would appear catalytically unproductive in renalase. To explain the slow reactivity of renalase towards both NADH and NADPH, we speculated that nicotinamide dinucleotides might access FAD through the putative substrate-binding cavity.

A further point that needs to be discussed is the recent report that the Glu37 allelic variant of the protein displays a higher catalytic efficiency (k_{cat}/K_m^{NADH}) in the reductase reaction, relative to the Asp37 form.[8] The crystal structure of the protein described here shows that residue 37 is located in a surface loop at the interface between the two domains, far from the active site. Moreover, consistent with structural evidences, we found no difference between the diaphorase activities of the two allelic variants of the enzyme. This discrepancy could be ascribed to the fact that we isolated renalase forms that underwent folding and FAD incorporation within *E. coli* cells,[15] while catalytic differences between variants were detected on proteins that were refolded *in vitro*.[8] Indeed, it has been shown that *in vitro* refolding may result in significant alterations in the properties of flavoproteins.[29]

In conclusion, the structural data first reported here are in keeping with the results of our previous and current functional studies, which point out that renalase is not a MAO and most probably not an oxidase. On the other hand, structural comparisons of renalase with its homologs do not allow us to shed additional light on the reaction catalyzed by this enzyme. Taken together, our observations suggest that the substrate of renalase may be a large polar molecule, possibly carrying a negative charge; the chemical process catalyzed by renalase on such substrate would be different from an oxidase reaction.

Materials and Methods

NAD^+, $NADP^+$, NADH, NADPH, 2′-phospho-AMP, 5′-AMP, INT, and WST1 were purchased from Sigma-Aldrich.

Renalase expression and purification

The variant of human renalase carrying Asp at position 37 was produced in the Rosetta(DE3) *E. coli* strain transformed with pET-SUMO-RNLS.[15] To obtain the other known

widespread variant of the protein,[8] we introduced a point mutation resulting in Asp37Glu substitution in the renalase coding sequence of the above plasmid, using the QuikChange® Lightning Site-Directed Mutagenesis Kit (Stratagene), in conjunction with the complementary oligonucleotides 5′ GGGACAAGGCTGAGGACTCAGGGGGAAG-3′ and 5′ CTTCCCCCTGAGTCCTCAGCCTTGTCCC-3 (base changes underlined). Both recombinant forms of renalase were produced and purified according to the procedure previously reported.[15] Renalase concentration was quantified on the basis of the extinction coefficient of 11.3 mM^{-1} cm^{-1} at 457 nm.[15]

Photoreduction experiments, ligand binding studies, and activity assays

All spectrophotometric measurements were performed either on a model 8453 diode-array (Agilent) or on a Cary 100 double-beam (Varian) spectrophotometer. Anaerobic stepwise photoreduction of the renalase FAD prosthetic group was carried out using the light/EDTA system.[30] Samples of ca 15 μM renalase in 10 mM phosphate–NaOH/10 mM pyrophosphate–NaOH (at pH values ranging from 5.5 to 9.5) containing 15 mM EDTA and ca 1.5 μM deazariboflavin were placed under anaerobic conditions in a sealed cuvette by successive cycles of N_2 flushing and vacuum application. Spectra were recorded before and after successive illumination periods, until a full reduction had been obtained within a total irradiation time of about 4 min. Sodium sulfite titration of renalase was performed in phosphate-buffered saline at 25 °C. Spectra were recorded before and after successive additions, allowing the reaction to reach equilibrium after each increase in ligand concentration. From the time course of the spectral change accompanying adduct formation, the pseudo-first-order rate constants of the process were obtained at different Na_2SO_3 concentrations. The secondary plot of this apparent constant as a function of ligand concentration yielded the individual constants for adduct formation and dissociation from the slope and the intercept of the plot, respectively. The putative reductive half-reaction catalyzed by renalase (i.e., the HT from NADH or NADPH to FAD) was monitored spectrophotometrically at 37 °C by recording the spectra of anaerobic solutions of 5 μM renalase in 50 mM Tris–HCl (pH 7.2) at various reaction times after the addition of NADH or NADPH at different concentrations. Spectrophotometric active-site titrations of renalase with $NADP^+$, NAD^+, 2′-P-AMP, or 5′-AMP were carried out at 25 °C in 50 mM Tris–HCl (pH 7.4), according to the procedure described elsewhere.[31] NADH-dependent and NADPH-dependent diaphorase activities of renalase were assayed at 37 °C in 50 mM Tris–HCl (pH 7.2), using a fixed concentration of either 100 μM INT or 500 μM WST1 as electron acceptor. The reaction mixture included 2.6 μM renalase and a variable concentration of reduced dinucleotide in the range of 0.05–2 mM. In the case of the INT-dependent reaction, 0.1% Triton X-100 was also included to avoid precipitation of the formazan product. The time course of the absorbance increase at the appropriate wavelength was monitored continuously, and steady-state rates were calculated using the extinction coefficients of 18.5 mM^{-1} cm^{-1} (at 490 nm) and 37 mM^{-1} cm^{-1} (at 450 nm) for INT and WST1, respectively.

Crystallization and structure solution

Renalase crystals were obtained in a sitting drop set-up, mixing 0.2 μl of protein (24 mg ml^{-1}; supplemented with freshly added 10 mM DDT) and 0.1 μl of reservoir solution [30% polyethylene glycol 8000, 0.1 M sodium cacodylate (pH 6.5), and 0.2 M ammonium sulfate]. Small crystals, with average dimensions of 50 μm × 25 μm × 25 μm, were grown in about 5 days at 20 °C. The crystals were transferred to a cryoprotectant solution [32% polyethylene glycol 8000, 0.1 M sodium cacodylate (pH 6.5), 0.2 M ammonium sulfate, and 25% glycerol] before being flash cooled in liquid nitrogen. Diffraction data were collected at European Synchrotron Radiation Facility beamline ID23-2. The crystal, belonging to the monoclinic space group $P2_1$, diffracted at 2.5 Å resolution. During data collection, the crystal suffered radiation damage, causing reduced completeness of data (84.7%). While the color of crystals used for data collection indicated that bound FAD was unequivocally oxidized, minor/partial reduction of the coenzyme during X-ray irradiation cannot be excluded. The final model was of no help in revealing the oxidation state of the cofactor, since the two nitrogen atoms of FAD were found to be not involved in hydrogen bonds. Renalase structure was solved by MR (program MOLREP).[32] The model used for MR search was built starting from the atomic coordinates of the q888a4 oxidoreductase of *Pseudomonas syringae* (a FAD-containing protein of unknown function; PDB ID: 3KKJ), divided into two domains: the FAD-binding domain (Mod1; amino acids 2–33, 124–181, and 278–329) and the cofactor-binding domain (Mod2; amino acids 82–99 and 185–275), including about 74% of the renalase residues. Since Matthews analysis suggested the presence of two molecules in the crystal asymmetric unit (solvent content, 57%), MR search (maximum resolution, 3.5 Å) was performed in two subsequent steps: to locate two copies of Mod1 (R-factor/S_{cor} = 0.572/0.445) and then the remaining two copies of Mod2 (R-factor/S_{cor} = 0.568/0.465). After rigid-body refinement (R/R_{free} = 0.522/0.514) and constrained refinement (R/R_{free} = 0.435/0.488; program Refmac),[33] we started mutating amino acids and manual rebuilding (program Coot).[34] A clear electron density was present in the FAD-binding site, and the ligand model was therefore built. The programs Parrot[35] and Buccaneer were used to help modelling during the manual (re)building procedures; omit maps were produced to correct for errors in the model; and the programs Refmac5 and Buster were used for final refinement. The final model contains 335 and 333 amino acids over 442 in molecules A and B, respectively, as well as 2 FAD molecules, 3 sulfate molecules, and 128 water molecules. Data collection and refinement statistics are reported in Table 2. Structural figures were prepared with PyMOL‡.

Accession number

The atomic coordinates of human renalase isoform 1 have been deposited in Research Collaboratory for Structural Bioinformatics PDB under accession code 3QJ4.

‡ http://www.pymol.org

References

1. Xu, J., Li, G., Wang, P., Velazquez, H., Yao, X., Li, Y. *et al.* (2005). Renalase is a novel, soluble monoamine oxidase that regulates cardiac function and blood pressure. *J. Clin. Invest.* **115**, 1275–1280.
2. Desir, G. V. (2009). Regulation of blood pressure and cardiovascular function by renalase. *Kidney Int.* **76**, 366–370.
3. Hennebry, S. C., Eikelis, N., Socratous, F., Desir, G. V., Lambert, G. & Schlaich, M. (2010). Renalase, a novel soluble FAD-dependent protein, is synthesized in the brain and peripheral nerves. *Mol. Psychiatry*, **15**, 234–236.
4. Desir, G. V. (2011). Role of renalase in the regulation of blood pressure and the renal dopamine system. *Curr. Opin. Nephrol. Hypertens.* **20**, *31–36*.
5. Desir, G. V. (2011). Novel insights into the physiology of renalase and its role in hypertension and heart disease. *Pediatr. Nephrol.*; [E-publication ahead of print; PMID 21424526].
6. Wu, Y., Xu, J., Velazquez, H., Wang, P., Li, G., Liu, D. *et al.* (2010). Renalase deficiency aggravates ischemic myocardial damage. *Kidney Int.* **79**, 853–860.
7. Zhao, Q., Fan, Z., He, J., Chen, S., Li, H., Zhang, P. *et al.* (2007). Renalase gene is a novel susceptibility gene for essential hypertension: a two-stage association study in northern Han Chinese population. *J. Mol. Med.* **85**, 877–885.
8. Farzaneh-Far, R., Desir, G. V., Na, B., Schiller, N. B. & Whooley, M. A. (2010). A functional polymorphism in renalase (Glu37Asp) is associated with cardiac hypertrophy, dysfunction, and ischemia: data from the heart and soul study. *PLoS ONE*, **5**, e13496.
9. Weinman, E. J., Biswas, R., Steplock, D., Wang, P., Lau, Y. S., Desir, G. V. & Shenolikar, S. (2011). Increased renal dopamine and the acute renal adaptation to a high phosphate diet. *Am. J. Physiol. Renal. Physiol.* **300**, F1123–F1129.
10. Gu, R., Lu, W., Xie, J., Bai, J. & Xu, B. (2011). Renalase deficiency in heart failure model of rats—a potential mechanism underlying circulating norepinephrine accumulation. *PLoS ONE*, **6**, e14633.
11. Wang, J., Qi, S., Cheng, W., Li, L., Wang, F., Li, Y. Z. & Zhang, S. P. (2008). Identification, expression and tissue distribution of a renalase homologue from mouse. *Mol. Biol. Rep.* **35**, 613–620.
12. Li, G., Xu, J., Wang, P., Velazquez, H., Li, Y., Wu, Y. & Desir, G. V. (2008). Catecholamines regulate the activity, secretion, and synthesis of renalase. *Circulation*, **117**, 1277–1282.
13. Boomsma, F. & Tipton, K. F. (2007). Renalase, a catecholamine-metabolising enzyme? *J. Neural Transm.* **114**, 775–776.
14. Medvedev, A. E., Veselovsky, A. V. & Fedchenko, V. I. (2010). Renalase, a new secretory enzyme responsible for selective degradation of catecholamines: achievements and unsolved problems. *Biochemistry (Moscow)*, **75**, 951–958.
15. Pandini, V., Ciriello, F., Tedeschi, G., Rossoni, G., Zanetti, G. & Aliverti, A. (2010). Synthesis of human renalase1 in *Escherichia coli* and its purification as a FAD-containing holoprotein. *Protein Expression Purif.* **72**, 244–253.
16. Massey, V. (1995). Introduction: flavoprotein structure and mechanism. *FASEB J.* **9**, 473–475.
17. Massey, V. (2000). The chemical and biological versatility of riboflavin. *Biochem. Soc. Trans.* **28**, 283–296.
18. Hynson, R. M., Kelly, S. M., Price, N. C. & Ramsay, R. R. (2004). Conformational changes in monoamine oxidase A in response to ligand binding or reduction. *Biochim. Biophys. Acta*, **1672**, 60–66.
19. Sablin, S. O., Yankovskaya, V., Bernard, S., Cronin, C. N. & Singer, T. P. (1998). Isolation and characterization of an evolutionary precursor of human monoamine oxidases A and B. *Eur. J. Biochem.* **253**, 270–279.
20. Massey, V., Müller, F., Feldberg, R., Schuman, M., Sullivan, P. A., Howell, L. G. *et al.* (1969). The reactivity of flavoproteins with sulfite. Possible relevance to the problem of oxygen reactivity. *J. Biol. Chem.* **244**, 3999–4006.
21. Li, M., Hubálek, F., Newton-Vinson, P. & Edmondson, D. E. (2002). High-level expression of human liver monoamine oxidase A in *Pichia pastoris*: comparison with the enzyme expressed in *Saccharomyces cerevisiae*. *Protein Expression Purif.* **24**, 152–162.
22. Dym, O. & Eisenberg, D. (2001). Sequence–structure analysis of FAD-containing proteins. *Protein Sci.* **10**, 1712–1728.
23. Fraaije, M. W. & Mattevi, A. (2000). Flavoenzymes: diverse catalysts with recurrent features. *Trends Biochem. Sci.* **25**, 126–132.
24. Fitzpatrick, P. F. (2010). Oxidation of amines by flavoproteins. *Arch. Biochem. Biophys.* **493**, 13–25.
25. De Colibus, L., Li, M., Binda, C., Lustig, A., Edmondson, D. E. & Mattevi, A. (2005). Three-dimensional structure of human monoamine oxidase A (MAO A): relation to the structures of rat MAO A and human MAO B. *Proc. Natl Acad. Sci. USA*, **102**, 12684–12689.
26. Binda, C., Mattevi, A. & Edmondson, D. E. (2002). Structure–function relationships in flavoenzyme-dependent amine oxidations: a comparison of polyamine oxidase and monoamine oxidase. *J. Biol. Chem.* **277**, 23973–23976.
27. Ballou, D. B., Entsch, B. & Cole, L. J. (2005). Dynamics involved in catalysis by single-component and two-component flavin-dependent aromatic hydroxylases. *Biochem. Biophys. Res. Commun.* **338**, *590–598*.
28. Wang, J., Ortiz-Maldonado, M., Entsch, B., Massey, V., Ballou, D. B. & Gatti, D. L. (2002). Protein and ligand dynamics in 4-hydroxybenzoate hydroxylase. *Proc. Natl Acad. Sci. USA*, **99**, 608–613.
29. Sevrioukova, I. F. (2011). Apoptosis-inducing factor: structure, function, and redox regulation. *Antioxid. Redox Signal.* **14**, 2545–2579.
30. Massey, V. & Hemmerich, P. (1977). A photochemical procedure for reduction of oxidation–reduction proteins employing deazariboflavin as catalyst. *J. Biol. Chem.* **252**, 5612–5614.
31. Milani, M., Balconi, E., Aliverti, A., Mastrangelo, E., Seeber, F., Bolognesi, M. & Zanetti, G. (2007). Ferredoxin–$NADP^+$ reductase from *Plasmodium*

falciparum undergoes $NADP^+$-dependent dimerization and inactivation: functional and crystallographic analysis. *J. Mol. Biol.* **367**, 501–513.
32. Vagin, A. & Teplyakov, A. (1997). MOLREP: an automated program for molecular replacement. *J. Appl. Crystallogr.* **30**, 1022–1025.
33. Murshudov, G. N., Vagin, A. A. & Dodson, E. J. (1997). Refinement of macromolecular structures by the maximum-likelihood method. *Acta Crystallogr. Sect. D*, **53**, 240–255.
34. Emsley, P., Lohkamp, B., Scott, W. & Cowtan, K. (2010). Features and development of Coot. *Acta Crystallogr. Sect. D*, **66**, 486–501.
35. Cowtan, K. (2010). Recent developments in classical density modification. *Acta Crystallogr. Sect. D*, **66**, 470–478.

Crystal structure of human renalase, a novel flavoenzyme involved in the pathogenesis of cardiovascular diseases

Sara Baroni[1], Mario Milani[1,2], Vittorio Pandini[1], Francesco Ciriello[1], Martino Bolognesi[1,2], Alessandro Aliverti[1]

[1]Dept. of Biomolecular Sciences & Biotechnology, Università degli Studi di Milano, Milano, Italy

[2]CNR-Istituto di Biofisica, Università degli Studi di Milano, Milano, Italy

Introduction

Renalase is a recently discovered flavoprotein [1], highly conserved in vertebrates with orthologs in many other organisms, including lower eukaryotes and bacteria. In mammals, renalase is synthetized in the kidneys, heart, skeletal muscles, brain and small intestine, being present in blood and urine [2]. Renalase has been shown to be active in lowering blood pressure, in exerting a cardioprotectant action and in promoting sodium and phosphate excretion [2]. Based on sequence similarity to other flavoenzymes including monoamine oxidases (MAOs), renalase has been proposed to act as a catecholamine-degrading enzyme, possibly via a mechanism requiring O_2 and/or NADH as co-substrates [2]. However, no clear evidence of such catalytic activity has been provided [3,4]. Thus, despite its medical relevance, the exact mechanism of renalase physiological actions is presently unknown. To gain insight into its activity at the molecular level, we produced recombinant human renalase in *Escherichia coli* and showed that it contains non-covalently bound FAD [5]. Here we report on some functional features of renalase and discuss them at the light of its crystal structure solved at 2.5 Å resolution [6].

Materials and Methods

The recombinant isoform 1 of human renalase was produced and isolated as reported [5]. Photoreduction experiments, steady-state assays, pre-steady state kinetics, ligand binding titration and protein crystal studies were performed as described elsewhere [6].

Results & Discussion

Recombinant renalase displays a typical flavoprotein spectrum, which slowly bleaches in the visible region when incubated with large concentrations of sodium sulfite, as shown in Fig. 1A.

2

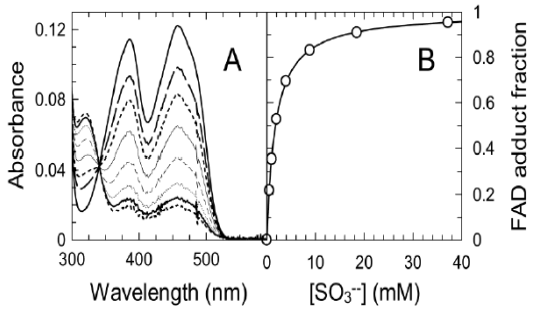

Figure 1. Spectral changes induced by Na_2SO_3 on renalase, at 25 °C. **A.** Spectra recorded after each addition of the ligand, after equilibrium conditions were reached. **B.** Fraction of FAD-sulfite adduct as a function of sulfite concentration.

From titration (Fig. 1B) and kinetic data, the following parameters for the sulfite-flavin adduct were obtained: K_d = 1.8 ± 0.2 mM, k_{on} = 3.36 ± 0.42 $h^{-1}mM^{-1}$, k_{off} = 1.5 ± 0.2 h^{-1}. The renalase-bound FAD could be easily reduced under anaerobiosis by the light/EDTA/deazariboflavin system. As shown in Figure 2, redox titrations carried out over a wide pH range show that the protein slightly stabilizes the neutral form of the FAD semiquinone at acidic or neutral pH values, with no clear evidence of formation of any FAD radical form above pH 7. The reactivity of renalase FAD prostetic group suggests that the enzyme is not an oxidase. To test the hypothesis that renalase is instead a NAD(P)H-dependent enzyme as recently proposed [2], we measured its NAD(P)H-diaphorase activity with different artificial electron acceptors, the best of which turned out to be *p*-iodonitrotetrazolium violet (INT). However, measured steady-state rates were extremely low, with k_{cat} values of 0.14 ± 0.04 min^{-1} and 0.26 ± 0.06 min^{-1}, and k_{cat}/K_m values of 7.8 ± 1.2 $min^{-1}mM^{-1}$ and 1.5 ± 0.14 $min^{-1}mM^{-1}$, for NADH and NADPH, respectively. The poor reactivity and selectivity of renalase towards nicotinamide dinucleotides were confirmed by studying the pre-steady state reactions of the enzyme with either NADH or NADPH (Fig. 3), and by performing spectrophotometric titrations with their corresponding oxidized forms, which yielded K_d values of 2.2 ± 0.1 mM and 1.6 ± 0.1 mM for NAD^+ and $NADP^+$, respectively. These data indicate that, most likely, neither NADH nor NADPH are physiological renalase substrates.

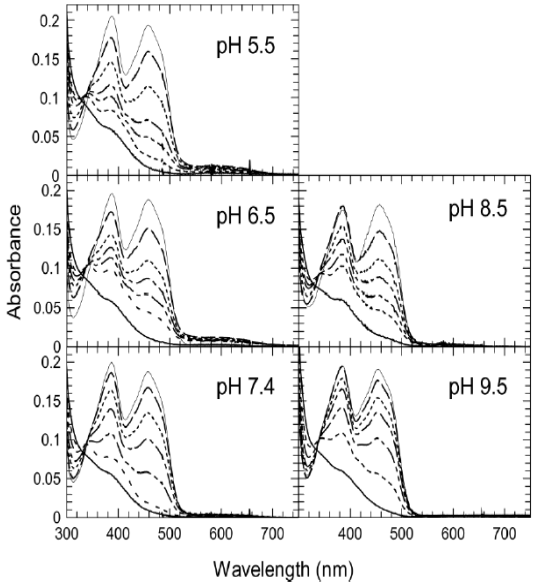

Figure 2. Anaerobic photoreduction of renalase at 15 °C by the light/EDTA/deazariboflavin system in 10 mM NaOH-phosphate/NaOH-pyrophosphate, at the indicated pH values.

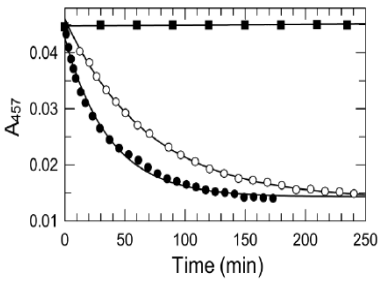

Figure 3. Time course of anaerobic reduction of renalase-bound FAD by 1 mM NADH (open circles) or 1 mM NADPH (filled circles) at 37 °C. Control data obtained in the absence of reducing agents are shown as filled squares.

The crystal structure of renalase (PDB ID: 3QJ4) was solved at 2.5 Å resolution by molecular replacement, using an uncharacterized oxidoreductase from *Pseudomonas syringae* (PDB ID: 3KKJ) as search model. The renalase molecule displays an elongated shape and a two-domain organization (FAD-binding and putative substrate-binding domains). The general fold of renalase assigns it to the *p*-hydroxybenzoate hydroxylase structural family of flavoproteins [7]. Notably, the majority of renalase homologs of known three-dimensional structure host a third domain that blocks solvent access to the isoalloxazine ring. In renalase, the absence of such domain leaves the pyrimidine side of the flavin ring exposed at the bottom of a funnel-shaped wide cavity that opens at the protein surface, as shown in Fig. 4A. The interactions established by the protein and the FAD cofactor are reported in Fig. 4B. The putative active site is represented by a roughly spherical 228 $Å^3$ cavity in front of the *re*-face of the flavin. The cavity shows an amphipathic character, with a polar region lined by basic groups and a hydrophobic side contributed by aromatic side-chains (Fig. 5). Notably, the renalase putative active site lacks both the "aromatic cage", present in amine oxidases, and the Lys residue interacting with the flavin N5 atom via a H_2O molecule that is conserved in most oxidases [8].

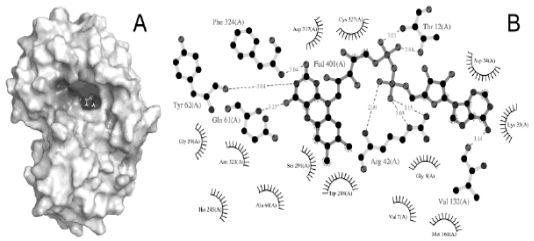

Figure 4. Crystal structure of human renalase. **A.** General shape of the protein molecule, showing its surface with the wide cavity opening to the putative active-site region, at the bottom of which part of the FAD isoalloxazine ring is visible. **B.** Scheme of the protein-FAD contacts.

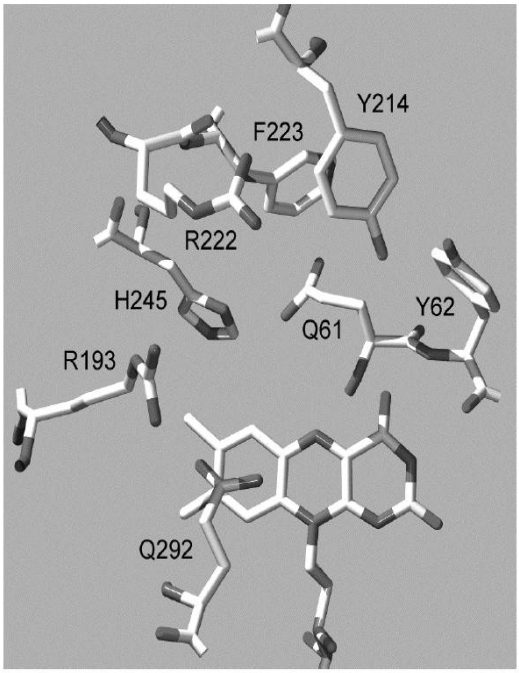

Figure 5. Spatial organization of human renalase putative active site. The FAD prosthetic group and the amino acid residues lining the proposed active-site cavity are shown.

Conclusions

Although our present results do not allow to assign a defined enzyme activity to renalase, we exclude that the enzyme may support an oxidase reaction. Our structural data suggest that renalase substrate should present an amphipathic character, possibly carrying one or more negatively charged groups.

References

1. J. Xu, G. Li, P. Wang, H. Velazquez, X. Yao, Y. Li, Y. Wu, A. Peixoto, S. Crowley, G.V. Desir (2005) Renalase is a novel, soluble monoamine oxidase that regulates cardiac function and blood pressure, *J. Clin. Invest.* **115**, 1275-1280.
2. G.V. Desir (2011) Role of renalase in the regulation of blood pressure and the renal dopamine system, *Curr. Opin. Nephrol. Hypertens.* **20**, 31-36.
3. F. Boomsma, K.F. Tipton (2007) Renalase, a catecholamine-metabolising enzyme? *J. Neural. Transm.* **114**, 775–776.
4. N. Eikelis, S.C. Hennebry, G.W. Lambert, M.P. Schlaich (2011) Does renalase degrade catecholamines? *Kidney Int.* **79**, 1380.
5. V. Pandini, F. Ciriello, G. Tedeschi, G. Rossoni, G. Zanetti, A. Aliverti (2010) Synthesis of human renalase1 in *Escherichia coli* and its purification as a FAD-containing holoprotein, *Protein Expr. Purif.* **72**, 244-253.
6. M. Milani, F. Ciriello, S. Baroni, V. Pandini, G. Canevari, M. Bolognesi, A. Aliverti (2011) FAD-binding site and NADP reactivity in human renalase: a new enzyme involved in blood pressure regulation, *J. Mol. Biol.* Epub ahead of print, PMID: 21699903.
7. M.W. Fraaije, A. Mattevi (2000) Flavoenzymes: diverse catalysts with recurrent features, *Trends Biochem. Sci.* **25**, 126-132.
8. C. Binda, A. Mattevi, D.E. Edmondson (2002) Structure-function relationships in flavenzyme-dependent amine oxidations: a comparison of polyamine oxidase and monoamine oxidase, *J. Biol. Chem.* **277**, 23973-23976.